Laboratory of Virology

Department of Virology, Parasitology and Immunology

Faculty of Veterinary Medicine

Ghent University

Invasion of feline, canine and porcine alphaherpesviruses through target mucosae of their respective host

Yewei Li

Dissertation submitted in fulfilment of the requirements for the degree of

Doctor of Philosophy (PhD) in Veterinary Science, 2017

Promoter

Prof. Dr. Hans J. Nauwynck

TABLE OF CONTENTS

CHAPTER 1
INTRODUCTION

1.1 The order *Herpesvirales*

The *Herpesviridae* are a large family of DNA viruses which have as their natural hosts mammals, birds, reptiles, bony fishes, frogs and molluscs (Davison, 2010). All members of the *Herpesviridae* are considered to have evolved from a common herpesvirus ancestor which originated 400 million years ago (Davison, 2007). During this evolution, the genomes of these herpesviruses became quite different in terms of nucleotide sequence, gene content, and genomic arrangement (McGeoch et al., 2000). Up till now, there are nine known human herpesviruses and a large number of animal herpesviruses. Phylogenetic studies have subdivided *Herpesviridae* into three distinct subfamilies: alpha-, beta- and gamma-herpesviruses (Leroy et al., 2016).

Among those subfamilies, members of the *Alphaherpesvirinae* are characterized by their short replication cycle, fast destruction of infected cells, induction of lifelong latency, primary in neurons, and a broad host cell range (Remeijer et al., 2004). There are four genera in the *Alphaherpesvirinae* subfamily: *Simplexvirus, Varicellovirus, Mardivirus* and *Iltovirus* (Arvin and Abendroth, 2007). Human herpes simplex virus 1 (HSV1) and 2 (HSV-2) belong to the *Simplexvirus genus*. Known species of the *Varicellovirus genus* are bovine herpesvirus 1 (BoHV1), equine herpesvirus 1 (EHV1), suid herpesvirus 1 (SuHV1, PrV), feline herpesvirus 1 (FeHV1), canine herpesvirus 1 (CaHV1) and human herpesvirus varicella-zoster virus (VZV). Table 1 provides an overview of members of the *Varicellovirus genus*. VZV is the prototype species in the genus, and PrV is also a well-studied varicellovirus.

Betaherpesvirinae contain four genera: *Cytomegalovirus, Muromegalovirus, Roseolovirus* and *Proboscivirus*. In this family, the virus' host range is quite restricted. Betaherpesviruses are characterized by a long replication cycle, which is different from alphaherpesviruses (Roizman and Baines, 1991). *Gammaherpesvirinae* prefer to enter the latency program instead of leading to a productive replication. Members of

this subfamily are subdivided into four genera: *Lymphocryptovirus, Rhadinovirus, Macavirus* and *Percavirus* (Davison et al., 2009).

Table 1. *Members of the Varicellovirus genus*

Name	Acronym	Common name	Host
Bovine herpesvirus 1	BoHV1	Infectious bovine rhinotracheitis virus	Cattle
Bovine herpesvirus 5	BoHV5	Bovine encephalitis herpesvirus	Cattle
Bubaline herpesvirus 1	BuHV1	Water buffalo herpesvirus	Buffalo
Canine herpesvirus 1	CaHV1	Canine herpesvirus	Dog
Caprine herpesvirus 1	CpHV1	Goat herpesvirus	Goat
Cercopithecine herpesvirus 9	CeHV9	Simian varicella virus	Monkey
Cervid herpesvirus 1	CvHV1	Red deer herpesvirus	Deer
Cervid herpesvirus 2	CvHV2	Reindeer herpesvirus	Deer
Equine herpesvirus 1	EHV1	Equine abortion virus	Horse
Equine herpesvirus 3	EHV3	Equine coital exanthema virus	Horse
Equine herpesvirus 4	EHV4	Equine rhinopneumonitis virus	Horse
Equine herpesvirus 8	EHV8	Asinine herpesvirus 3	Horse
Feline herpesvirus 1	FeHV1	Feline rhinotracheitis virus	Cats
Human herpesvirus 3	HHV3	Varicella-zoster virus	Human
Phocine herpesvirus 1	PhoHV1	Harbour seal herpesvirus	Seal
Suid herpesvirus 1	SuHV1/PrV	Pseudorabies virus	Pig

1.1.1 Virion structure of alphaherpesviruses

Mature (fully assembled) herpesvirus particles contain four morphologically distinct elements: the genome, capsid, tegument, and envelope. The general architecture of a herpesvirus particle is given in Figure 1. Mature (fully assembled) alphaherpesvirus particles have a diameter of about 200 nm. Variation is caused by the variable dimension of the tegument. The core contains a double stranded DNA genome, which

is packaged into the capsid. The tegument is a poorly defined layer of proteinaceous material between the capsid and envelope. The envelope is a lipid bilayer containing a number of different integral viral (glyco)proteins (Owen et al., 2015b).

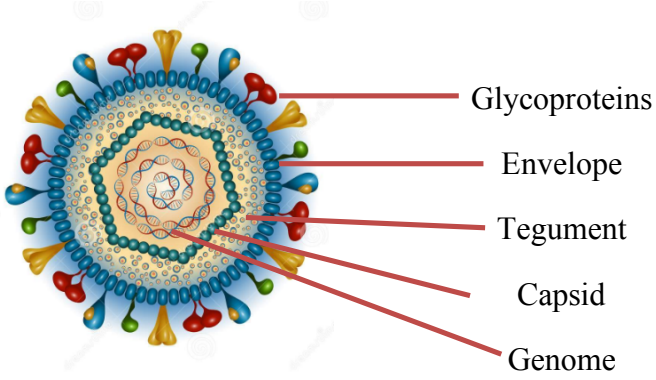

Figure 1. Morphology of alphaherpesviruses. *Mature (fully assembled) herpesvirus particles contain four morphologically distinct elements: the genome, capsid, tegument and envelope.*

Alphaherpesvirus genomes are linear and double stranded. Circularization of DNA occurs immediately after the viral DNA becomes released from the capsid into the nucleus of the infected cell (Strang and Stow, 2005). The genome length may differ between alphaherpesviruses (Parsons et al., 2015). These differences are mainly due to the variable copy numbers of terminal and internal repeat sequences (Roizman, 1979). Alphaherpesvirus genomes have two unique regions, intermitted and flanked by reiterated DNA sequences (Ziemann et al., 1998). For instance, PrV has a classical arrangement of varicelloviruses with one unique long (UL), one internal repeat (IR), one unique short (US) and one terminal repeat (TR) sequence. In the past, 70 different genes of PrV were identified (Pomeranz et al., 2005). Among these genes, 11 encode viral surface glycoproteins that are involved in virus attachment, cell penetration and egress, cell-to-cell spread, pathogenicity and virulence (Table 2). These and most other genes have homologs in other related alphaherpesviruses (Pomeranz et al., 2005).

Table 2. *Alphaherpesviruses glycoprotein functions*

Name	Gene	Proposed function(s)
gB	UL27	Viral entry (fusion); cell-cell spread
gC	UL44	Viral entry (virion attachment); binds to heparan sulfate
gD	US6	Viral entry (cellular receptor binding protein)
gE	US8	Cell-cell spread; complexed with gI; C-terminus interacts with UL49; protein sorting in axons
gG	US4	Unknown
gH	UL22	Viral entry (fusion); cell-cell spread; complexed with gL
gI	US7	Cell-cell spread; complexed with gE
gK	UL53	Viral egress (secondary envelopment); gK/UL20 inhibit glycoprotein-mediated membrane fusion
gL	UL1	Viral entry (fusion); cell-cell spread; membrane anchored via complex with gH
gM	UL10	Inhibits glycoprotein-mediated membrane fusion; C terminus interacts with tegument protein UL49; complexed with gN
gN	UL49.5	Immune evasion (TAP inhibitor); complexed with Gm

1.1.2 Phylogenetic relationship between alphaherpesviruses

Phylogenetic analysis of herpesviruses is well described nowadays. These studies have generated a tree that is well resolved and robust by primarily concatenated alignments of amino acid sequences from a set of up to eight core genes (McGeoch et al., 2006). Within these analyses, it is well know that PrV is found to be the closest relative of BoHV1 and 5 (Ros and Belak, 1999). The tree's structure allowed the addition of data for more species as they became available. In 2016, a full genome sequence of CaHV1 was reported and a phylogenetic analysis was performed. The

analysis was based on UL30 genes of CaHV1 and some other related herpesviruses (Figure 2). It showed that CaHV1 is most related to FeHV1 and then to equine herpesviruses (Papageorgiou et al., 2016).

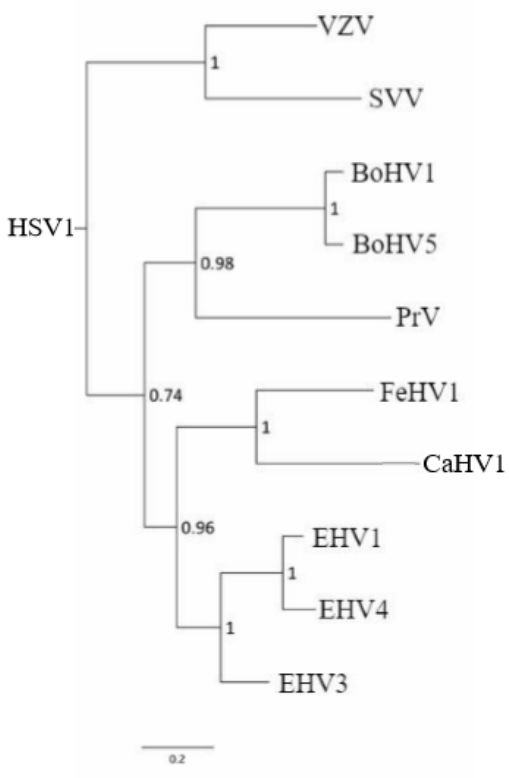

Figure 2. Phylogenetic tree of varicellovirus DNA polymerases (based on UL30) (Papageorgiou et al., 2016). *The tree was rooted on HSV1, which is a member of genus Simplexvirus. Bootstrap values are indicated at nodes as fractions. The scale bar indicates substitutions per amino acid residue.*

1.2 Replication cycle of alphaherpesviruses

An overview of the alphaherpesvirus replication cycle is described in Figure 3.

1.2.1 Entry

The replication cycle of an alphaherpesvirus starts with the binding of the virus to a cellular receptor on a permissive cell. Some cellular surface receptors and viral

glycoproteins have been associated with this process. gD is the main HSV receptor-binding protein. It binds three classes of receptors: herpes virus entry mediator (HVEM), a member of the TNF receptor family; nectin-1 and nectin-2, cell adhesion molecules of the immunoglobulin superfamily; and 3-O-sulfated heparan sulfate (Connolly et al., 2011, Spear et al., 2000). In addition to gD, gB can bind to paired immunoglobulin-like type 2 receptor alpha (PILRα) and this interaction can trigger viral fusion in the presence of gD (Connolly et al., 2011). Besides, two recently-identified receptors also have been shown to interact with gB and trigger HSV-1 entry: non-muscle myosin heavy chain IIA (NMHC-IIA) and myelin-associated glycoprotein (MAG), a protein expressed on neural tissues (Connolly et al., 2011). Human nectin-1 and nectin-2, but not HVEM or 3-O-sulfated heparan sulfate, could mediate entry of PrV into CHO cells, with nectin-1 being the most effective (Pomeranz et al., 2005; Spear et al., 2000). Alphaherpesvirus entry into cells requires a multipartite fusion apparatus made of gB, gD and gH/gL (Krummenacher et al., 2013). Generally, the virus attaches to cell membranes by the interaction of gC with heparan sulfate proteoglycans (Rue and Ryan, 2003). Next, gD contacts with a cellular receptor to attain a stable binding (Krummenacher et al., 2013).

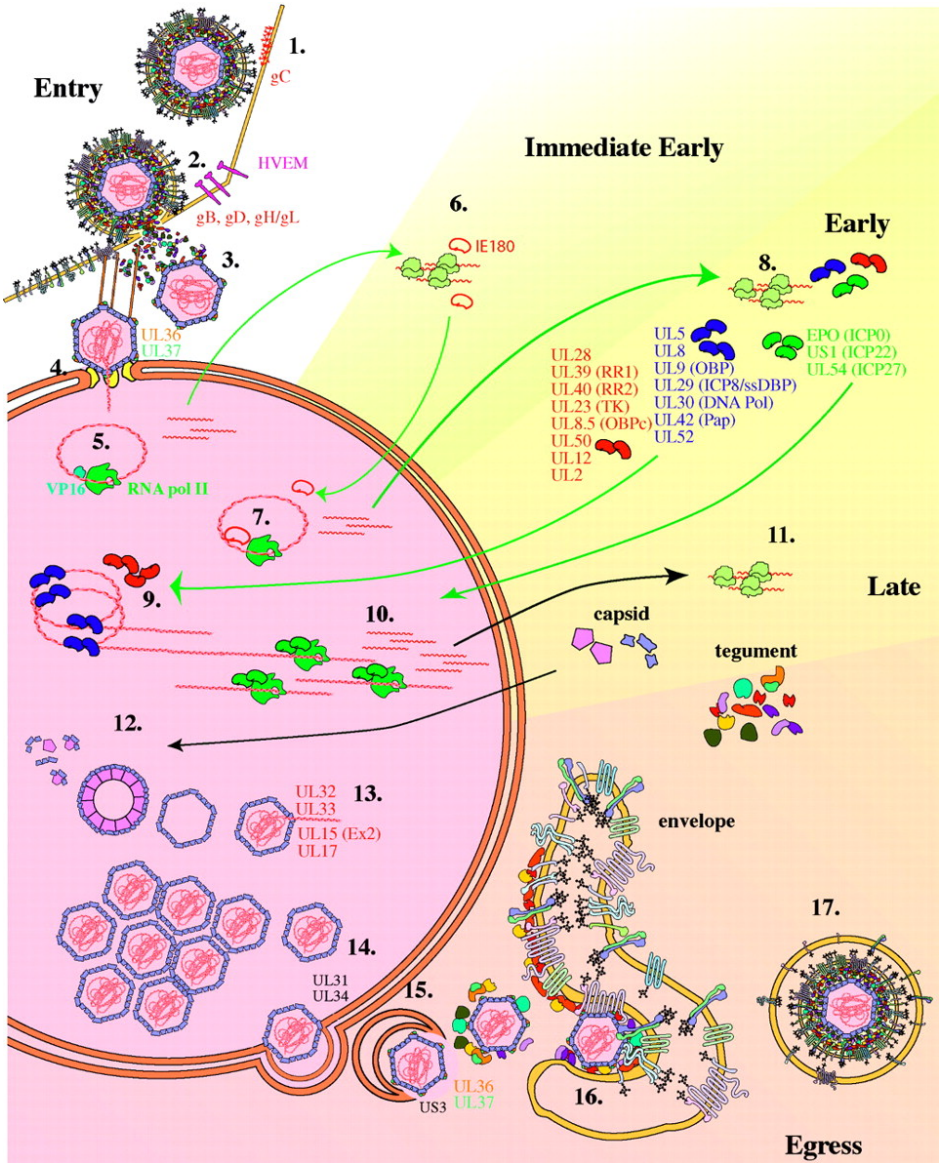

Figure 3. Productive replication cycle of PrV (Pomeranz et al., 2005). *1. Entry starts with attachment or binding of the virus particle to the cell surface: interaction between gC in the virion envelope and heparan sulfate on the surface of the cell. 2. The next steps of entry require gD, gB, gH, and gL. 3. The capsid and tegument proteins are released into the cell. 4. The capsid and tightly bound inner tegument proteins are transported along microtubules to the cell nucleus. 5. The VP16 tegument protein localizes to the nucleus independent of the capsid and transactivates cellular RNA polymerase II transcription of the only immediate-early protein of PRV, the HSV ICP4 homolog IE180. 6. The newly produced IE180 protein is transported back to the nucleus. 7. There, it transactivates RNA polymerase II transcription of the early genes. 8. Early proteins fall into two main categories. 9. Seven of*

these proteins (UL5, UL8, UL9/OBP, UL29/ssDNABP, UL30/DNA Pol, UL42/Pap, and UL52) (shown in blue) are essential for replication of the viral DNA. 10. The second category comprises three proteins (EP0, US1, and UL54) thought to act as transactivators of transcription. 11. Onset of DNA synthesis signals the start of the late stage of the PRV replication cycle and synthesis of true late proteins. 12. The capsid proteins are transported to the nucleus. 13. The mature capsid is composed of five proteins (UL19/VP5, UL18/VP23, UL25, UL38, and UL35). The product of the UL6 gene acts as a portal for insertion of the genomic DNA. 14. The fully assembled nucleocapsid buds out of the nucleus, temporarily entering the perinuclear space. This process involves the products of the UL31 and UL34 genes along with the US3 kinase. 15 and 16. The nucleocapsid (15) loses its primary envelope and (16) gains its final envelope by associating with tegument and envelope proteins and budding into the trans-Golgi apparatus. 17. The mature virus is brought to the cell surface within a sorting compartment/vesicle derived from the envelopment compartment.

1.2.2 Replication and transcription

Upon nuclear entry, the linear genome circularizes. Afterwards, transcription starts immediately and gene expression happens in a cascade manner. Alphaherpesvirus genes belong to three categories that are sequentially transcribed: immediate-early (IE), early (E) and late (L) genes (Nicoll et al., 2012). After entry in the nucleus, IE genes are transcribed by using the host nuclear machinery (Nauwynck et al., 2007). For PrV, the only IE gene is IE 180. IE180 protein, expressed in the cytoplasm, is transported back to the nucleus (Pomeranz et al., 2005). The E gene products are formed which mainly play a role in nucleotide metabolism and DNA synthesis. L genes mainly encode structural proteins, such as capsid, tegument and envelope proteins (Lehman and Boehmer, 1999).

1.2.3 Assembly and release

In the nucleus, capsid precursors assemble by the interaction of pUL19 and pUL6 with a scaffold composed of the conserved pUL26 and pUL26.5 proteins (Singer et al., 2005; Walters et al., 2003). At this stage, individual genome copies enter into pre-formed capsids through a nuclear pore complex (Zeev-Ben-Mordehai et al., 2015). Afterwards, the mature nucleocapsid moves out of the nucleus and reaches the cytoplasm via primary envelopment and de-envelopment at the inner and outer nuclear membrane, respectively. At the trans-Golgi network, these capsids are packaged into infectious particles. Then, these infectious particles are transported to the cell surface by Golgi-derived vesicles. These particles can be released by exocytosis or cytolysis or cell-to-cell contact and cell fusion (Owen et al., 2015a).

1.3 Pathogenesis of alphaherpesviruses

Horizontal transmission of alphaherpesviruses in animals occurs mainly via direct contact and to a lesser extent, via aerosol and semen. Vertical transmission is also possible. General features of alphaherpesviruses and current knowledge on FeHV1, CaHV1 and PrV are described in the following paragraphs, since they are the viruses examined in this thesis.

1.3.1 Feline herpesvirus 1 (FeHV1)

Most cats are exposed to FeHV1 during their lifetime. The virus can survive in the environment and on objects for several days. It is easily inactivated by disinfectants, antiseptics and detergents. The virus can be transmitted to other cats via ocular, oral and nasal secretions. Especially respiratory secretions are causing infections via sneezing, contaminated fomites and unhygienic handling practices.

The viral primary infection mainly occurs after 8 weeks of age, since maternal antibodies decline at this time (Gould, 2011). Epithelial cells of nasal mucosa, conjunctiva and tonsils are the preferential primary replication sites of the virus

(Gould, 2011). After several days post infection, ocular and respiratory problems may be observed. Conjunctivitis and keratitis are characterized by the formation of punctate and dendritic epithelial ulcers. It has been shown that the epithelial ulcers might persist for up to 24 days upon experimental inoculation (Nasisse et al., 1989).

Upon primary infection, FeHV1 establishes a lifelong latency in sensory neurons of the trigeminal nerve. The viral genome persists in the cell nuclei of the trigeminal ganglia, and latency associated transcripts (LATs) are produced in this phase (Ohmura et al., 1993).

Latent FeHV1 can be reactivated by a compromised immune system of the host, leading to recrudescent clinical disease. This can occur spontaneously or in association with various stressors including systematic treatment with corticosteroids, co-infections with other agents, and by mental stress due to environment changes (Gaskell and Povey, 1977). Although the molecular mechanism of viral reactivation is unknown, it is clear that the virus migrates from the neuronal cell body, through sensory axons to epithelial tissues and results in clinical or subclinical disease.

1.3.2 Canine herpesvirus 1 (CaHV1)

CaHV1 is associated with reproductive failure and causes a fetal hemorrhagic disease in neonatal puppies. Reproductive failure due to CaHV1 is characterized by infertility, resorption, abortion, stillbirth, delivery of poorly developed and compromised neonates, or neonatal death (Evermann et al., 2011). Pregnant dogs may deliver weak or stillborn puppies after a CaHV1 infection at midgestation or later. Although puppies might seem normal at parturition, they may die later. Since maternally derived immunity protects the puppies during the first weeks of life, virus infectious diseases are not observed in subsequent litters (Decaro et al., 2008).

At less than two weeks of age, susceptible puppies infected with CaHV1 might result in a fatal generalized necrotizing and hemorrhagic disease. In contrast, older puppies and adult dogs infected with CaHV1 often do not show any clinical sign (Carmichael et al., 1965). In older dogs infected with CaHV1, the infection seems to be limited to the upper respiratory organs. Only a mild rhinitis, pharyngitis and tracheobronchitis may be observed (Appel et al., 1969; Okuda et al., 1993).

CaHV1 can be transmitted by direct or indirect contact between animals, primarily through contaminated nasal secretions and aerosols. Similar with FeHV1 infections in cats, reactivation of latent virus may be provoked by environmental or social stress or, experimentally, by immunosuppressive drugs (corticosteroids) or antilymphocyte serum (Burr et al., 1996). Latent virus persists in the trigeminal ganglia and other sites, such as lumbosacral ganglia, tonsils, and parotid salivary glands. Latently infected dogs represent a source of infection for susceptible animals, and this is of particular concern in breeding dogs that can ensure CaHV1 transmission through genital secretions (Decaro et al., 2008).

1.3.3 Pseudorabies virus (PrV)

The natural host of PrV is the pig, but the virus may also infect cattle, sheep, horses, cats and dogs. In many species, the virus causes a fatal encephalitis except its natural host, pigs. PrV has been eradicated from domestic pigs in many countries, but it remains enzootic in free-ranging animals which may form a dangerous virus reservoir (Wozniakowski and Samorek-Salamonowicz, 2015).

The respiratory tract, especially the upper respiratory tract, is the main entry site for the virus. After infection in the respiratory tract, the virus may develop a systemic infection through the lymphatic system and blood circulation. In viremic pigs, a low number of cell-associated and cell-free virus can be detected (Nawynck and Pensaert,

1995; Wittmann et al., 1980). In pregnant sows, mononuclear blood cells infected by PrV may spread the infection, leading to reproductive disorders (Nauwynck and Pensaert, 1992). In the first trimester of pregnancy, sows infected with PrV will usually reabsorb the fetuses in utero. In the second and third trimester of pregnancy, the typical result of the infection is abortion, stillbirths, or weak piglets that die within 2 days after birth (Pomeranz et al., 2005).

Infections in neonatal piglets cause neurological signs such as vomiting, scratching, trembling, ataxia, paralysis and convulsions. The infected piglets may die from severe encephalomyelitis. When a PrV infection occurs during the first two weeks of age, neonatal piglets are most susceptible with a mortality that reaches 100%. The mortality rate decreases to 50% during the third and fourth week of age (Nauwynck, 1997). PrV establishes latency mainly in neurons of the trigeminal ganglion (Rziha et al., 1986).

PrV reactivation in animals normally requires a modulation of the immune system, e.g. by a stressful experience (Meier et al., 2015). Identified stressors increasing PrV activity include treatment with immunosuppressive agents, concomitant disease conditions, transport, poor animal husbandry and farrowing (Pomeranz et al., 2005).

1.4 Characteristics of ocular, respiratory and genital mucosae

Pathogens face a range of barriers that hamper their invasion during primary contact with susceptible hosts. At mucosae, mucus, epithelium, basement membrane and lamina propria are firm barriers that alphaherpesviruses need to cross prior to cause a generalized infection. The general structure and components of these barriers will be described briefly below.

1.4.1 Ocular mucosa

The research in this thesis was mainly conducted on feline ocular mucosa. The ocular mucosa consists of corneal and conjunctival mucosae. The two mucosae are close to each other. The cornea mucosa is the clear front surface of the eye. It is avascular and gets its nutrition from tears on the outside, aqueous fluid on the inside, and from blood vessels located at the periphery. The conjunctival mucosa extends from the limbo-corneal junction of the globe to the mucocutanous junction of the eyelid, covering the exposed surface of the ocular globe and lining the inner surface of the eyelids. It is richly vascularized, variably pigmented, which is different from the corneal mucosa.

1.4.1.1 Corneal mucosa

The cornea has the same function and structure in cat eyes as in human eyes. The corneal mucosa is located at the anterior surface of the eyeball. For cats, there is no significant differences between central and peripheral corneal thickness (Gilger et al., 1993).The cornea mucosa is composed of five layers: epithelial layer, Bowman's layer, stroma, Descemet's membrane and endothelial layer (Casaroli-Marano et al., 2015) (Figure 4). The basement membrane is located between the epithelial layer and Bowman's layer. The Bowman's layer (anterior limiting lamina), stroma (substantia propria), Descemet's membrane (posterior limiting lamina) are corresponding to the lamina propria of other mucosal tissues.

Mucus - The normal airway mucus provides important immune functions by detoxifying noxious molecules and by trapping and removing pathogens and particulates from the airway via mucociliary clearance (Voynow and Rubin, 2009). The mucus layer is composed predominantly of mucin glycoproteins. The mucin glycoproteins help the spread of the aqueous layer across the eye to ensure that the eye remains wet. In the apical surface cells of corneal epithelium, MUC1 and MUC16

proteins are found. MUC4 is only located in the central part of the cornea (Gipson, 2004).

Corneal Epithelium - The outermost layer of the cornea is its epithelium. The epithelium is 5-7 cell layers thick, and is composed of a single layer of basal cells and cell layers of non-keratinized, stratified squamous epithelial cells (wing cells and superficial cells) (Zieske et al., 1994). The basal cells of the central cornea are more mature-looking than the basal cells of all other stratified squamous epithelia (Srinivasan and Eakins, 1979). The basal cells from the limbo-corneal epithelium are proposed to be the stem cells of the corneal epithelium (Lavker and Sun, 2000; Sun and Lavker, 2004). The wing cell layer lies between the basal cell layer and the superficial cell layer. These cells are progressively displaced anteriorly. They eventually become superficial cells, which are eventually desquamated from the corneal surface (Masters and Thaer, 1994). The superficial cells are terminally differentiated, flattened cells. Superficial cells are held together by tight junctions, to form an effective barrier against fluid loss and pathogen penetration. The corneal epithelium is completely renewed every 5 to 7 days.

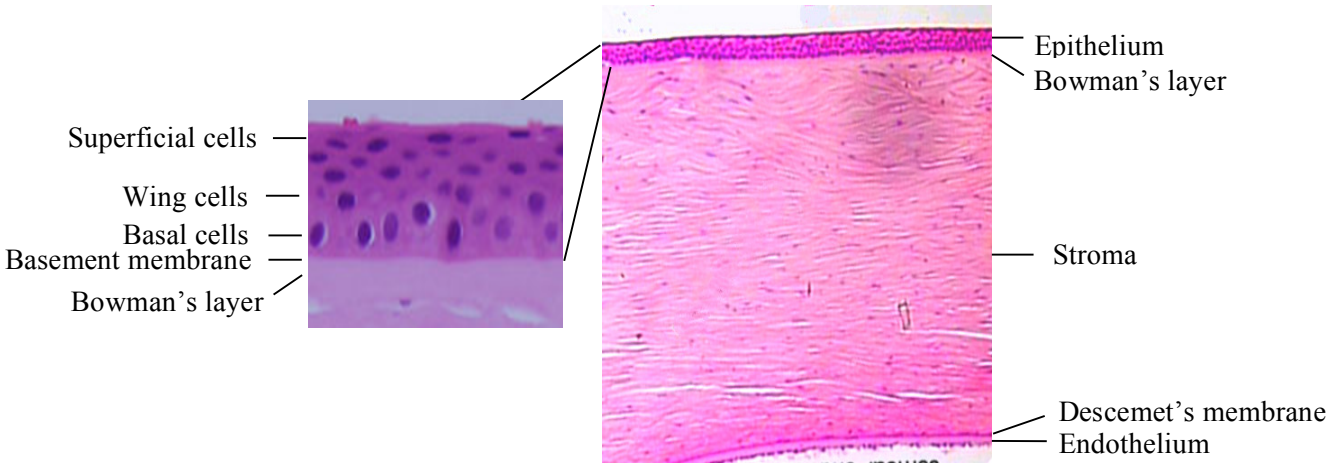

Figure 4. Histologic full-thickness section of a normal human cornea. *The cornea consists of 5 layers: the epithelium, Bowman's layer, stroma, Descemet's membrane and endothelium. The epithelium has 5-7 cell layers, is composed of superficial cells, wing cells and basal cells.*

The epithelial basement membrane is lying underneath the basal cell layer. The Bowman's layer is a smooth, acellular membrane, located between the superficial epithelium and the stroma in the cornea of the eye. The stroma consists of collagen fibril lamellae. Descemet's membrane is a thin layer of tissue. The endothelium is a single layer of cells on the inner surface of the cornea. Image adapted from images.misssionforvisionusa.org

Basement membrane - The corneal basement membrane is positioned between the basal epithelial cells and the Bowman's layer. The corneal basement membrane is different from that in other tissues (Torricelli et al., 2013). This highly specialized extracellular matrix anchors epithelial cells to the stroma and provides scaffolding during migration, differentiation, and maintenance of the differentiated epithelial phenotype (Torricelli et al., 2013). It undergoes a considerable change during embryonic development and appears to have a regional heterogeneity from the center to outer limbus (Torricelli et al., 2013). The corneal basement membrane is associated with many inherited and acquired corneal diseases (Torricelli et al., 2013). In general, the primary components of the basement are collagens, laminins, heparin sulfate proteoglycans and nidogens. The functions of these components will be discussed in 1.4.2.

Lamina propria - Bowman's layer (anterior limiting lamina), stroma (substantia propria), Descemet's membrane (posterior limiting lamina) are corresponding to the lamina propria of other mucosal tissues (conjunctival mucosa, tracheal mucosal et al.).

The Bowman's layer is located between the epithelial basement membrane and the anterior corneal stroma (Lagali et al., 2009). The Bowman's layer does not correspond to the basement membrane, and it is the anteriormost part of the corneal stroma (Pavelka and Roth, 2010). It is a smooth, acellular, non-regenerating layer. Major components of the Bowman's layer are collagen fibrils and proteoglycans (Yadav et al., 2012). According to Hayashi and co-workers (Hayashi et al., 2002), the cat cornea

has a Bowman's layer which is thinner than the Bowman's layer in the human eye. The Bowman's layer have no critical function in corneal physiology, and may be a visible indicator of stromal-epithelial interactions (Wilson and Hong, 2000). In a previous study, the layer was postulated as a barrier that prevents traumatic contact with the cornea stroma. It is highly associated with stromal wound healing and the restoration of anterior corneal transparency at the morphological level (Lagali et al., 2009). In addition, the Bowman's layer can serve as a barrier to protect the nerve plexus (Lagali et al., 2009).

The corneal stroma is avascular and has a relatively low keratocyte density. It is the thickest layer of the cornea. It contains collagen fibers and keratocytes. The stromal fibrils are further organized into bundles, or lamellae, and the lamellae course lines the full width of the cornea without a break (Bron, 2001). The keratocytes occupy 10% of the stroma. Descemet's membrane is a thin layer of tissue that forms the deepest layer of the stroma. It separates the stroma from its innermost cellular layer, the endothelium, which consists a single layer of low cuboidal cells. The major components of Descemet's membrane are collagen type IV fibrils and collagen type I fibrils (Dua et al., 2013).

1.4.1.2 Conjunctival mucosa

The feline conjunctiva is structurally similar to the human. It is divided into three parts: the palpebral (tarsal) conjunctiva, the bulbar (ocular) conjunctiva and the fornix conjunctiva (Figure 5a). The palpebral conjunctiva starts at the mucocutaneous junction at the eyelid margin and is firmly adherent to the tarsal plates. The fornix conjunctiva is loose and folded, and it is the junction between the bulbar and palpebral conjunctivas. The bulbar conjunctiva lines the anterior sclera.

Mucus - The conjunctival mucosa produces mucus to keep the eye surface moist and protected. The mucin glycoproteins are the major molecular constituents of normal mucus. They are large, heavily glycosylated proteins with a defining feature of tandemly repeating sequences of amino acids (Voynow and Rubin, 2009). In conjunctival epithelium, MUC1, MUC4 and MUC16 are widely distributed. In addition, MUC5AC, a gel-forming mucin, is expressed by goblet cells of the conjunctiva (Gipson, 2004).

a b

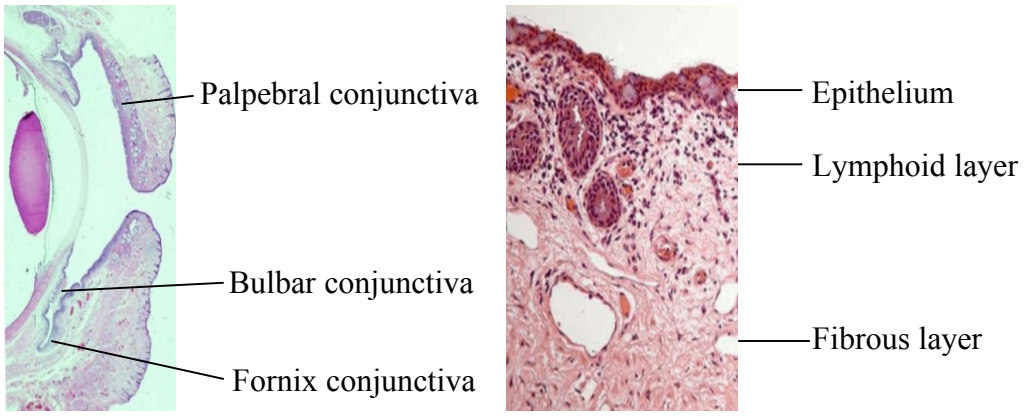

Figure 5. Vertical section of the human conjunctiva (a) and histologic section of a human conjunctiva (b).*The different regions of the conjunctiva are shown on the left (a). The conjunctival submucosa has two layers: lymphoid and fibrous (b). The conjunctival epithelium has 2-3 cell layers. The lymphoid layer consists of a fine network of connective tissue with lymphocytes. The fibrous layer contains conjunctival blood vessels and nerves. Image adapted from http://www.images.missionforvisionusa.org/anatomy/2005/11/ conjunctiva-answers.html website and https://entokey.com/ pathology-of-conjunctiva/ website with courtesy of Dr. Tatyana Milman*

Epithelium - The conjunctival epithelium is thinner than the corneal epithelium. The cell conjunction is less tight in the conjunctival epithelium than in the corneal epithelium. It is composed of a non-keratinized, stratified squamous epithelium with

goblet cells, as well as a stratified columnar epithelium. The morphology of the conjunctival epithelium varies from region to region. The fornix and bulbar epitheliums consist of 3 layers: the superficial layer with cylindrical cells, the middle layer with polyhedral cells and the deepest layer with cuboidal cells. The fornix conjunctival epithelium holds the highest density of goblet cells (Wei et al., 1993). The palpebral conjunctival epithelium does not have the middle layer.

In the conjunctiva, both epithelial cells and goblets cells synthesize mucins to provide a barrier against the external environment (Dartt and Masli, 2014). Stratified squamous cells synthesize mucins that are trafficked to the surface. Goblet cells can also synthesize and secrete a high molecular weight mucin MUC5AC (Gipson, 2004). MUC5AC is very protective for the ocular surface against chronic inflammatory diseases.

Basement membrane - Most basement membrane components have the same distribution pattern in the conjunctival mucosa and the corneal mucosa. Only alpha subchains of type IV collagen show a different distribution pattern in the two tissues (Fukuda et al., 1999).

Lamina propria The conjunctival submucosa or substantia propria consists of two layers (Figure 5b): lymphoid and fibrous. Numerous lymphocytes, mast cells, plasma cells, and neutrophils are present within this connective tissue layer. The deepest fibrous layer contains the nerves and vessels providing innervation and blood supply to the conjunctiva (Giuliano et al., 2002; Singh, 2003). Contrary to the cornea where blood supply is totally lacking, voluminous blood supply exists in the conjunctiva (Friedenwald, 1951).

1.4.2 Respiratory mucosa

We will focus in this section on the tracheal mucosa, because is the main entry site for alphaherpesviruses. The mucus, epithelium, basement membrane and lamina propria of the trachea will be described below.

1.4.2.1 Tracheal mucus

The mucus layer of trachea epithelium is mainly produced by goblet cells, submucosal mucous and serous glands. These glands are complex structures that normally produce mucus in response to a wide range of different stimulation (Ianowski et al., 2007). The thickness of the layer is different between species, location and host health status. In the upper respiratory tract, the major mucins are MUC5AC and MUC5B, although more types were described (Corfield, 2015).

1.4.2.2 Tracheal epithelium

The ciliated pseudostratified epithelium of the nose/trachea is composed of morphologically distinct epithelial cell types, including basal cells, ciliated cells, goblet cells and brush cells. In the ciliated pseudostratified columnar epithelium, basal cells are the stem or progenitor cells for the epithelium and differentiate to form the other cells during repair after an injury. Ciliated cells are the main cell type in the respiratory epithelium. These cells provide the mechanism for moving the mucus blanket. Goblet cells are a type of columnar epithelial cells that secrete mucus (Yaghi and Dolovich, 2016). Brush cells are characterized by the presence of a tuft of blunt, squat microvilli on the cell surface, and express components of the taste-signaling cascade and, consequently, are considered to act as chemosensory cells (Kaske et al., 2007). Furthermore, some other cell types, like immune cells and inflammatory cells migrate to and remain within the respiratory mucosa. Immune cells include mast cells, intraepithelial lymphocytes, dendritic cells and macrophages (Knight and Holgate,

2003). Inflammatory cells refer to neutrophils, macrophages, monocytes, eosinophils or basophils that take part in the inflammatory response to a foreign substance.

1.4.2.3 Tracheal basement membrane

Basement membranes are conserved forms of extracellular matrix (ECM), which are located at the basal side of the epithelium. The thickness of a standard basement membrane is less than 100 nm (Halfter et al., 2015). The basement membrane forms an organized scaffold to provide structural support to the tissue, and also offer functional input to modulate cellular function (LeBleu et al., 2007). The basement membrane determines the polarity of the epithelium and is a barrier for the epithelial cell migration. Proliferating cells are close to the basement membrane and their daughter cells are migrating at the upper side (Watt, 1984). Cells interact with the basement membrane by binding basement membrane components through basal cell surface integrin receptors (Lee and Streuli, 2014). The basement membrane consists of a core set of proteins, including laminin, type IV collagen, the glycoprotein nidogen and perlecan and agrin (Figure 6).

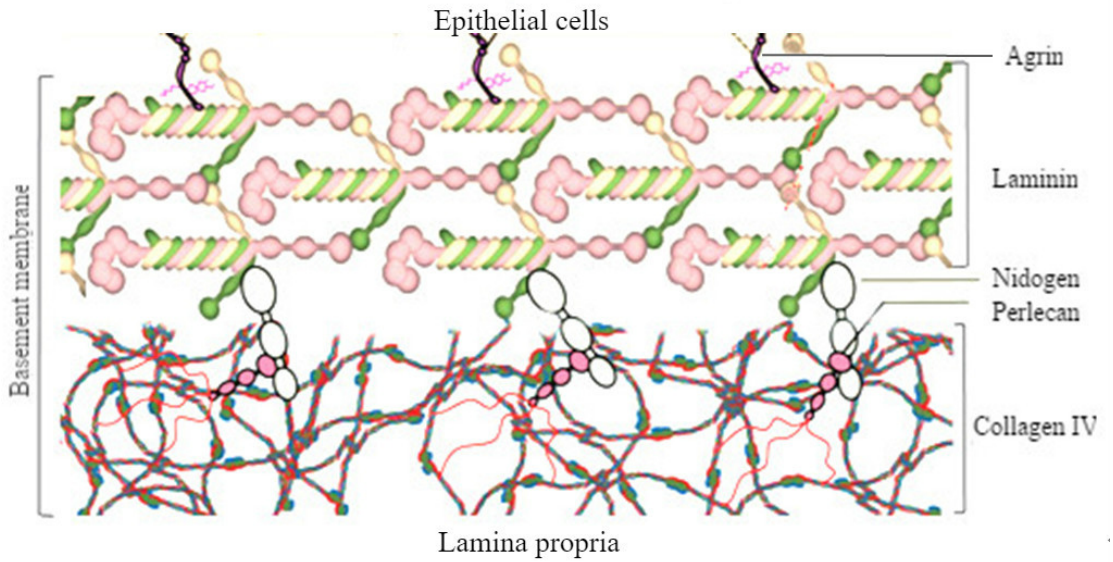

Figure 6. General structure of the basement membrane. *Epithelial cells secrete at their basal side ECM components to synthesize the basement membrane that functions as a support/platform and anchorage for the cells. The basement membrane consists of laminin, collagen IV, nidogens and the heparin sulphate proteoglycans (HSPG) perlecan and agrin. Figure adapted from (Singh et al., 2012).*

Laminin is a heavily glycosylated protein with a 12-27% carbohydrate content often present as complex-type carbohydrates (Terres et al., 2003). The laminin molecule is composed of one α, one β, and one γ polypeptide chain. Up till now, five α, four β, and three γ variants were reported. The molecular weight of the laminin is variable from 400 to 900 kDa (Yao, 2016). Laminins are contributors to basement membrane assembly. The basement membrane diversity arises from the variety in laminin isoforms, resulting in highly tissue-specific basement membrane architecture and function (Horejs, 2016).

Collagens are the most abundant proteins in mammals. They are the main component of connective tissue and are associated with maintaining tissue architecture, cell adhesion, angiogenesis and development (Myllyharju and Kivirikko, 2004). The major collagen in the basement membrane, collagen type IV, consists of 6 different kinds of α-chains (α1–α6), which form three heterotrimers (α1α1α2, α3α4α5, α5α5α6) (Horejs, 2016). Among those heterotrimers, α1α1α2 is observed in the basement membrane of almost all tissues, while the other two have somewhat limited tissue distributions (Khoshnoodi et al., 2008).

Nidogen interconnects the laminin and collagen networks with the help of perlecan and thus forms a rigid basement membrane (Figure 6). Nidogens are the smallest glycoproteins in the basement membrane, with a size around 150 kDa (Halfter et al., 2015). Two types of nidogens (nidogen-1 and 2) have been identified. Both nidogens

can bind with collagens I and IV. Nidogen-2 binds to laminin and promotes high-affinity binding of nidogen-1 (Kohfeldt et al., 1998; Timpl et al., 1983).

Perlecan, agrin and collagen XVIII are heparan sulfate proteoglycans in the basement membrane (Halfter et al., 2015). Perlecan is well studied while the other proteoglycans are not. Collagen XVIII is a component of basement membranes with the structural properties of both a collagen and a proteoglycan (Marneros and Olsen, 2005). With the cooperation of nidogen, perlecan is responsible for a non-covalent linkage of the collagen and laminin networks (Breitkreutz et al., 2013). Agrin functions as a bridge between laminin α chains and integrins that interact with the coiled-coil region in the β-chain (Singh et al., 2012).

1.4.2.4 Lamina propria

The lamina propria is located underneath the basement membrane. Functionally, the lamina propria regions from the upper respiratory tract and female reproductive tract are the mucosal immunity effector sites, while local and regional draining lymph nodes and mucosa associated lymphoid tissue are the inductive sites (McGhee and Fujihashi, 2012). The lamina propria contains collagenous elastic fibers, fibroblasts, lots of lymphocytes, macrophages, occasional mast cells, and eosinophils. The immune cells in the lamina propria play a major role in the local immunity (Uematsu et al., 2008). Myofibroblasts, a cell type between fibroblasts and smooth muscle cells, play a key role in inflammation and wound healing responses. In some conditions, myofibroblasts are able to release cytokines and chemokines (Wiseman et al., 2003).

1.4.3 Genital mucosa

The research in this thesis was mainly conducted on genital epithelium of the canine vagina. Layers can be found within vaginal mucosa: mucus, epithelium, basement membrane and lamina propria.

1.4.3.1 Genital mucins

Similar with the ocular and respiratory tract, the genital tract is also covered by a thick mucus layer. Mucin types are differentially expressed during the different stages of the oestrous cycle, which is also related to fluctuations in sex steroid hormones (Cortes et al., 2012). In humans, the vaginal epithelium expresses mucins 1 and 4, and vaginal expression of MUC4 seems patchy (Gipson et al., 1997)

1.4.3.2 Vaginal epithelium

The lower female reproductive tract, consisting of the vagina and ectocervix, is lined with a non-keratinized stratified squamous epithelium attached to a basement membrane. The different cell types in the epithelium layers are basal cells, parabasal cells, intermediate cells and superficial cells (Figure 7). Basal cells are round cells with small nuclei, and are considered as the stem or progenitor cell population (Purkis et al., 1990). Parabasal cells, another type of progenitor cells, are also round with small nuclei. They are the most immature cells in the vaginal epithelium (Brizzolara et al., 1999). In addition, they are important markers of intense inflammation. This cell population increases during vaginitis (Utian, 1975). Intermediate cells can be differentiated in large (with glycogen) and small (without glycogen) cells (Post, 1985). During pregnancy and under the strong influence of progestins or androgens, these cells show a canoe or boat form and are called navicular cells (Dos Santos et al., 2017). Superficial cells show the greatest degree of maturation. They are polygonal in shape and distinctly flat, sometimes having the appearance of being rolled up (Anderson et al., 2014).

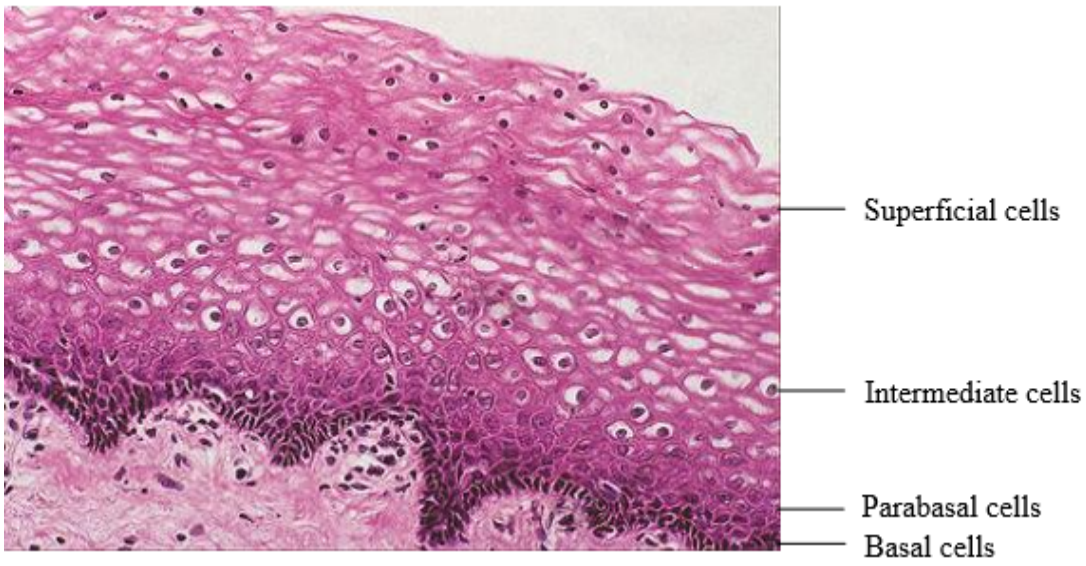

Figure 7. Histologic section of of the human vaginal epithelium. Vaginal epithelial cells are classified as superficial, intermediate, parabasal and basal cells. Image adapted from http://www.histology-world.com/photoalbum/displayimage.php

1.4.3.3 Genital basement membrane

Epithelia are separated from the underlying lamina propria by the basement membrane. The components of the vaginal basement membrane does not differ significantly from the non-reproductive skin and mucosa except the amnion placentae (Chi et al., 2010). A description of these components is discussed in 1.4.2.3.

1.4.3.4 Genital lamina propria

The vaginal mucosal lamina propria contains many elastic fibers as well as a dense network of blood vessels, lymphatic and nerve supply, but does not contain glands or mucosal muscular layer (Lorenzen et al., 2015). It is responsible for the support and nutrition of the vaginal lining and is fundamental for the architecture of the vaginal wall. The defensive cells in the lamina propria contain neutrophils, macrophages, lymphocytes, plasma cells, and mast cells. Neutrophils and macrophages may migrate from the lamina propria to the vaginal epithelium (Hussin et al., 2014).

1.5 Plasminogen activator-plasmin system

Many pathogens break extracellular matrix proteins of interstitial spaces and connective tissues by the use of many proteases or surface-bound plasminogen and matrix metalloproteinases recruited from the host (Singh et al., 2012). Proteases are enzymes that hydrolyse peptide bonds, and are necessary to degrade extracellular matrix (DeClerck et al., 2004). They are classified according to their catalytic activity: serine-, cysteine-, metallo- and aspartic peptidases. Previous studies demonstrated that serine protease activity is involved in PrV invasion through the basement membrane (Glorieux et al., 2011). The plasminogen activator-plasmin system is the principal serine protease mediating extracellular matrix degradation (Skrzydlewska et al., 2005). As a valuable candidate, some components of the system are expressed/found in epithelial cells and the extracellular matrix (Mehta and Shapiro, 2008). In this part, the detail of plasminogen activator-plasmin system will be discussed.

Plasminogen is the inactive zymogen form of plasmin, an enzyme that plays a crucial role in the dissolution of fibrin clots, the extracellular matrix and other key proteins involved in immunity and tissue repair (Law et al., 2013). Plasminogen is produced primarily by the liver, circulates in plasma at a high concentration (2 μM), and is also found at high concentrations in interstitial fluid (Hoover-Plow, 2010). Plasminogen is also present in tissues and organs (Raum et al., 1980; Zhang et al., 2002). Under physiological conditions, plasminogen is activated by tissue-type plasminogen activator (tPA) and urokinase-type plasminogen activator (uPA) via the classical cleavage mechanism (Verhamme et al., 2015) (Figure 8). Some other proteases, such as kallikrein, factors XIa and XIIa are also capable of functioning as plasminogen activators (Backes et al., 2000; Miles et al., 2003). Besides, the process of plasminogen activation is also controlled by inhibitors and their receptors (Castellino and Ploplis, 2005).

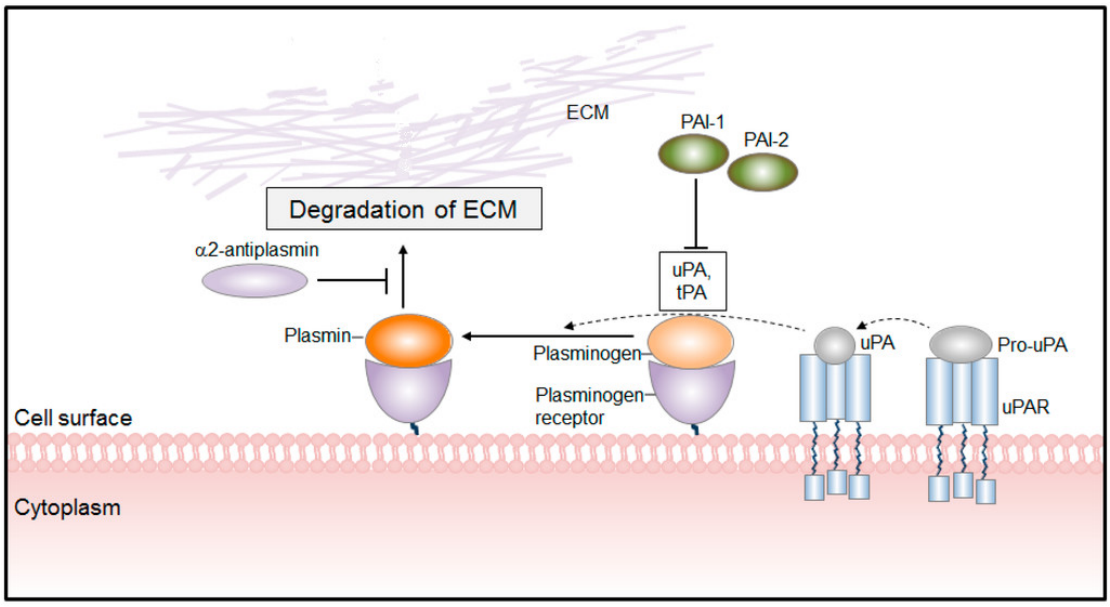

Figure 8. Schematic representation of the plasminogen activator-plasmin system digesting the extracellular matrix. *Plasminogen binds to its receptors and is subsequently converted to plasmin by plasminogen activators (uPA, tPA). The proteolytic activities of uPA and plasmin are antagonized by plasminogen activator inhibitor-1 and -2 (PAI-1, PAI-2) and by α2-antiplasmin, respectively. tPA is mainly antagonized by PAI-1. ECM, extracellular matrix. Image adapted from (Didiasova et al., 2014).*

1.5.1 Plasminogen and plasmin

There are two types of plasminogen: Glu-plasminogen and Lys-plasminogen. Glu-plasminogen, the circulating form of plasminogen, is a single-chain multidomain protien composed of 791 amino acids, which has seven different structural domains: an N-terminal pre-activation peptide (amino-terminal glutamic acid (Glu) plasminogen N-terminal peptide), 5 kringle domains and the C-terminal trypsin-like serine protease domain (Figure 9) (Law et al., 2012). Lys-plasminogen is a modified form of Glu-plasminogen, after removal of a 77-residue amino-terminal peptide by plasmin (Zhang et al., 2003). Lys-plaminogen can be activated to plasmin more readily than Glu-plasminogen.

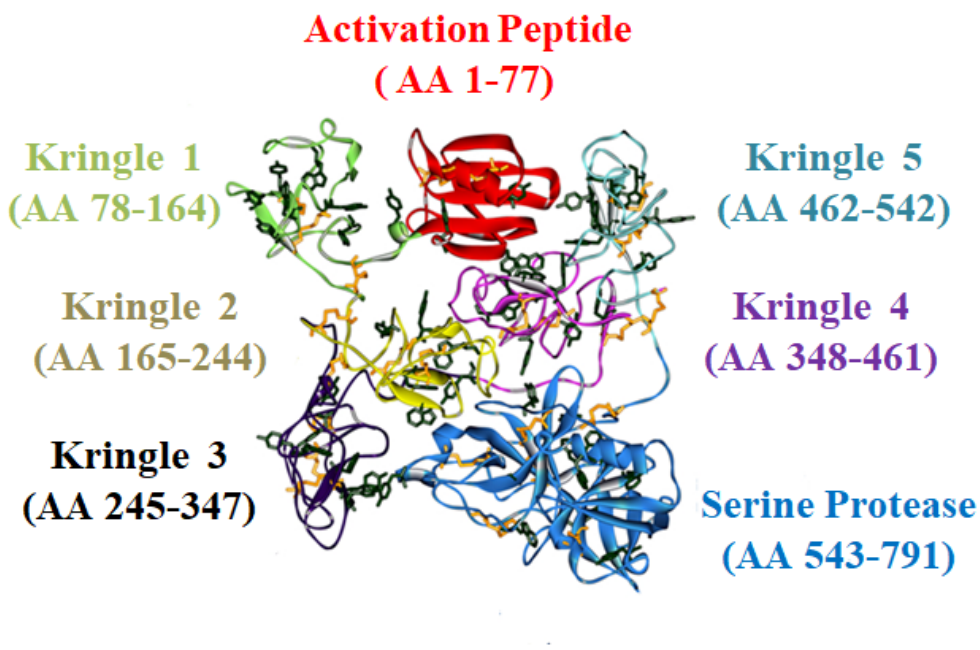

Figure 9. Full length native 3D structure of native human Glu-plasminogen. *The activation peptide, the 5 kringle domains, and the serine protease domain (where the catalytic site is located) are highlighted with different colors. After removal of a 77-residue amino-terminal peptide (AA 1-77, indicated in red), Glu-plasminogen is converted into Lys-plasminogen. The cleavage of the Arg561-Val562 peptide bond in plasminogen leads to the formation of plasmin. Image adapted from Correia et al. (2015).*

Kringle domains are autonomous protein domains that fold into large loops stabilized by 3 disulfide linkages. The kringle domains mainly help plasminogen binding to large substrates (bacterial proteins, fibrinogen and cell surface) and also to some small ligands. These kringle domains appear to function independently. When plasminogen kringles are formed in combination, it can inhibit cell migration (Castellino and Ploplis, 2005). Kringle domains are also found in other proteins of the fibrinolytic system, such as tPA, uPA, and in the contact pathway of coagulation protein, FXII (Gunzler et al., 1982; Magnusson et al., 1975).

The C-terminal trypsin-like serine protease domain, also known as the catalytic domain, contains the cleavage site for plasminogen activator. The cleavage of the Arg561-Val562 peptide bond in plasminogen leads to the formation of plasmin, which contains a heavy chain of 561 amino acid residues, disulfide linked to a light chain of 230 amino acid residues. The heavy chain consists of the activation peptide and 5 kringles. The activation peptide is called this way since cleavage of it (normally promoted by plasmin) from full-length Glu-plasminogen results in Lys-plasminogen that exists in a more relaxed conformation, making it more easy to become activated by plasminogen activators (Mauro et al., 2013). The plasmin light chain contains the carboxyl terminus of plasminogen, which comprises the catalytic domain that resembles that of the serine protease family (Bhattacharya et al., 2012). It is a compact molecule that can recruit adapter molecules. The catalytic triad of amino acids that define the serine protease activists consists of His603, Asp646, and Ser741 for human plasmin (Castellino and Powell, 1981).

Plasminogen can adapt two distinct conformations, termed closed and open, which highly influences its activation capability. The closed state (tight conformation) is a compact state seen in full-length plasminogen. In this conformation, plasminogen is poorly activated (Urano et al., 1987). uPA or tPA cannot easily activate the full-length plasminogen in its closed conformation. The lysine binding sites in the heavy chain are buried, which results in a functionally inactive molecule (Law et al., 2013). In case of binding to fibrin or the cell surface, full-length plasminogen switches into an open conformation (Law et al., 2013). This open conformation is more flexible. It is readily activated when the activation peptide is displaced from its kringle binding sites (Bhattacharya et al., 2012).

1.5.2 Plasminogen activators

Plasminogen activators (PAs) include physiological and non-physiological molecules. Two physiological PA have been recognized: tissue-type PA (tPA) and urokinase-type PA (uPA), which binds to a cellular uPA receptor (uPAR) (Lijnen et al., 1991; McCoy et al., 1991). Both uPA and tPA are weak proteolytic enzymes with the function to cleave plasminogen into the active serine protease plasmin, which results in a two-chain plasmin molecule that are connected by a single cysteine bridge. uPA seems to be the primary plasminogen activator in eukaryotic cell migration processes, and is recognized as a vital component for plasmin generation during cell migration and invasion, under physiological and pathological conditions (Fortenberry, 2013; Ghosh and Vaughan, 2012; Kindell et al., 2015). tPA is the main plasminogen activator in fibrinolysis, regulates airway disease and maintenance of vascular patency (Lijnen and Collen, 1995; Nassar et al., 2010). Besides, invasive pathogens have evolved plasminogen activators, such as streptokinase and staphylokinase. Neither streptokinase nor staphylokinase is an enzyme, which is different from tPA and uPA (Dahiya et al., 2005). Streptokinase and staphylokinase form a bimolecular 1:1 complex with plasminogen that in turn catalyzes the conversion of free plasminogen into plasmin (Dahiya et al., 2005). The activities of PAs are controlled by specific plasminogen activator inhibitors thereby restricting the generation of plasmin for extra cellular matrix (ECM) as well as intravascular fibrin degradation (Andreasen et al., 1986; Vassalli et al., 1984).

1.5.2.1 Tissue Plasminogen Activator (tPA)

tPA is a serine protease that is secreted in a single-chain, which contains five structural domains (Figure 10): the fibronectin finger, epidermal growth factor domain, kringle 1 and 2, and serine protease domain. The fibronectin finger domain, together with the kringle 2, provides tPA with a high affinity for fibrin (Banyai et al., 1983; Verheijen et al., 1986). A large serine protease catalytic domain is located at the carboxyl terminus, similar to uPA. The single chain tPA is cleaved at the Arg275-Ile276 bond by plasmin or kallikrein, creating a two-chain molecule held together through a single disulfide bond (Wallen et al., 1983). The heavy chain consists of a fibronectin finger, an epidermal growth factor domain and two kringle domains. The light chain is able to activate plasminogen, but requires the heavy chain for fibrin-binding and fibrin-stimulation. Both the single-chain and the two-chain forms of tPA are active, but the two-chain form has relatively higher proteolytic activity (Rijken et al., 1982).

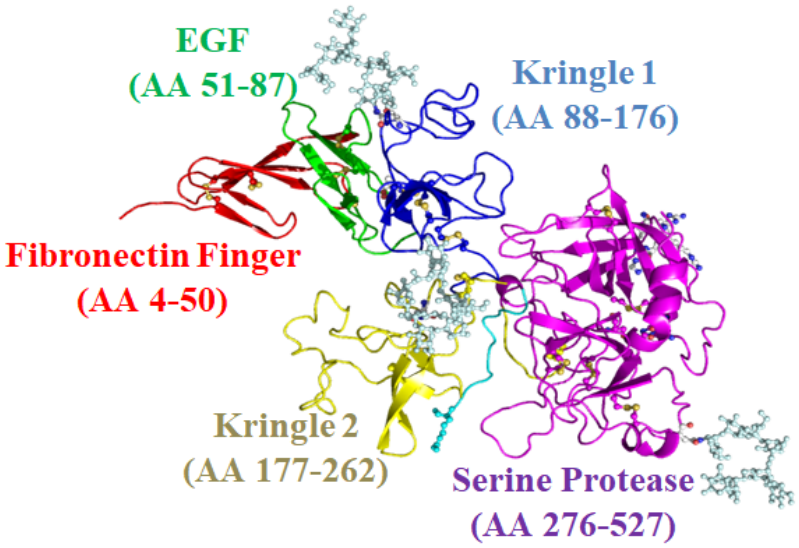

Figure 10. A theoretical structure of the full tissue plasminogen activator in humans. *The kringle domains, fibronectin finger, epidermal growth factor (EGF) and serine protease domains are marked.*

Image adapted from https://commons.wikimedia.org/wiki/File%3AT-PA.png

Normal physiological tPA concentrations do not induce systemic plasmin generation. Fibrin is generally thought to regulate plasminogen activation leading to fibrinolysis through recruitment and co-localization of both tPA and plasminogen on its surface. The stimulation of endothelial cells at the site of damage ensures rapid local release of active unbound tPA to be incorporated into the clot (Oliver et al., 2005). tPA binds to fibrin and activates fibrin-bound plasminogen more rapidly than it activates plasminogen in the circulation (Lijnen, 2001). Binding sites for tPA have been identified on endothelial cells. This involves annexin 2 (A2), a calcium and phospholipid binding protein on the plasma membrane that has been shown to enhance tPA-dependent plasminogen activation that is C terminal lysine dependent (Hajjar et al., 1987). A2 has also been identified on the surface of at least one herpesvirus, CMV (Raynor et al., 1999).

1.5.2.2 Urokinase Plasminogen Activator (uPA)

The serine protease uPA (50 kDa) is the product of the *PLAU* gene, synthesized by vascular endothelial and smooth muscle cells, by epithelial cells, fibroblasts, monocytes/macrophages, and also by cells of malignant tumors of different origin (Stepanova and Tkachuk, 2002). This protein is secreted as a single chain form. The lack of viable crystals for structure determination of intact uPA is probably due to the high degree of structural and motile independence of the domains. An overview of the uPA molecule is shown schematically in Figure 11. The single chain form is a prozymogen, which upon plasmin-mediated proteolytic cleavage is converted to an active two-chain form (Skriver et al., 1988). This uPA consists of an A-chain (157 residues) and a glycosylated B-chain (253 residues), which are linked by the disulfide bridge at cys148 and cys279. Further cleavages at lys135 and arg156 produce low-molecular-weight (31 kDa) uPA. Both high- and low-molecular-weight species are enzymatically active (Schaller and Gerber, 2011). The epidermal growth factor

domain (EGF) contains a binding site for the uPA receptor (uPAR). The kringle domain lacks lysine binding sites, which plays an important role in the binding to the cell surface and fibrin (Schaller and Gerber, 2011). uPA has a characteristic, basic sequence motif that has an affinity for heparin, which may be involved in the binding of uPA to components of the extracellular matrix such as laminin-nidogen (Siren et al., 1992; Vaheri et al., 1992).

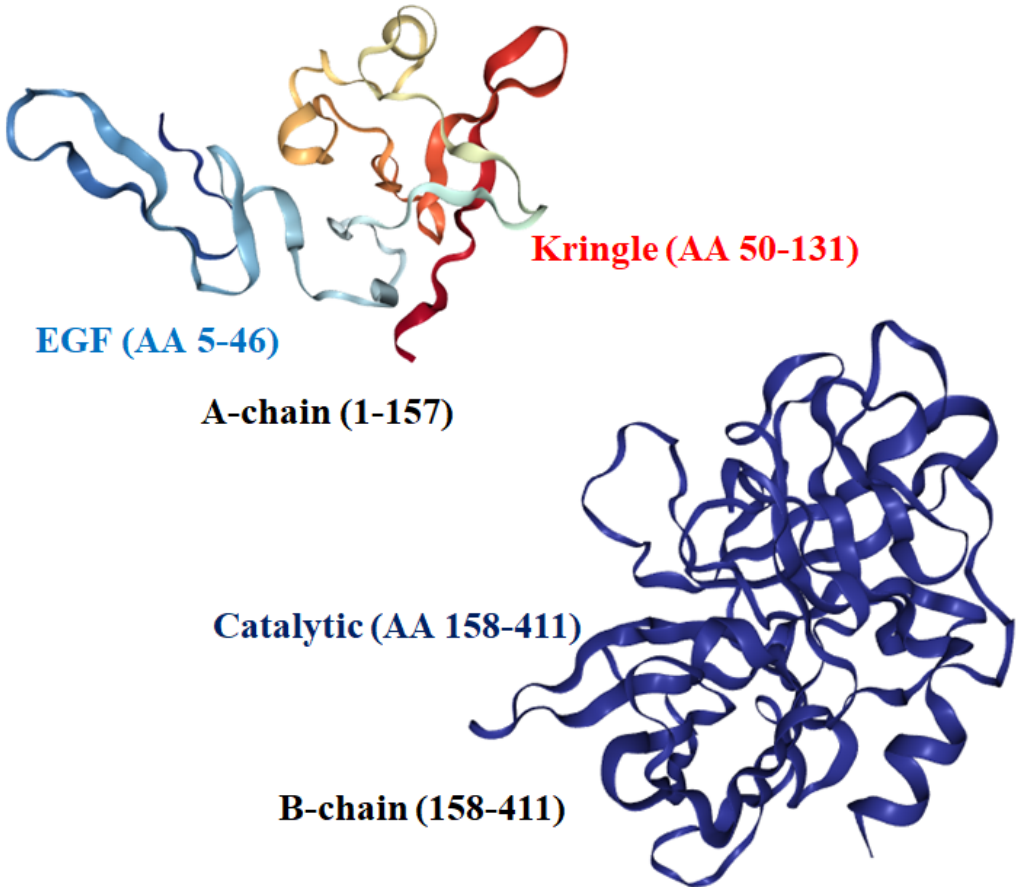

Figure 11. The schematic representation of the A-chain and B-chain of urokinase-type plasminogen activator (uPA). *uPA consists of an A-chain (157 residues) and a glycosylated B-chain (253 residues). The epidermal growth factor domain (EGF, AA 5-46), the kringle domain (kringle, AA 50-131) and the catalytic domain (catalytic, AA 148-411) are highlighted with different colors. Image adapted from the RCSB PDB (www.rcsb.org) of PDB ID 2I9A and 4XSK.*

uPA provides a system for pericellular plasminogen activation. uPA binds with high affinity to uPAR on the cell surface. Those two components are key members in processes that require concentrated proteolytic activities, including pathological processes (such as tumor invasion), as well as physiological processes, such as wound healing. On the surface of extravascular cells, uPA/uPAR complexes mediate plasminogen conversion into plasmin. The plasmin generated at the cell surface is involved in proteolytic degradation of the extracellular matrix. This remodeling process contributes to the upregulation of cell migration and proliferation (Dano et al., 1985). Jimenez et al. (1997) have demonstrated that uPA can accelerate the wound healing process in a murine model. In addition, the migration of corneal epithelial cells has been shown to require degradation of the basement membrane by the release of cellular uPA (Legrand et al., 2001).

1.5.3 Plasminogen activator inhibitors

The plasminogen activator inhibitor-1 (PAI-1), PAI-2 or PAI-3 regulate uPA and tPA. All of them are glycoproteins that belong to the family of serine proteases (Kruithof, 1988). During the physiological condition, these inhibitors have a variety of conformations. They are stable when they snap into their target protease. PAI-3 can inhibit both uPA and tPA albeit with a much slower rate than PAI-1 and -2 (Rijken, 1995). Besides, PAI-1 is the most universal and most rapidly acting physiological inhibitor of both uPA and tPA. On the other hand, PAI-2 can inhibit both two-chain uPA and two-chain tPA, but is less effective towards single-chain tPA and does not inhibit single-chain uPA (Bhattacharya et al., 2012).

1.5.3.1 Plasminogen activator inhibitor-1

PAI-1, also known as endothelial plasminogen activator inhibitor or serpin E1, is a 54 kDa protein that exists in (i) a native inhibitory form, (ii) an inactive latent form, (iii) complexed with proteinases and (iv) a cleaved form (Hekman and Loskutoff, 1985).

PAI-1 assembles complexes both with single-chain and two chain tPA and with two-chain uPA, but is more selective for tPA (De Taeye et al., 2004). In plasma, there is a large molar excess of active PAI-1 over tPA. Most of tPA is in complex with PAI-1 to regulate constitutive plasminogen activation (Schaller and Gerber, 2011). Platelets have much PAI-1 in its inactive form (Booth et al., 1988). Platelets that are involved in the formation of a fibrin clot are activating PAI-I by their α-granules (Juhanvague et al., 1984). There is enough active PAI-I to inhibit the plasminogen activator tPA and uPA and protect clot formation (Brogren et al., 2004). In contrast, activated platelets are thought to provide a surface for enhanced plasminogen activation by promoting an interaction between tPA and plasminogen and for protection of plasmin from α2-antiplasmin (Loscalzo et al., 1995).

1.5.3.2 Plasminogen activator inhibitor-2

The PAI-2 can be found in two forms: a nonglycosylated intracellular form (42kDa) and a glycosylated, secreted extracellular form (60kDa) (Genton et al., 1987). PAI-2 rapidly inhibits uPA, but tPA very slowly (Kawano et al., 1970; Kruithof et al., 1995). PAI-2 secreted by monocytes is involved in uPA-mediated cell migration, whereas intracellular PAI-2 prevents apoptosis (Dickinson et al., 1995; Kirchheimer and Remold, 1989; Kumar and Baglioni, 1991).

1.5.3.3 Plasminogen activator inhibitor-3

PAI-3, also known as Protein C inhibitor, is synthesized in the liver and in numerous steroid-responsive organs. It is a serine proteinase inhibitor that can inhibit enzymes in blood coagulation, fibrinolysis and fertility. The role of PAI-3 in regulating the blood coagulation mechanism is still unknown, as it can inhibit both procoagulant and anticoagulant enzymes (Meijers et al., 2002).

1.5.4 α2-antiplasmin

α2-antiplasmin is the chief physiological inhibitor of plasmin. This glycoprotein forms a complex with plasmin by binding to kringle 1-3 of plasmin (Wiman and Collen, 1979). Since the same lysine-binding kringle sites mediate plasminogen binding to receptors, receptor-bound plasminogen/plasmin is resistant to inhibition by α2-antiplasmin.

1.5.4 α2-macroglobulin

Another broad-spectrum proteinase inhibitor, α2-macroglobulin, can also inhibit plasmin. α2-macroglobulin forms a noncovalent complex with plasmin, and this process happens when the α2-antiplasmin concentration is low (Aoki et al., 1978).

1.5.4 Virus and plasmino(gen) interaction

The roles of the plasminogen activator-plasmin system in normal and pathologic processes have expanded significantly with the introduction of new gene-targeting techniques, and the roles of the plasminogen activator-plasmin in viral infections have become more clear.

Plasminogen is involved in the infection and replication of various enveloped viruses. During H1 or H3 influenza virus infection, plasmin can make a HA0 cleavage in cell cultures (Hamilton and Whittaker, 2013). Annexin A2 is a cellular protein which promotes the formation of lipid micro-domains that are necessary for the budding of virus from infected host cells. When incorporated in influenza virus by converting plasminogen into plasmin, annexin A2 was shown to enhance viral replication (LeBouder et al., 2008). Plasminogen was shown to promote influenza virus replication through annexin A2 in the absence of neuraminidase (LeBouder et al., 2010).

HSV1 enhance the generation of plasmin and plasmin enhances cell infection by HSV. It was shown that plasmin generation from its purified precursor plasminogen by tissue plasminogen activator increased in the presence of purified HSV1, and this process relied on the protease activated receptors (Pryzdial et al., 2014). This simultaneous generation of clot-dissolving and -forming proteases may explain why some enveloped viruses such as HSV1 rarely cause thrombosis (Pryzdial et al., 2014).

Severe cute respiratory syndrome coronavirus (SARS-CoV) is a virus may cause acute respiratory disease and acute lung injury. Following SARS-CoV infection, uPA activity increased in a dose-dependent manner, and dysregulation of the urokinase pathway caused more severe lung pathology (Gralinski et al., 2013). In addition, the urokinase pathway and ECM remodeling are important for regulating SARS-CoV pathogenic outcomes (Gralinski et al., 2013). Serpine1 is a negative regulator of urokinase pathway, and it inhibits uPA activity. In SARS patients, Serpine1 is highly expressed (de Lang et al., 2007). In a Serpine1 knockout mouse model, the virus infection resulted in lethal disease with extreme lung pathology (Gralinski et al., 2013). By contrast, in a tPA-deficient mice model, the virus infection increased exudates in the lung (Gralinski and Baric, 2015). These results indicate that the dysregulation of these components are closely associated with SARS-CoV infection.

1.6 Concluding remarks

Viruses must be able to overcome cellular and non-cellular physical barriers in order to successfully establish an infection. During the mucosa infection, they have developed mechanisms to establish primary infection and cross the basement membrane barrier. ECM degradation and remodelling have been demonstrated to play a key role in governing organ branching by providing structural integrity and regulating diverse cellular processes. However, there are still some challenging issues that remain to be resolved. One aspect of BM passage that we have not discussed here is the role of the local cellular immunity in breaking down ECM during a microbial invasion. Immune cells can produce large quantities of proteases upon stimulation at

the site of inflammation, and this may break important defense barriers such as the BM, allowing pathogens to invade deeper tissues. But on the other hand, inflammation also increases the risk that pathogens will be recognized and neutralized by the immune system.

As the BM represents one of the first barriers encountered by the pathogen, dissecting pathogen interactions with, and mechanisms to cross the BM may provide interesting leads towards developing novel antimicrobial drugs. However, it is important to bear in mind that the *in vitro* knowledge on this topic does not automatically lead to an effective *in vivo* implementation. Improved *in vitro* models that can more accurately reflect the *in vivo* environment will provide excellent tools for the identification and characterization of putative adhesion and invasion mechanisms before progressing to the use of animal models.

The invasive capacity of various microorganisms is directly linked to the characteristics of the species in addition to host proteases that degrade structural ECM proteins. Generally, underlying mechanisms for binding to and breakdown of the BM are better studied for bacteria and fungi than for viruses. Bacteria and fungi degrade ECM by many ways, including binding to host plasminogen. In recent years, protease inhibitors have been considered as an effective antimicrobial therapeutic approach to control the invasive capacity of pathogens and also to hinder host ECM degradation (Doyle et al., 2007; Hiemstra, 2002). It will be interesting to identify the possible viral factors that are required for efficient penetration through the BM and ECM. If the protease activity plays a role, as recently demonstrated by a herpesvirus (Pryzdial et al., 2014), then the use of protease-inhibitors might be a useful anti-viral strategy. Still, to further develop the potential use of protease-inhibitors as antimicrobial targets, there is a need for identification of all concerned signals, factors and domains during microbial invasion.

In conclusion, viruses have evolved different strategies to cross the basement membrane. For herpesvirus basement membrane penetration, it may be associated with plasminogen activator-plasminogen system activation. Plasminogen is associated with virus infection and replication by many ways. Fundamental insights in these invasion mechanisms of herpesviruses could be a promising road towards new therapeutic approaches in various host species.

References

Anderson, D.J., Marathe, J., Pudney, J., 2014. The structure of the human vaginal stratum corneum and its role in immune defense. Am J Reprod Immunol 71(6), 618-623.

Andreasen, P.A., Nielsen, L.S., Kristensen, P., Grondahl-Hansen, J., Skriver, L., Dano, K., 1986. Plasminogen activator inhibitor from human fibrosarcoma cells binds urokinase-type plasminogen activator, but not its proenzyme. J Biol Chem 261(17), 7644-7651.

Aoki, N., Moroi, M., Tachiya, K., 1978. Effects of Alpha-2-Plasmin Inhibitor on Fibrin Clot Lysis - Its Comparison with Alpha-2-Macroglobulin. Thromb Haemostasis 39(1), 22-31.

Appel, M.J., Menegus, M., Parsonson, I.M., Carmichael, L.E., 1969. Pathogenesis of canine herpesvirus in specific-pathogen-free dogs: 5- to 12-week-old pups. Am J Vet Res 30(12), 2067-2073.

Arvin, A., Abendroth, A., 2007. VZV: immunobiology and host response. In: Arvin, A., Campadelli-Fiume, G., Mocarski, E., Moore, P.S., Roizman, B., Whitley, R., Yamanishi, K. (Eds.), Human Herpesviruses: Biology, Therapy, and Immunoprophylaxis, Cambridge.

Backes, B.J., Harris, J.L., Leonetti, F., Craik, C.S., Ellman, J.A., 2000. Synthesis of positional-scanning libraries of fluorogenic peptide substrates to define the extended substrate specificity of plasmin and thrombin (vol 18, pg 188, 2000). Nat Biotechnol 18(5), 559-559.

Banyai, L., Varadi, A., Patthy, L., 1983. Common evolutionary origin of the fibrin-binding structures of fibronectin and tissue-type plasminogen activator. FEBS Lett 163(1), 37-41.

Bhattacharya, S., Ploplis, V.A., Castellino, F.J., 2012. Bacterial plasminogen receptors utilize host plasminogen system for effective invasion and dissemination. J Biomed Biotechnol 2012, 482096.

Booth, N.A., Macgregor, I.R., Bennett, B., 1988. Plasminogen-Activator Inhibitor (Pai-1) in Plasma and Platelets. Brit J Haematol 68(4), 509-509.

Breitkreutz, D., Koxholt, I., Thiemann, K., Nischt, R., 2013. Skin basement membrane: the foundation of epidermal integrity--BM functions and diverse roles of bridging molecules nidogen and perlecan. Biomed Res Int 2013, 179784.

Brizzolara, S., Killeen, J., Severino, R., 1999. Vaginal pH and parabasal cells in postmenopausal women. Obstet Gynecol 94(5 Pt 1), 700-703.

Brogren, H., Karlsson, L., Andersson, M., Wang, L., Erlinge, D., Jern, S., 2004. Platelets synthesize large amounts of active plasminogen activator inhibitor 1. Blood 104(13), 3943-3948.

Bron, A.J., 2001. The architecture of the corneal stroma. Br J Ophthalmol 85(4), 379-381.

Burr, P.D., Campbell, M.E., Nicolson, L., Onions, D.E., 1996. Detection of canine herpesvirus 1 in a wide range of tissues using the polymerase chain reaction. Vet Microbiol 53(3-4), 227-237.

Carmichael, L.E., Squire, R.A., Krook, L., 1965. Clinical and pathologic features of a fatal viral disease of newborn pups. Am J Vet Res 26(113), 803-814.

Casaroli-Marano, R.P., Nieto-Nicolau, N., Martinez-Conesa, E.M., Edel, M., A, B.A.-P., 2015. Potential Role of Induced Pluripotent Stem Cells (IPSCs) for Cell-Based Therapy of the Ocular Surface. J Clin Med 4(2), 318-342.

Castellino, F.J., Ploplis, V.A., 2005. Structure and function of the plasminogen/plasmin system. Thromb Haemostasis 93(4), 647-654.

Castellino, F.J., Powell, J.R., 1981. Human plasminogen. Methods Enzymol 80 Pt C, 365-378.

Chi, C.C., Wang, S.H., Prenter, A., Cooper, S., Wojnarowska, F., 2010. Basement membrane zone and dermal extracellular matrix of the vulva, vagina and amnion: An immunohistochemical study with comparison with

non-reproductive epithelium. Australas J Dermatol 51(4), 243-247.

Connolly, S.A., Jackson, J.O., Jardetzky, T.S., Longnecker, R., 2011. Fusing structure and function: a structural view of the herpesvirus entry machinery. Nat Rev Microbiol 9(5), 369-381.

Corfield, A.P., 2015. Mucins: A biologically relevant glycan barrier in mucosal protection. Bba-Gen Subjects 1850(1), 236-252.

Correia, M., Snabe, T., Thiagarajan, V., Petersen, S.B., Campos, S.R., Baptista, A.M., Neves-Petersen, M.T., 2015. Photonic activation of plasminogen induced by low dose UVB. PLoS One 10(1), e0116737.

Cortes, M.E., Hauyon, R., Gonzalez, F., Vigil, P., 2012. Evidence of Fractality in a Pattern of Crystallization of Bovine Cervical Mucus Obtained at Oestrus. Int J Morphol 30(4), 1461-1465.

Dahiya, M., Rajamohan, G., Dikshit, K.L., 2005. Enhanced plasminogen activation by staphylokinase in the presence of streptokinase beta/betagamma domains: plasminogen kringles play a role. FEBS Lett 579(7), 1565-1572.

Dano, K., Andreasen, P.A., Grondahl-Hansen, J., Kristensen, P., Nielsen, L.S., Skriver, L., 1985. Plasminogen activators, tissue degradation, and cancer. Adv Cancer Res 44, 139-266.

Dartt, D.A., Masli, S., 2014. Conjunctival epithelial and goblet cell function in chronic inflammation and ocular allergic inflammation. Curr Opin Allergy Clin Immunol 14(5), 464-470.

Davison, A.J., 2007. Comparative analysis of the genomes. In: Arvin, A., Campadelli-Fiume, G., Mocarski, E., Moore, P.S., Roizman, B., Whitley, R., Yamanishi, K. (Eds.), Human Herpesviruses: Biology, Therapy, and Immunoprophylaxis, Cambridge.

Davison, A.J., 2010. Herpesvirus systematics. Vet Microbiol 143(1), 52-69.

Davison, A.J., Eberle, R., Ehlers, B., Hayward, G.S., McGeoch, D.J., Minson, A.C., Pellett, P.E., Roizman, B., Studdert, M.J., Thiry, E., 2009. The order

Herpesvirales. Arch Virol 154(1), 171-177.

de Lang, A., Baas, T., Teal, T., Leijten, L.M., Rain, B., Osterhaus, A.D., Haagmans, B.L., Katze, M.G., 2007. Functional genomics highlights differential induction of antiviral pathways in the lungs of SARS-CoV-infected macaques. PLoS Pathog 3(8), e112.

De Taeye, B., Gils, A., Declerck, P.J., 2004. The story of the serpin plasminogen activator inhibitor I: is there any need for another mutant? Thromb Haemostasis 92(5), 898-924.

Decaro, N., Martella, V., Buonavoglia, C., 2008. Canine adenoviruses and herpesvirus. Vet Clin North Am Small Anim Pract 38(4), 799-814, viii.

Dickinson, J.L., Bates, E.J., Ferrante, A., Antalis, T.M., 1995. Plasminogen activator inhibitor type 2 inhibits tumor necrosis factor alpha-induced apoptosis. Evidence for an alternate biological function. J Biol Chem 270(46), 27894-27904.

Didiasova, M., Wujak, L., Wygrecka, M., Zakrzewicz, D., 2014. From plasminogen to plasmin: role of plasminogen receptors in human cancer. Int J Mol Sci 15(11), 21229-21252.

Dos Santos, A.C., Viana, D.C., Oliveira, G.B., Silva, R.S., Oliveira, M.F., Assis-Neto, A.C., 2017. Follicular development and morphological changes in the vaginal epithelium during the estrous cycle of Galea spixii. Microsc Res Tech 80(2), 167-176.

Doyle, P.S., Zhou, Y.M., Engel, J.C., McKerrow, J.H., 2007. A cysteine protease inhibitor cures Chagas' disease in an immunodeficient-mouse model of infection. Antimicrob Agents Chemother 51(11), 3932-3939.

Dua, H.S., Faraj, L.A., Said, D.G., Gray, T., Lowe, J., 2013. Human corneal anatomy redefined: a novel pre-Descemet's layer (Dua's layer). Ophthalmology 120(9), 1778-1785.

Evermann, J.F., Ledbetter, E.C., Maes, R.K., 2011. Canine reproductive, respiratory,

and ocular diseases due to canine herpesvirus. Vet Clin North Am Small Anim Pract 41(6), 1097-1120.

Fukuda, K., Chikama, T., Nakamura, M., Nishida, T., 1999. Differential distribution of subchains of the basement membrane components type IV collagen and laminin among the amniotic membrane, cornea, and conjunctiva. Cornea 18(1), 73-79.

Fortenberry, Y.M., 2013. Plasminogen activator inhibitor-1 inhibitors: a patent review (2006-present). Expert Opin Ther Pat 23(7), 801-815.

Friedenwald, J.S., 1951. Growth pressure and metaplasia of conjunctival and corneal epithelium. Doc Ophthalmol 5-6, 184-192.

Gaskell, R.M., Povey, R.C., 1977. Experimental induction of feline viral rhinotracheitis virus re-excretion in FVR-recovered cats. Vet Rec 100(7), 128-133.

Genton, C., Kruithof, E.K.O., Schleuning, W.D., 1987. Phorbol Ester Induces the Biosynthesis of Glycosylated and Nonglycosylated Plasminogen-Activator Inhibitor-2 in High Excess over Urokinase-Type Plasminogen-Activator in Human U-937 Lymphoma-Cells. J Cell Biol 104(3), 705-712.

Ghosh, A.K., Vaughan, D.E., 2012. PAI-1 in tissue fibrosis. J Cell Physiol 227(2), 493-507.

Gilger, B.C., Wright, J.C., Whitley, R.D., McLaughlin, S.A., 1993. Corneal thickness measured by ultrasonic pachymetry in cats. Am J Vet Res 54(2), 228-230.

Gipson, I.K., 2004. Distribution of mucins at the ocular surface. Exp Eye Res 78(3), 379-388.

Gipson, I.K., Ho, S.B., Spurr-Michaud, S.J., Tisdale, A.S., Zhan, Q., Torlakovic, E., Pudney, J., Anderson, D.J., Toribara, N.W., Hill, J.A., 3rd, 1997. Mucin genes expressed by human female reproductive tract epithelia. Biol Reprod 56(4), 999-1011.

Giuliano, E.A., Moore, C.P., Phillips, T.E., 2002. Morphological evidence of M cells in healthy canine conjunctiva-associated lymphoid tissue. Graefes Arch Clin

Exp Ophthalmol 240(3), 220-226.

Glorieux, S., Favoreel, H.W., Steukers, L., Vandekerckhove, A.P., Nauwynck, H.J., 2011. A trypsin-like serine protease is involved in pseudorabies virus invasion through the basement membrane barrier of porcine nasal respiratory mucosa. Vet Res 42, 58.

Gould, D., 2011. Feline herpesvirus-1: ocular manifestations, diagnosis and treatment options. J Feline Med Surg 13(5), 333-346.

Gralinski, L.E., Bankhead, A., 3rd, Jeng, S., Menachery, V.D., Proll, S., Belisle, S.E., Matzke, M., Webb-Robertson, B.J., Luna, M.L., Shukla, A.K., Ferris, M.T., Bolles, M., Chang, J., Aicher, L., Waters, K.M., Smith, R.D., Metz, T.O., Law, G.L., Katze, M.G., McWeeney, S., Baric, R.S., 2013. Mechanisms of severe acute respiratory syndrome coronavirus-induced acute lung injury. MBio 4(4).

Gralinski, L.E., Baric, R.S., 2015. Molecular pathology of emerging coronavirus infections. J Pathol 235(2), 185-195.

Gunzler, W.A., Steffens, G.J., Otting, F., Buse, G., Flohe, L., 1982. Structural Relationship between Human High and Low-Molecular Mass Urokinase. H-S Z Physiol Chem 363(2), 133-141.

Hajjar, K.A., Hamel, N.M., Harpel, P.C., Nachman, R.L., 1987. Binding of tissue plasminogen activator to cultured human endothelial cells. J Clin Invest 80(6), 1712-1719.

Halfter, W., Oertle, P., Monnier, C.A., Camenzind, L., Reyes-Lua, M., Hu, H., Candiello, J., Labilloy, A., Balasubramani, M., Henrich, P.B., Plodinec, M., 2015. New concepts in basement membrane biology. FEBS J 282(23), 4466-4479.

Hamilton, B.S., Whittaker, G.R., 2013. Cleavage activation of human-adapted influenza virus subtypes by kallikrein-related peptidases 5 and 12. J Biol Chem 288(24), 17399-17407.

Hayashi, S., Osawa, T., Tohyama, K., 2002. Comparative observations on corneas, with special reference to Bowman's layer and Descemet's membrane in mammals and amphibians. J Morphol 254(3), 247-258.

Hekman, C.M., Loskutoff, D.J., 1985. Endothelial-Cells Produce a Latent Inhibitor of Plasminogen Activators That Can Be Activated by Denaturants. J Biol Chem 260(21), 11581-11587.

Hiemstra, P.S., 2002. Novel roles of protease inhibitors in infection and inflammation. Biochem Soc Trans 30(2), 116-120.

Hoover-Plow, J., 2010. Does plasmin have anticoagulant activity? Vasc Health Risk Manag 6, 199-205.

Horejs, C.M., 2016. Basement membrane fragments in the context of the epithelial-to-mesenchymal transition. Eur J Cell Biol 95(11), 427-440.

Hussin, A.M., Zaid, N.W., Hussain, S.O., 2014. Compensatory structural adaptive modifications of vagina in response to functional demand in goat. Vet Med Int 2014, 789816.

Ianowski, J.P., Choi, J.Y., Wine, J.J., Hanrahan, J.W., 2007. Mucus secretion by single tracheal submucosal glands from normal and cystic fibrosis transmembrane conductance regulator knockout mice. J Physiol 580(Pt 1), 301-314.

Jimenez, P.A., Teliska, M., Liu, B., Antonaccio, M.J., 1997. Urokinase-type plasminogen activator stimulates wound healing in the diabetic mouse. Inflamm Res 46 Suppl 2, S169-170.

Juhanvague, I., Moerman, B., Decock, F., Aillaud, M.F., Collen, D., 1984. Plasma-Levels of a Specific Inhibitor of Tissue-Type Plasminogen-Activator (and Urokinase) in Normal and Pathological Conditions. Thromb Res 33(5), 523-530.

Kaske, S., Krasteva, G., Konig, P., Kummer, W., Hofmann, T., Gudermann, T., Chubanov, V., 2007. TRPM5, a taste-signaling transient receptor potential ion-channel, is a ubiquitous signaling component in chemosensory cells. BMC

Neurosci 8, 49.

Kawano, T., Morimoto, K., Uemura, Y., 1970. Partial Purification and Properties of Urokinase Inhibitor from Human Placenta. J Biochem-Tokyo 67(3), 333-&.

Khoshnoodi, J., Pedchenko, V., Hudson, B.G., 2008. Mammalian collagen IV. Microsc Res Tech 71(5), 357-370.

Kindell, D.G., Keck, R.W., Jankun, J., 2015. Comparison between the clot-protecting activity of a mutant plasminogen activator inhibitor-1 with a very long half-life and 6-aminocaproic acid. Exp Ther Med 9(6), 2339-2343.

Kirchheimer, J.C., Remold, H.G., 1989. Endogenous receptor-bound urokinase mediates tissue invasion of human monocytes. J Immunol 143(8), 2634-2639.

Knight, D.A., Holgate, S.T., 2003. The airway epithelium: structural and functional properties in health and disease. Respirology 8(4), 432-446.

Kohfeldt, E., Sasaki, T., Gohring, W., Timpl, R., 1998. Nidogen-2: a new basement membrane protein with diverse binding properties. J Mol Biol 282(1), 99-109.

Kruithof, E.K., 1988. Plasminogen activator inhibitors--a review. Enzyme 40(2-3), 113-121.

Kruithof, E.K.O., Baker, M.S., Bunn, C.L., 1995. Biological and Clinical Aspects of Plasminogen-Activator Inhibitor Type-2. Blood 86(11), 4007-4024.

Krummenacher, C., Carfi, A., Eisenberg, R.J., Cohen, G.H., 2013. ENTRY OF HERPESVIRUSES INTO CELLS: The Enigma Variations. Adv Exp Med Biol 790, 178-195.

Kumar, S., Baglioni, C., 1991. Protection from tumor necrosis factor-mediated cytolysis by overexpression of plasminogen activator inhibitor type-2. J Biol Chem 266(31), 20960-20964.

Lagali, N., Germundsson, J., Fagerholm, P., 2009. The role of Bowman's layer in corneal regeneration after phototherapeutic keratectomy: a prospective study using in vivo confocal microscopy. Invest Ophthalmol Vis Sci 50(9), 4192-4198.

Lavker, R.M., Sun, T.T., 2000. Epidermal stem cells: properties, markers, and location. Proc Natl Acad Sci U S A 97(25), 13473-13475.

Law, R.H.P., Abu-Ssaydeh, D., Whisstock, J.C., 2013. New insights into the structure and function of the plasminogen/plasmin system. Curr Opin Struc Biol 23(6), 836-841.

Law, R.H.P., Caradoc-Davies, T., Cowieson, N., Horvath, A.J., Quek, A.J., Encarnacao, J.A., Steer, D., Cowan, A., Zhang, Q., Lu, B.G.C., Pike, R.N., Smith, A.I., Coughlin, P.B., Whisstock, J.C., 2012. The X-ray crystal structure of full-length human plasminogen. J Thromb Haemost 10(6), E23-E23.

LeBleu, V.S., Macdonald, B., Kalluri, R., 2007. Structure and function of basement membranes. Exp Biol Med (Maywood) 232(9), 1121-1129.

LeBouder, F., Lina, B., Rimmelzwaan, G.F., Riteau, B., 2010. Plasminogen promotes influenza A virus replication through an annexin 2-dependent pathway in the absence of neuraminidase. J Gen Virol 91(Pt 11), 2753-2761.

LeBouder, F., Morello, E., Rimmelzwaan, G.F., Bosse, F., Pechoux, C., Delmas, B., Riteau, B., 2008. Annexin II incorporated into influenza virus particles supports virus replication by converting plasminogen into plasmin. J Virol 82(14), 6820-6828.

Lee, J.L., Streuli, C.H., 2014. Integrins and epithelial cell polarity. J Cell Sci 127(Pt 15), 3217-3225.

Legrand, C., Polette, M., Tournier, J.M., de Bentzmann, S., Huet, E., Monteau, M., Birembaut, P., 2001. uPA/plasmin system-mediated MMP-9 activation is implicated in bronchial epithelial cell migration. Exp Cell Res 264(2), 326-336.

Leroy, B., Gillet, L., Vanderplasschen, A., Wattiez, R., 2016. Structural Proteomics of Herpesviruses. Viruses 8(2).

Lijnen, H.R., 2001. Elements of the fibrinolytic system. Ann Ny Acad Sci 936, 226-236.

Lijnen, H.R., Collen, D., 1995. Mechanisms of Physiological Fibrinolysis. Bailliere Clin Haem 8(2), 277-290.

Lijnen, H.R., Stassen, J.M., Vanlinthout, I., Fukao, H., Okada, K., Matsuo, O., Collen, D., 1991. Comparative fibrinolytic properties of staphylokinase and streptokinase in animal models of venous thrombosis. Thromb Haemost 66(4), 468-473.

Llevadot, J., Giugliano, R.P., Antman, E.M., 2001. Bolus fibrinolytic therapy in acute myocardial infarction. JAMA 286(4), 442-449.

Loscalzo, J., Pasche, B., Ouimet, H., Freedman, J.E., 1995. Platelets and plasminogen activation. Thromb Haemost 74(1), 291-293.

Lorenzen, E., Follmann, F., Jungersen, G., Agerholm, J.S., 2015. A review of the human vs. porcine female genital tract and associated immune system in the perspective of using minipigs as a model of human genital Chlamydia infection. Vet Res 46, 116.

Magnusson, S., Sottrupjensen, L., Claeys, H., Zajdel, M., Petersen, T.E., 1975. Complete Primary Structure of Prothrombin - Partial Primary Structures of Plasminogen and Hirudin. Thromb Diath Haemost 34(2), 562-563.

Marneros, A.G., Olsen, B.R., 2005. Physiological role of collagen XVIII and endostatin. FASEB J 19(7), 716-728.

Masters, B.R., Thaer, A.A., 1994. In vivo human corneal confocal microscopy of identical fields of subepithelial nerve plexus, basal epithelial, and wing cells at different times. Microsc Res Tech 29(5), 350-356.

Mauro, M.A., Murphy, K.P., Thomson, K.R., Venbrux, A.C., Morgan, R.A., 2013. Image-Guided Interventions E-Book: Expert Radiology Series. Elsevier Health Sciences.

McCoy, H.E., Broder, C.C., Lottenberg, R., 1991. Streptokinases produced by pathogenic group C streptococci demonstrate species-specific plasminogen activation. J Infect Dis 164(3), 515-521.

McGeoch, D.J., Dolan, A., Ralph, A.C., 2000. Toward a comprehensive phylogeny for mammalian and avian herpesviruses. J Virol 74(22), 10401-10406.

McGeoch, D.J., Rixon, F.J., Davison, A.J., 2006. Topics in herpesvirus genomics and evolution. Virus Res 117(1), 90-104.

McGhee, J.R., Fujihashi, K., 2012. Inside the mucosal immune system. PLoS Biol 10(9), e1001397.

Mehta, R., Shapiro, A.D., 2008. Plasminogen deficiency. Haemophilia 14(6), 1261-1268.

Meier, R.K., Ruiz-Fons, F., Ryser-Degiorgis, M.P., 2015. A picture of trends in Aujeszky's disease virus exposure in wild boar in the Swiss and European contexts. BMC Vet Res 11, 277.

Meijers, J.C.M., Marquart, J.A., Bertina, R.M., Bouma, B.N., Rosendaal, F.R., 2002. Protein C inhibitor (plasminogen activator inhibitor-3) and the risk of venous thrombosis. Brit J Haematol 118(2), 604-609.

Miles, L.A., Castellino, F.J., Gong, Y., 2003. Critical role for conversion of Glu-plasminogen to Lys-plasminogen for optimal stimulation of plasminogen activation on cell surfaces. Trends Cardiovas Med 13(1), 21-30.

Myllyharju, J., Kivirikko, K.I., 2004. Collagens, modifying enzymes and their mutations in humans, flies and worms. Trends Genet 20(1), 33-43.

Nasisse, M.P., Guy, J.S., Davidson, M.G., Sussman, W.A., Fairley, N.M., 1989. Experimental ocular herpesvirus infection in the cat. Sites of virus replication, clinical features and effects of corticosteroid administration. Invest Ophthalmol Vis Sci 30(8), 1758-1768.

Nassar, T., Yarovoi, S., Abu Fanne, R., Akkawi, S., Jammal, M., Allen, T.C., Idell, S., Cines, D.B., Higazi, A., 2010. Regulation of Airway Contractility by Plasminogen Activators through N-Methyl-D-Aspartate Receptor-1. Am J Resp Cell Mol 43(6), 703-711.

Nauwynck, H., Glorieux, S., Favoreel, H., Pensaert, M., 2007. Cell biological and

molecular characteristics of pseudorabies virus infections in cell cultures and in pigs with emphasis on the respiratory tract. Vet Res 38(2), 229-241.

Nauwynck, H.J., 1997. Functional aspects of Aujeszky's disease (pseudorabies) viral proteins with relation to invasion, virulence and immunogenicity. Vet Microbiol 55(1-4), 3-11.

Nauwynck, H.J., Pensaert, M.B., 1992. Abortion induced by cell-associated pseudorabies virus in vaccinated sows. Am J Vet Res 53(4), 489-493.

Nawynck, H.J., Pensaert, M.B., 1995. Cell-free and cell-associated viremia in pigs after oronasal infection with Aujeszky's disease virus. Vet Microbiol 43(4), 307-314.

Nicoll, M.P., Proenca, J.T., Efstathiou, S., 2012. The molecular basis of herpes simplex virus latency. FEMS Microbiol Rev 36(3), 684-705.

Ohmura, Y., Ono, E., Matsuura, T., Kida, H., Shimizu, Y., 1993. Detection of feline herpesvirus 1 transcripts in trigeminal ganglia of latently infected cats. Arch Virol 129(1-4), 341-347.

Okuda, Y., Ishida, K., Hashimoto, A., Yamaguchi, T., Fukushi, H., Hirai, K., Carmichael, L.E., 1993. Virus reactivation in bitches with a medical history of herpesvirus infection. Am J Vet Res 54(4), 551-554.

Oliver, J.J., Webb, D.J., Newby, D.E., 2005. Stimulated tissue plasminogen activator release as a marker of endothelial function in humans. Arterioscl Throm Vas 25(12), 2470-2479.

Owen, D.J., Crump, C.M., Graham, S.C., 2015a. Tegument Assembly and Secondary Envelopment of Alphaherpesviruses. Viruses 7(9), 5084-5114.

Owen, D.J., Crump, C.M., Graham, S.C., 2015b. Tegument Assembly and Secondary Envelopment of Alphaherpesviruses. Viruses-Basel 7(9), 5084-5114.

Papageorgiou, K.V., Suarez, N.M., Wilkie, G.S., McDonald, M., Graham, E.M., Davison, A.J., 2016. Genome Sequence of Canine Herpesvirus. PLoS One 11(5), e0156015.

Parsons, L.R., Tafuri, Y.R., Shreve, J.T., Bowen, C.D., Shipley, M.M., Enquist, L.W., Szpara, M.L., 2015. Rapid genome assembly and comparison decode intrastrain variation in human alphaherpesviruses. MBio 6(2).

Pavelka, M., Roth, J., 2010. Bowman's Layer, Functional Ultrastructure: Atlas of Tissue Biology and Pathology. Springer Vienna, Vienna, pp. 284-285.

Pomeranz, L.E., Reynolds, A.E., Hengartner, C.J., 2005. Molecular biology of pseudorabies virus: impact on neurovirology and veterinary medicine. Microbiol Mol Biol Rev 69(3), 462-500.

Post, K., 1985. Canine vaginal cytology during the estrous cycle. Can Vet J 26(3), 101-104.

Pryzdial, E.L., Sutherland, M.R., Ruf, W., 2014. The procoagulant envelope virus surface: contribution to enhanced infection. Thromb Res 133 Suppl 1, S15-17.

Purkis, P.E., Steel, J.B., Mackenzie, I.C., Nathrath, W.B., Leigh, I.M., Lane, E.B., 1990. Antibody markers of basal cells in complex epithelia. J Cell Sci 97 (Pt 1), 39-50.

Raum, D., Marcus, D., Alper, C.A., Levey, R., Taylor, P.D., Starzl, T.E., 1980. Synthesis of Human-Plasminogen by the Liver. Science 208(4447), 1036-1037.

Raynor, C.M., Wright, J.F., Waisman, D.M., Pryzdial, E.L., 1999. Annexin II enhances cytomegalovirus binding and fusion to phospholipid membranes. Biochemistry 38(16), 5089-5095.

Remeijer, L., Osterhaus, A., Verjans, G., 2004. Human herpes simplex virus keratitis: the pathogenesis revisited. Ocul Immunol Inflamm 12(4), 255-285.

Rijken, D.C., 1995. Plasminogen activators and plasminogen activator inhibitors: biochemical aspects. Baillieres Clin Haematol 8(2), 291-312.

Rijken, D.C., Hoylaerts, M., Collen, D., 1982. Fibrinolytic properties of one-chain and two-chain human extrinsic (tissue-type) plasminogen activator. J Biol Chem 257(6), 2920-2925.

Roizman, B., 1979. The organization of the herpes simplex virus genomes. Annu Rev Genet 13, 25-57.

Roizman, B., Baines, J., 1991. The diversity and unity of Herpesviridae. Comp Immunol Microbiol Infect Dis 14(2), 63-79.

Ros, C., Belak, S., 1999. Studies of genetic relationships between bovine, caprine, cervine, and rangiferine alphaherpesviruses and improved molecular methods for virus detection and identification. J Clin Microbiol 37(5), 1247-1253.

Rue, C.A., Ryan, P., 2003. A role for glycoprotein C in pseudorabies virus entry that is independent of virus attachment to heparan sulfate and which involves the actin cytoskeleton. Virology 307(1), 12-21.

Rziha, H.J., Mettenleiter, T.C., Ohlinger, V., Wittmann, G., 1986. Herpesvirus (Pseudorabies Virus) Latency in Swine - Occurrence and Physical State of Viral-DNA in Neural Tissues. Virology 155(2), 600-613.

Schaller, J., Gerber, S.S., 2011. The plasmin-antiplasmin system: structural and functional aspects. Cell Mol Life Sci 68(5), 785-801.

Singer, G.P., Newcomb, W.W., Thomsen, D.R., Homa, F.L., Brown, J.C., 2005. Identification of a region in the herpes simplex virus scaffolding protein required for interaction with the portal. J Virol 79(1), 132-139.

Singh, B., Fleury, C., Jalalvand, F., Riesbeck, K., 2012. Human pathogens utilize host extracellular matrix proteins laminin and collagen for adhesion and invasion of the host. Fems Microbiol Rev 36(6), 1122-1180.

Singh, D., 2003. Conjunctival lymphatic system. J Cataract Refract Surg 29(4), 632-633.

Siren, V., Stephens, R.W., Salonen, E.M., Vaheri, A., Summanen, P., Immonen, I., 1992. Retinal pigment epithelial cells secrete urokinase-type plasminogen activator and its inhibitor PAI-1. Ophthalmic Res 24(4), 203-212.

Skriver, L., Petersen, L.C., Lund, L.R., Nielsen, L.S., Dano, K., 1988. One-Chain Urokinse-Type Plasminogen-Activator from Human Sarcoma-Cells Is a

Proenzyme with Little or No Intrinsic Activity. Eur J Cancer Clin On 24(9), 1553-1553.

Skrzydlewska, E., Sulkowska, M., Koda, M., Sulkowski, S., 2005. Proteolytic-antiproteolytic balance and its regulation in carcinogenesis. World J Gastroenterol 11(9), 1251-1266.

Spear, P.G., Eisenberg, R.J., Cohen, G.H., 2000. Three classes of cell surface receptors for alphaherpesvirus entry. Virology 275(1), 1-8.

Srinivasan, B.D., Eakins, K.E., 1979. The reepithelialization of rabbit cornea following single and multiple denudation. Exp Eye Res 29(6), 595-600.

Stepanova, V.V., Tkachuk, V.A., 2002. Urokinase as a multidomain protein and polyfunctional cell regulator. Biochemistry-Moscow+ 67(1), 109-118.

Strang, B.L., Stow, N.D., 2005. Circularization of the herpes simplex virus type 1 genome upon lytic infection. J Virol 79(19), 12487-12494.

Sun, T.T., Lavker, R.M., 2004. Corneal epithelial stem cells: past, present, and future. J Investig Dermatol Symp Proc 9(3), 202-207.

Terres, A.M., Windle, H.J., Ardini, E., Kelleher, D.P., 2003. Soluble extracts from Helicobacter pylori induce dome formation in polarized intestinal epithelial monolayers in a laminin-dependent manner. Infect Immun 71(7), 4067-4078.

Timpl, R., Dziadek, M., Fujiwara, S., Nowack, H., Wick, G., 1983. Nidogen: a new, self-aggregating basement membrane protein. Eur J Biochem 137(3), 455-465.

Torricelli, A.A., Singh, V., Santhiago, M.R., Wilson, S.E., 2013. The corneal epithelial basement membrane: structure, function, and disease. Invest Ophthalmol Vis Sci 54(9), 6390-6400.

Uematsu, S., Fujimoto, K., Jang, M.H., Yang, B.G., Jung, Y.J., Nishiyama, M., Sato, S., Tsujimura, T., Yamamoto, M., Yokota, Y., Kiyono, H., Miyasaka, M., Ishii, K.J., Akira, S., 2008. Regulation of humoral and cellular gut immunity by lamina propria dendritic cells expressing Toll-like receptor 5. Nat Immunol 9(7), 769-776.

Urano, T., Sator de Serrano, V., Chibber, B.A., Castellino, F.J., 1987. The control of the urokinase-catalyzed activation of human glutamic acid 1-plasminogen by positive and negative effectors. J Biol Chem 262(33), 15959-15964.

Utian, W.H., 1975. Definitive symptoms of post-menopause--incorporating use of vaginal parabasal cell index. Front Horm Res 3, 74-93.

Vaheri, A., Bizik, J., Salonen, E.M., Tapiovaara, H., Siren, V., Myohanen, H., Stephens, R.W., 1992. Regulation of the pericellular activation of plasminogen and its role in tissue-destructive processes. Acta Ophthalmol Suppl(202), 34-41.

Vareille, M., Kieninger, E., Edwards, M.R., Regamey, N., 2011. The Airway Epithelium: Soldier in the Fight against Respiratory Viruses (vol 24, pg 210, 2011). Clin Microbiol Rev 24(3), 631-631.

Vassalli, J.D., Dayer, J.M., Wohlwend, A., Belin, D., 1984. Concomitant secretion of prourokinase and of a plasminogen activator-specific inhibitor by cultured human monocytes-macrophages. J Exp Med 159(6), 1653-1668.

Verhamme, I.M., Panizzi, P.R., Bock, P.E., 2015. Pathogen activators of plasminogen. J Thromb Haemost 13, S106-S114.

Verheijen, J.H., Caspers, M.P., Chang, G.T., de Munk, G.A., Pouwels, P.H., Enger-Valk, B.E., 1986. Involvement of finger domain and kringle 2 domain of tissue-type plasminogen activator in fibrin binding and stimulation of activity by fibrin. EMBO J 5(13), 3525-3530.

Voynow, J.A., Rubin, B.K., 2009. Mucins, mucus, and sputum. Chest 135(2), 505-512.

Wallen, P., Pohl, G., Bergsdorf, N., Ranby, M., Ny, T., Jornvall, H., 1983. Purification and characterization of a melanoma cell plasminogen activator. Eur J Biochem 132(3), 681-686.

Walters, J.N., Sexton, G.L., McCaffery, J.M., Desai, P., 2003. Mutation of single hydrophobic residue I27, L35, F39, L58, L65, L67, or L71 in the N terminus

of VP5 abolishes interaction with the scaffold protein and prevents closure of herpes simplex virus type 1 capsid shells. J Virol 77(7), 4043-4059.

Watt, F.M., 1984. Selective migration of terminally differentiating cells from the basal layer of cultured human epidermis. J Cell Biol 98(1), 16-21.

Wei, Z.G., Wu, R.L., Lavker, R.M., Sun, T.T., 1993. In vitro growth and differentiation of rabbit bulbar, fornix, and palpebral conjunctival epithelia. Implications on conjunctival epithelial transdifferentiation and stem cells. Invest Ophthalmol Vis Sci 34(5), 1814-1828.

Wilson, S.E., Hong, J.W., 2000. Bowman's layer structure and function: critical or dispensable to corneal function? A hypothesis. Cornea 19(4), 417-420.

Wiman, B., Collen, D., 1979. Mechanism of the Reaction between Human Alpha-2-Antiplasmin and Plasmin. J Biol Chem 254(18), 9291-9297.

Wiseman, O.J., Fowler, C.J., Landon, D.N., 2003. The role of the human bladder lamina propria myofibroblast. Bju Int 91(1), 89-93.

Wittmann, G., Jakubik, J., Ahl, R., 1980. Multiplication and distribution of Aujeszky's disease (pseudorabies) virus in vaccinated and non-vaccinated pigs after intranasal infection. Arch Virol 66(3), 227-240.

Wozniakowski, G., Samorek-Salamonowicz, E., 2015. Animal herpesviruses and their zoonotic potential for cross-species infection. Ann Agr Env Med 22(2), 191-194.

Yadav, R., Kottaiyan, R., Ahmad, K., Yoon, G., 2012. Epithelium and Bowman's layer thickness and light scatter in keratoconic cornea evaluated using ultrahigh resolution optical coherence tomography. J Biomed Opt 17(11), 116010.

Yaghi, A., Dolovich, M.B., 2016. Airway Epithelial Cell Cilia and Obstructive Lung Disease. Cells 5(4).

Yao, Y., 2016. Laminin: loss-of-function studies. Cell Mol Life Sci.

Yoshizaki, T., 2002. Promotion of metastasis in nasopharyngeal carcinoma by Epstein-Barr virus latent membrane protein-1. Histol Histopathol 17(3),

845-850.

Zeev-Ben-Mordehai, T., Weberruss, M., Lorenz, M., Cheleski, J., Hellberg, T., Whittle, C., El Omari, K., Vasishtan, D., Dent, K.C., Harlos, K., Franzke, K., Hagen, C., Klupp, B.G., Antonin, W., Mettenleiter, T.C., Grunewald, K., 2015. Crystal Structure of the Herpesvirus Nuclear Egress Complex Provides Insights into Inner Nuclear Membrane Remodeling. Cell Rep 13(12), 2645-2652.

Zhang, L., Gong, Y., Grella, D.K., Castellino, F.J., Miles, L.A., 2003. Endogenous plasmin converts Glu-plasminogen to Lys-plasminogen on the monocytoid cell surface. J Thromb Haemost 1(6), 1264-1270.

Zhang, L., Seiffert, D., Fowler, B.J., Jenkins, G.R., Thinnes, T.C., Loskutoff, D.J., Parmer, R.J., Miles, L.A., 2002. Plasminogen has a broad extrahepatic distributions. Thromb Haemostasis 87(3), 493-501.

Ziemann, K., Mettenleiter, T.C., Fuchs, W., 1998. Gene arrangement within the unique long genome region of infectious laryngotracheitis virus is distinct horn that of other alphaherpesviruses. J Virol 72(1), 847-852.

Zieske, J.D., Mason, V.S., Wasson, M.E., Meunier, S.F., Nolte, C.J., Fukai, N., Olsen, B.R., Parenteau, N.L., 1994. Basement membrane assembly and differentiation of cultured corneal cells: importance of culture environment and endothelial cell interaction. Exp Cell Res 214(2), 621-633.

CHAPTER 2
Aims

The mucosal surfaces represent preferential sites of entry for many alphaherpesviruses. The basement membrane, a barrier underlying the epithelium which involves serine protease activity, hampers free passage of alphaherpesviruses towards deeper cell layers. Previous studies have demonstrated that alphaherpesviruses have developed different mechanisms to overcome this barrier. Many alphaherpesviruses spread across the basement membrane in a plaque-wise manner, in which the virus replicates and spreads by direct cell-to-cell contact, resulting in (local) breakdown of the basement membrane. The mechanism underlying this breakdown of the basement membrane is not well understood. A better understanding will generate new leads towards the development of novel antiviral strategies.

The alphaherpesviruses feline herpesvirus 1 (FeHV 1) and canine herpesvirus 1 (CaHV 1) cause important diseases in cats and dogs. Before this PhD research, it remained unknown if FeHV 1 and/or CaHV 1 cross the basement membrane. In the present thesis, feline and canine ocular, respiratory and genital mucosa explants were established *ex vivo* and the viral dynamics of FeHV 1 and CaHV 1 were analyzed using these mucosal explants (Chapter 3 and Chapter 4).

In addition, by the use of pseudorabies virus (PrV) and porcine respiratory mucosa explants, the mechanism of alphaherpesvirus invasion across the basement membrane was examined (Chapter 5).

CHAPTER 3

Viral dynamics of Feline herpesvirus 1 in *ex vivo* modeling of ocular and respiratory mucosae, the primary targets of infection

Yewei Li, Jolien Van Cleemput, Yu Qiu, Vishwanatha R.A.P. Reddy, Bart Mateusen, Hans J. Nauwynck

Virus Research 210 (2015) 227–231

3.1 Abstract

Feline herpesvirus 1 (FeHV1) is a major cause of rhinotracheitis and ocular diseases in cats. In the present study, the viral replication at the primary infection sites was studied using feline respiratory and ocular mucosa explants. The explants of three cats were maintained in an air-liquid culture up to 96 hours without loss of viability. After inoculation with FeHV1 (C27), no evidence of infection was noted in corneal epithelium, while plaque-wise replication was observed in conjunctival and tracheal mucosae beginning from 24 h post inoculation (hpi). The viral plaque diameters increased over time in trachea and conjunctiva and were larger in tracheal explants than in conjunctival explants at 48 hpi. FeHV1 penetrated the basement membrane in conjunctival and tracheal explants between 24 and 48 hpi. At 48 and 72 hpi, viral invasion was going deeper in tracheal explants than in conjunctival explants. Our study indicates that FeHV1 has a better capacity to invade the respiratory mucosa than the conjunctival mucosa, and prefers the conjunctiva, but not the cornea as a portal of entry during ocular infection.

3.2 Introduction

Feline herpesvirus 1 (FeHV1), a member of the alphaherpesvirus subfamily, causes infections in Felidae worldwide, and is responsible for the upper respiratory tract infections known as feline viral rhinotracheitis in domestic cats (Gaskell et al., 2007). The characteristics of FeHV1 replication are similar to those of many other alphaherpesviruses: a short replication cycle, lifelong latency mainly in neurons, and a narrow host range (Maes, 2012). Clinically, primary FeHV1 infections typically cause acute upper respiratory tract and ocular diseases in domestic cats, characterized by sneezing and nasal discharge, conjunctivitis and cornea ulceration, and usually end with latent and chronic infections (Thiry et al., 2009). The virus may be reactivated, especially when the host is immunocompromised, and cats that experience frequent FeHV1 recurrences can be difficult to treat (Gaskell et al., 2007; Maggs, 2005).

FeHV1 primarily replicates in epithelial cells of ocular and respiratory mucosae, which include conjunctivae, nasal septum, turbinates, nasopharynx and upper trachea, resulting in surface epithelial erosion and inflammation (Binns et al., 2000; Filoni et al. 2006; Jacobi and Dubielzig, 2008). After release from these cells, the virus enters axons of sensory neurons and travels to the trigeminal ganglion where it establishes lifelong latency (Maes, 2012). Sometimes, a severe conjunctivitis may be accompanied by cornea ulceration, but whether the cornea epithelium is a portal for primary FeHV1 infection is unclear. A feline cornea cell line has been found to be susceptible for FeHV1, but primary cornea FeHV1 infection is rarely observed in cats under natural conditions (Andrew, 2001; Sandmeyer et al., 2005; Townsend et al., 2013). Upon experimental inoculation into the conjunctival sacs of cats, FeHV1 was isolated from both corneal and conjunctival samples. However, histologic lesions were nearly exclusively found in conjunctival samples (Townsend et al., 2013). Ocular inoculation by intrastromal injection or topical application after scarifying the epithelium resulted in viral replication in both cornea and conjunctiva. Viral antigens were mainly observed in the conjunctival epithelium and to a lesser extent in the corneal epithelium (Nasisse et al., 1989). The host possesses several barriers that hamper invasion of pathogens. One essential barrier is the basement membrane (BM) underneath the epithelia (Martinez-Hernandez and Amenta, 1983). Previous studies in our laboratory have shown that alphaherpesviruses behave differently at the BM. The replication of equine herpesvirus 4 (EHV4) is restricted to the respiratory epithelium of the upper respiratory tract (Vandekerckhove et al., 2011). Herpes simplex virus 1 (HSV1), suid herpesvirus 1 (PRV) and bovine herpesvirus 1 (BoHV1) penetrate through the BM, to reach and infect susceptible cells located in the underlying connective tissues (Glorieux et al., 2011a,b; Steukers et al., 2012b). Equine herpesvirus 1 (EHV1) infects epithelial cells, but not underlying fibroblasts. Instead, it hijacks monocytes in the epithelium to invade its host (Vandekerckhove et al., 2010). Little is known about how FeHV1 behaves at respiratory and ocular mucosae. Since

FeHV1 ocular and respiratory infections in domestic cats resemble HSV1 infections in humans in many aspects, a better characterization of the pathogenesis of FeHV1 infections may contribute to better insights in human alphaherpesvirus infections. Feline tracheal mucosa explants have already been used to study the mode of spread of FeHV1 in the respiratory epithelium (Leeming et al., 2006). The present study is, however, the first to set up mucosa explant models of feline ocular tissues. Kinetics of FeHV1 dissemination, including the interaction with the BM and the connective tissue underneath, were studied in both ocular and respiratory explants. The ex vivo explants have proven to be valuable for the investigation of the mucosal invasion of various alphaherpesviruses from horses, pigs, cattle and humans (Vandekerckhove et al., 2011; Steukers et al., 2012b; Glorieux et al., 2011a,b).

3.3 Materials and methods

3.3.1 Animals

This study was approved by the Ethical Committee of the Faculty of Veterinary Medicine, Ghent University (application EC2012/043). Cats were examined in veterinary clinics, blood was collected to determine FeHV1 specific antibody titers with a complement-dependent seroneutralization (SN)-test. Gender and breed were not considered in this experiment. Three seronegative cats without any ocular or respiratory symptoms were selected for this experiment. Two cats were 4 years old, the third was 9 years old. Cats were sedated by intramuscular injection of a mixture of Ketamin (0.05 mL/kg; Anesketin®, Eurovet, Heusden Zolder, Belgium) and Midazolam (0.05 mL/kg; Dormicum®, Roche, Brussels, Belgium). Then, cats were euthanized by intracardial injection of 20% sodium pentobarbital (1 mL/1.5 kg; Kela Laboratories, Hoogstraten, Belgium). Within 10 min, the whole cornea, palpebral conjunctiva and proximal trachea were harvested in a laminar flow hood using sterile equipment.

3.3.2 Air-liquid explant culture

The protocols for making feline ocular and respiratory explants were similar. In brief, tissues were transferred in ice-cold medium containing phosphate-buffered saline (PBS), supplemented with 1 μg/mL gentamycin (Invitrogen, Paisley, UK), 1 mg/mL streptomycin (Certa, Braine l'Alleud, Belgium), 1 mg/mL kanamycin (Sigma, St. Louis, MO, USA), 1000 U/mL penicillin (Continental Pharma, Puurs, Belgium) and 5 μg/mL amphotericin (Bristol-Myers Squibb, New York, USA). Then, the tissues were cut into equal sections with a size of approximately 16 mm^2. The tracheal tissues were taken with cartilage. Then, the tissues were placed with the epithelium upwards on sterile gauzes in individual wells of a 6-well plate. To mimic the air-liquid interface, only a thin film of culture medium covered the surface of the explants at 37 °C and 5% CO_2 up to 96 h. The culture medium consisted of 50% DMEM (Invitrogen)/50% Ham's F-12 Gluta-MAX (Invitrogen), supplemented with 0.1 mg/mL streptomycin (Certa), 100 U/mL penicillin (Continental Pharma) and 1 μg/mL gentamycin (Invitrogen). For cornea culture, the system was optimized by adding 5% dextran in the culture medium to prevent excessive swelling of the cornea (Redbrake e et al., 1997). At each time point, one explant from each tissue of each animal was randomly selected for viability analysis. At 24 h post cultivation, the remaining explants were used for viral inoculation.

3.3.3 Tissue viability

Tracheal tissues were observed under an inverted microscope, and only tissues with strong cilia beating were used. An In Situ Cell Death Detection Kit (Roche Diagnostics, Switzerland) was used for detection of apoptotic cells, based on terminal deoxynucleotidyl transferase-mediated dUTP nick end labeling (TUNEL). A Hoechst staining was performed to stain the cell nucleus. The test was performed according to the manufacturer's guidelines. The amount of TUNEL-positive cells was counted in five randomly selected fields of 100 cells in both epithelium and lamina

propria/stroma at 0, 24, 48, 72 and 96 h post cultivation. A fluorescence microscope (Leica TCS SP2 confocal microscopy) was used to analyze all samples.

3.3.4 Virus inoculation

FeHV1 strain C27 was kindly provided by Dr. R. Maes (College of Veterinary Medicine, Michigan State University, USA). The strain C27 had previously received an unknown number of passages. The virus was passaged once more in Crandell Rees feline kidney (CRFK) cells in our laboratory and this virus was used to inoculate the explants. At 24 h after cultivation, the explants were washed twice in culture medium in a 24-well plate (Nunc). Then, explants were inoculated with 1 ml medium containing $10^{7.0}$ $TCID_{50}$/mL FeHV1 for 1 h at 37 °C. After inoculation, explants were washed three times and then replaced on the gauze. Explants were collected at 0, 24, 48 and 72 hpi. All samples were embedded in a cryoprotection medium (Methocel, Fluka (Sigma)) and frozen at −70 °C.

3.3.5 Immunostaining

Immunostaining of sections was performed as previously described (Steukers et al., 2012b). Sections were fixed in methanol (-20 °C, 100%). To evaluate the distribution of FeHV1 infected epithelial cells and FeHV1 penetration underneath the BM, a double staining was performed. Mouse anti-collagen VII antibodies (Sigma) (1:100 in PBS, 1 h, 37 °C) and goat anti-mouse Texas Red® antibodies (Molecular Probes) (1:50 in PBS, 1 h, 37 °C) were applied to visualize the BM. After washing, an FITC-labeled anti-FeHV1 polyclonal antiserum (VMRD, Pullman, WA, USA) (undiluted, 1 h, 37 °C) was used to visualize virus positive cells in the explants. At each examined timepoint, a mock-inoculated tissue was enclosed. Sections were mounted and analyzed by confocal microscopy (Leica TCS SP2 confocal microscopy). A quantitative reproducible and complete three-dimensional picture of the horizontal and vertical spread of FeHV1 in the mucosa was obtained by confocal microscope

analysis of serial tissue sections. An extended focus image in the confocal microscope was used to display three dimensional information.

3.3.6 Statistical analysis

Prior to statistical analyses, all variables were checked for assumptions of ANOVA (normality and homoscedasticity) by Shapiro–Wilk's and Levene's test. Viral plaque diameter values were log-transformed to meet assumptions of normality and homoscedasticity. A three-way ANOVA, mixed effects model, was used to identify significant differences in viral plaque diameter (i) over different time points post inoculation, (ii) between respiratory and ocular mucosa explants and (iii) between three random seronegative cats. A post-hoc Scheffé's test was carried out in order to compare separate groups.

Since TUNEL-staining data and viral plaque penetration depth data were heteroscedastic after log-transformation, a Kruskal–Wallis' test followed by Mann–Whitney's post-hoc test were performed. For all statistical tests used, P-values <0.05 were considered statistically significant. All analyses were conducted in IBM SPSS Statistics for Windows, version 22.0 (IBM Corp, Armonck, NY, USA).

3.4 Results

3.4.1 Viability

The effect of cultivation on the viability of explants is shown in Table 1. The percentages of apoptotic cells in both epithelium and lamina propria were determined by confocal microscopy at each time point. The percentage of apoptotic epithelial cells slightly but significantly increased over time post cultivation in cornea, conjunctiva and trachea explants (all $P < 0.05$). Similar results were found for cells present in the lamina propria. The highest percentage of apoptosis (8.2 ± 5.3) was

observed in tracheal explants among cells in the lamina propria but mean viability remained above 90%.

Table 1. *Occurrence of apoptosis in epithelium and lamina propria as a parameter for the effect of in vitro culture on the viability of feline ocular and respiratory mucosa explants. TUNEL-positive cells were counted from five randomly chosen fields of 100 cells. Values are given as means ± SD.*

Tissue	Layer	% of TUNEL-positive cells at … h post cultivation				
		0	24	48	72	96
Cornea	Epithelium	1.3±0.3	1.5±0.5	0.9±0.3	1.3±0.7	2.1±0.8
	Lamina propria	0.8±0.6	2.9±0.5	2.3±2.5	3.8±2.6	5.2±3.5
Conjunctiva	Epithelium	0.6±0.5	0.8±0.7	1.5±0.5	2.1±0.6	2.3±1.0
	Lamina propria	0.7±0.6	2.5±3.2	5.6±3.5	7.4±2.7	7.2±3.5
Trachea	Epithelium	0.3±0.5	0.8±0.7	0.7±0.5	2.7±1.3	4.3±2.7
	Lamina propria	1.1±3.1	3.5±4.3	4.5±2.6	5.2±3.5	8.2±5.3

3.4.2 Evolution of FeHV1 mucosal spread

Mock-inoculated samples (negative controls) did not show any FeHV1 positive cells in conjunctival and tracheal mucosa explants throughout the culture period. As shown in Figure 1, FeHV1 was found to spread in a plaque-wise manner as the result of direct cell-to-cell spread. Individual plaques were visible starting from 24 hpi in explant tissues derived from all cats. In the cornea, virus infection was observed at the borders of the explants, but plaques were absent in the centers of the explants at all time points. The evolution of plaque diameter and penetration depth underneath the BM was investigated at 0, 24, 48 and 72 hpi in conjunctival and tracheal mucosa explants.

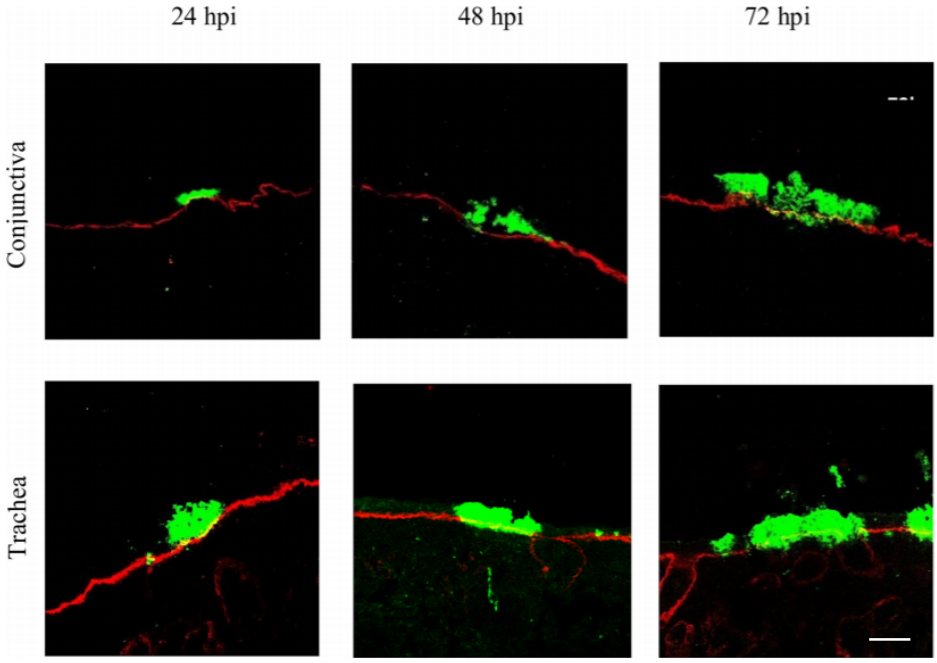

Figure 1. Confocal photomicrograph of FeHV1 infected feline conjunctiva and trachea explants at 24, 48 and 72 h post inoculation (hpi). *Collagen VII of the basement membrane is stained red; viral antigen positive cells are stained green. Scale bar = 100 µm.*

Plaque diameter (Figure 2) - In explant tissues derived from all cats, plaques were present in conjunctival and tracheal explants starting at 24 hpi. A statistically significant difference in viral plaque diameter was observed between different timepoints ($P < 0.001$) and between the two mucosa explants ($P < 0.05$). Viral plaque diameter did not differ significantly between the three cats ($P = 0.138$). Viral plaque diameter increased significantly over time from 24 hpi (96 ± 30µm) to 48 hpi (194 ± 60µm) and from 48 to 72 hpi (287 ± 67µm). At 24 and 72 hpi, viral plaque diameter did not differ significantly between trachea and conjunctiva ($P = 0.33$ and 0.98 respectively). However, at 48 hpi viral plaques in the trachea were on average 38 ± 15µm wider than in conjunctiva ($P < 0.05$).

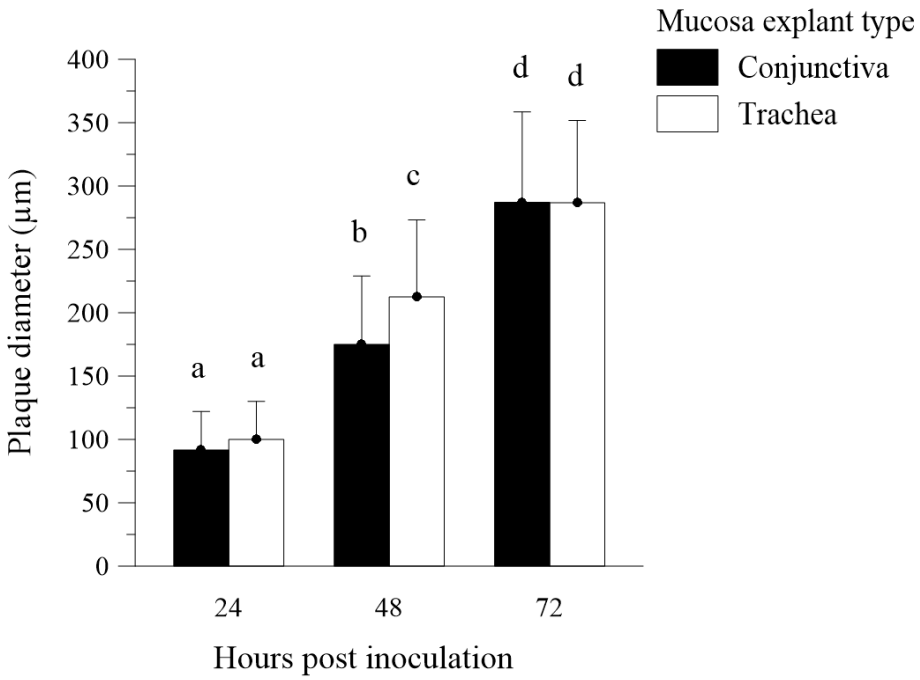

Figure 2. Evolution of the mean FeHV1 plaque diameter in conjunctival and tracheal mucosa explants at 24, 48 and 72 hpi (3 cats, 10 plaques per cat). *Three-way ANOVA, followed by Scheffé's post-hoc test, were performed. Different letters indicate significant differences (P < 0.05). Data are represented as mean + SD.*

Penetration depth (Figure 3) - Similarly to the viral plaque diameter, a significant difference in plaque penetration depth underneath the BM was observed between different time points ($P < 0.001$) and between the two types of mucosa explants ($P < 0.05$). No significant difference was found between the three cats ($P = 0.120$). Except for one plaque in a tracheal explant, that penetrated 17µm underneath the BM, no vertical spread of virus was observed at 24 hpi. FeHV1 plaques penetrated 21 ± 18µm underneath the BM at 48 hpi and 34 ± 21µm at 72 hpi. Plaque penetration depth increased significantly over all different time points (all $P < 0.05$). At 48 and 72 hpi, plaques in trachea explants extended on average 13 ± 4µm and 13 ± 6µm further underneath the BM than in conjunctiva explants (all $P < 0.05$).

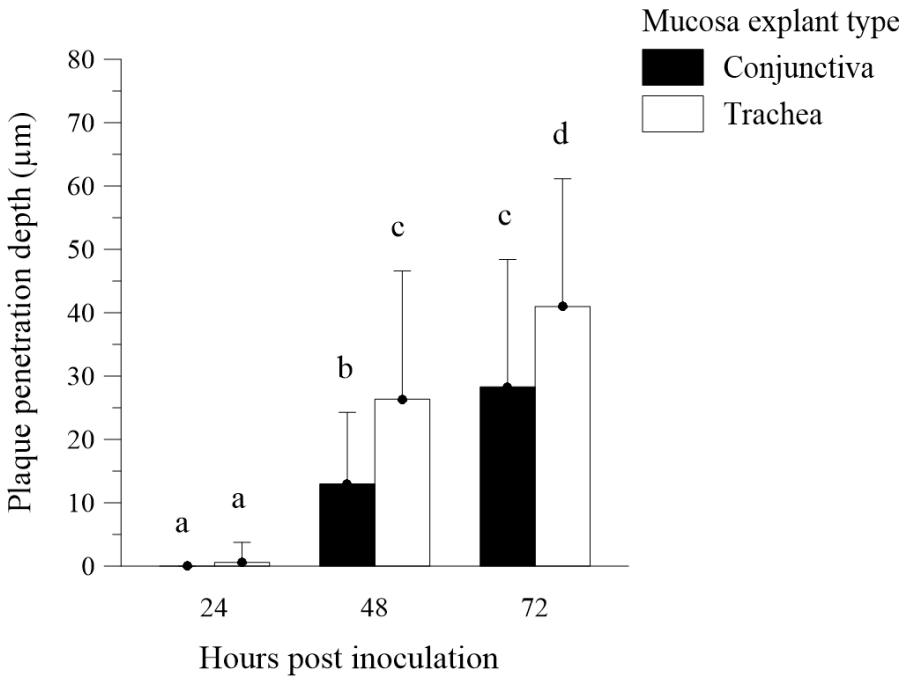

Figure 3. Evolution of the mean FeHV1 plaque penetration depth underneath the BM in conjunctival and tracheal mucosa explants at 24, 48 and 72 hpi (3 cats, 10 plaques per cat). *A Kruskal-Wallis' test, followed by Mann-Whitney's post hoc test, were performed. Different letters indicate significant differences ($P < 0.05$). Data are represented as mean + SD.*

3.5 Discussion

In the present study, we described FeHV1 replication in ocular and respiratory mucosae during the first 72 hpi using in vitro mucosa explants. Our study shows that (i) FeHV1 replicated in conjunctival and respiratory mucosa, but not in the cornea; (ii) FeHV1 replicated in a plaque-wise manner and penetrated the BM after 24 hpi. Our finding is in line with previous reports in experimentally infected cats. FeHV1 was found to preferentially infect and induce necrosis in the conjunctiva rather than in the cornea (Nasisse et al., 1989; Townsend et al., 2013). Our study shows that virus infection occurred at the edges, but not in the intact center of corneal tissues. This suggests that the FeHV1 C27 strain may spread in a cell associated manner from the open edges into corneal tissues. Similar to FeHV1, HSV1 exhibits an eye tropism. In

vivo studies in mice have shown that some, but not all, HSV1 strains require scarification prior to inoculation in order to successfully infect the cornea. Non-traumatic inoculation with HSV1, results in viral replication in the conjunctiva, but not in the cornea (Kaye et al., 1992; Tullo et al., 1983; Zheng et al., 2001). Absence of herpesvirus infection in the intact corneal tissue in the present study may be due to several factors. First, the mucins at the cornea surface may hamper the attachment of herpesviruses to corneal epithelial cells, in a similar way as they do in the respiratory tract (Yang et al., 2012). Secondly, it is possible that receptors are absent at the surface of the epithelial cells, leading to a state of resistance. Thirdly, viral replication of the FeHV1 C27 strain might be attenuated or modified by passage. This could impair its ability to infect the intact cornea. It is known that passage often leads to a loss of glycoproteins involved in cell entry, and this could explain the apparent inability to infect the cornea, particularly since there is extensive ocular and corneal involvement *in vivo*.

Our data show that FeHV1 crossed the BM more efficiently in tracheal mucosa than in conjunctival mucosa. At 48 hpi and 72 hpi, more plaques penetrated the BM in the trachea than in the conjunctiva, indicating that the virus requires more time to penetrate the BM in conjunctiva. A trypsin-like serine protease, which can degrade collagen in the BM, has been demonstrated to mediate penetration of herpesviruses through the BM (Glorieux et al., 2011b). Because the BM barriers can vary in composition and thickness depending on the tissue/organ, it is possible that the BM of the conjunctival mucosa is thicker, more complex and/or has more components, and is, therefore, more difficult for virus particles to penetrate (Steukers et al., 2012a). Although FeHV1 is phylogenetically most closely related to CaHV1, EHV1 and EHV4, they all behave differently in penetrating the BM (Davison, 2002; Gaskell and Willoughby, 1999). CaHV1 penetrates the BM in a plaque-wise manner, but more slowly than FeHV1 does (unpublished data). EHV1 and EHV4 replication is restricted

to epithelial cells. In addition, EHV1 uses monocytic cells and T-lymphocytes as "Trojan horses" to transport the virus through the BM (Vandekerckhove et al., 2010; Vandekerckhove et al., 2011). FeHV1 exhibited a plaque-wise mucosal spread very similar to BoHV1 and PRV, but with smaller plaque diameters and depths than those of BoHV1 and PRV (Davison, 2002; Field et al., 2006; Glorieux et al., 2009; Steukers et al., 2012b; Vandekerckhove et al., 2010). These different behaviors of alphaherpesviruses in their respective hosts are probably the result of a lifelong co-evolution.

To our knowledge, this is the first report describing a feline ocular mucosa model, consisting of explants. Experimental animal infection models allow studies that are close to the field situation, but raise many ethical issues especially in companion animals such as cats. The use of an explant model reduces the number of experimental animals, and is a compromise between in vitro cell cultures and in vivo laboratory animals. Tracheal mucosa explants have previously been used to study FeHV1 infections (Leeming et al., 2006). However, the viability of these explants was only monitored based on the ciliary beating of the epithelial layer. No information was available on the viability of the lamina propria. The in vitro model should mimic in vivo conditions with an intact BM and viable cells in both epithelial and lamina propria for a better understanding of the pathogen invasion. Here, both the ocular and respiratory mucosa explants that were kept at an air-liquid interface, were in an optimal condition and thus, closely represent the in vivo situation. However, like any other experimental models, it has important limitations. First, the explant system can only mimic the acute infection within the first 3 days. In addition, the in vitro system can only mimic the effects of in vivo local factors. Immunological factors originating from blood are absent.

Clinically, the ocular disease induced by FeHV1 is very similar to that of herpes simplex virus 1 (HSV1). In both cats and humans, naturally occurring primary ocular infections consistently cause conjunctivitis, with minimal corneal involvement. Primary HSV1 keratitis may appear as multiple scattered microdendritic figures, similar to those observed in cats following primary exposure to FeHV1. For both FeHV1 and HSV1, infection of the natural host results in a dendritic keratitis that is usually self-limiting (AlDujaili et al., 2011; Stiles, 2014; Townsend et al., 2013). Based on their similarities, FeHV1 infection of the eyes in cats is a valuable homologous model to study herpesvirus-induced ocular diseases in humans. Thus, the feline ocular model is ideal to study herpesvirus eye interactions since human ocular tissue is difficult to obtain. Especially, this model provides a useful tool for the investigation of ocular antiviral drugs.

In conclusion, we successfully developed in vitro feline ocular and respiratory mucosa explant models to study FeHV1 invasion at the primary replication sites. FeHV1 did not replicate in corneal tissues, but was found to spread in a plaque-wise manner in both conjunctival and tracheal tissues. Plaque penetration of the BM started at 24 hpi and at 72 hpi most plaques crossed the BM. Furthermore, FeHV1 invaded the BM and underlying connective tissue more efficiently in tracheal than in conjunctival mucosa.

3.6 Acknowledgements

The authors would like to express their gratitude to the cat owners for their essential contribution to the work. Special thanks go to Dr. R. Maes for providing the FeHV1C27 strain. Ivy K. Brown is acknowledged for the linguistic support. Yewei Li received financial support from the China Scholarship Council (CSC). This research was supported by Ghent University (Concerted Research Action 01G01311). Jolien Van Cleemput is a reseacher sponsored by the Research Foundation Flanders (FWO) (11Y5415N). Yewei Li, Jolien Van Cleemput, Vishwanatha R.A.P. Reddy, and Hans

J. Nauwynck are members of the BELVIR consortium (IAP, phase VII) sponsored by Belgian Science Policy Office (BELSPO).

3.7 References

Al-Dujaili, L.J., Clerkin, P.P., Clement, C., McFerrin, H.E., Bhattacharjee, P.S., Varnell, E.D., Kaufman, H.E., Hill, J.M., 2011. Ocular herpes simplex virus: how are latency, reactivation, recurrent disease and therapy interrelated? Future Microbiology 6(8), 877-907.

Andrew, S.E., 2001. Ocular manifestations of feline herpesvirus. J Feline Med Surg 3(1), 9-16.

Binns, S.H., Dawson, S., Speakman, A.J., Cuevas, L.E., Hart, C.A., Gaskell, C.J., Morgan, K.L., Gaskell, R.M., 2000. A study of feline upper respiratory tract disease with reference to prevalence and risk factors for infection with feline calicivirus and feline herpesvirus. J Feline Med Surg 2(3), 123-133.

Davison, A.J., 2002. Evolution of the herpesviruses. Vet Microbiol 86(1-2), 69-88.

Field, H.J., Biswas, S., Mohammad, I.T., 2006. Herpesvirus latency and therapy--from a veterinary perspective. Antiviral Res 71(2-3), 127-133.

Filoni, C., Catao-Dias, J.L., Bay, G., Durigon, E.L., Jorge, R.S., Lutz, H., Hofmann-Lehmann, R., 2006. First evidence of feline herpesvirus, calicivirus, parvovirus, and Ehrlichia exposure in Brazilian free-ranging felids. J Wildl Dis 42(2), 470-477.

Gaskell, R., Dawson, S., Radford, A., Thiry, E., 2007. Feline herpesvirus. Vet Res 38(2), 337-354.

Gaskell, R., Willoughby, K., 1999. Herpesviruses of carnivores. Vet Microbiol 69(1-2), 73-88.

Glorieux, S., Bachert, C., Favoreel, H.W., Vandekerckhove, A.P., Steukers, L.,

Rekecki, A., Van den Broeck, W., Goossens, J., Croubels, S., Clayton, R.F., Nauwynck, H.J., 2011a. Herpes simplex virus type 1 penetrates the basement

membrane in human nasal respiratory mucosa. PLoS One 6(7), e22160.

Glorieux, S., Favoreel, H.W., Meesen, G., de Vos, W., Van den Broeck, W., Nauwynck, H.J., 2009. Different replication characteristics of historical pseudorabies virus strains in porcine respiratory nasal mucosa explants. Vet Microbiol 136(3-4), 341-346.

Glorieux, S., Favoreel, H.W., Steukers, L., Vandekerckhove, A.P., Nauwynck, H.J., 2011b. A trypsin-like serine protease is involved in pseudorabies virus invasion through the basement membrane barrier of porcine nasal respiratory mucosa. Vet Res 42, 58.

Jacobi, S., Dubielzig, R.R., 2008. Feline early life ocular disease. Vet Ophthalmol 11(3), 166-169.

Kaye, S.B., Shimeld, C., Grinfeld, E., Maitland, N.J., Hill, T.J., Easty, D.L., 1992. Non-traumatic acquisition of herpes simplex virus infection through the eye. Br J Ophthalmol 76(7), 412-418.

Leeming, G., Meli, M.L., Cripps, P., Vaughan-Thomas, A., Lutz, H., Gaskell, R., Kipar, A., 2006. Tracheal organ cultures as a useful tool to study Felid herpesvirus 1 infection in respiratory epithelium. J Virol Methods 138(1-2), 191-195.

Maes, R., 2012. Felid herpesvirus type 1 infection in cats: a natural host model for alphaherpesvirus pathogenesis. ISRN Vet Sci 2012, 495830.

Martinez-Hernandez, A., Amenta, P.S., 1983. The basement membrane in pathology. Lab Invest 48(6), 656-677.

Nasisse, M.P., Guy, J.S., Davidson, M.G., Sussman, W.A., Fairley, N.M., 1989. Experimental ocular herpesvirus infection in the cat. Sites of virus replication, clinical features and effects of corticosteroid administration. Invest Ophthalmol Vis Sci 30(8), 1758-1768.

Sandmeyer, L.S., Keller, C.B., Bienzle, D., 2005. Effects of cidofovir on cell death and replication of feline herpesvirus-1 in cultured feline corneal epithelial cells.

Am J Vet Res 66(2), 217-222.

Steukers, L., Glorieux, S., Vandekerckhove, A.P., Favoreel, H.W., Nauwynck, H.J., 2012a. Diverse microbial interactions with the basement membrane barrier. Trends Microbiol 20(3), 147-155.

Steukers, L., Vandekerckhove, A.P., Van den Broeck, W., Glorieux, S., Nauwynck, H.J., 2012b. Kinetics of BoHV1 dissemination in an in vitro culture of bovine upper respiratory tract mucosa explants. ILAR J 53(1), E43-54.

Stiles, J., 2014. Ocular manifestations of feline viral diseases. Vet J 201(2), 166-173.

Thiry, E., Addie, D., Belak, S., Boucraut-Baralon, C., Egberink, H., Frymus, T., Gruffydd-Jones, T., Hartmann, K., Hosie, M.J., Lloret, A., Lutz, H., Marsilio, F., Pennisi, M.G., Radford, A.D., Truyen, U., Horzinek, M.C., 2009. Feline herpesvirus infection. ABCD guidelines on prevention and management. J Feline Med Surg 11(7), 547-555.

Townsend, W.M., Jacobi, S., Tai, S.H., Kiupel, M., Wise, A.G., Maes, R.K., 2013. Ocular and neural distribution of feline herpesvirus-1 during active and latent experimental infection in cats. BMC Vet Res 9, 185.

Tullo, A.B., Shimeld, C., Blyth, W.A., Hill, T.J., Easty, D.L., 1983. Ocular infection with herpes simplex virus in nonimmune and immune mice. Arch Ophthalmol 101(6), 961-964.

Vandekerckhove, A.P., Glorieux, S., Gryspeerdt, A.C., Steukers, L., Duchateau, L., Osterrieder, N., Van de Walle, G.R., Nauwynck, H.J., 2010. Replication kinetics of neurovirulent versus non-neurovirulent equine herpesvirus type 1 strains in equine nasal mucosal explants. J Gen Virol 91(Pt 8), 2019-2028.

Vandekerckhove, A.P., Glorieux, S., Gryspeerdt, A.C., Steukers, L., Van Doorsselaere, J., Osterrieder, N., Van de Walle, G.R., Nauwynck, H.J., 2011. Equine alphaherpesviruses (EHV1 and EHV4) differ in their efficiency to infect mononuclear cells during early steps of infection in nasal mucosal explants. Vet Microbiol 152(1-2), 21-28.

Yang, X., Forier, K., Steukers, L., Van Vlierberghe, S., Dubruel, P., Braeckmans, K., Glorieux, S., Nauwynck, H.J., 2012. Immobilization of pseudorabies virus in porcine tracheal respiratory mucus revealed by single particle tracking. PLoS One 7(12), e51054.

Zheng, X., Silverman, R.H., Zhou, A., Goto, T., Kwon, B.S., Kaufman, H.E., Hill, J.M., 2001. Increased severity of HSV1 keratitis and mortality in mice lacking the 2-5A-dependent RNase L gene. Invest Ophthalmol Vis Sci 42(1), 120-126.

CHAPTER 4

Viral dynamics of Canine herpesvirus 1 in canine respiratory and genital mucosae by the use of *ex vivo* models

Yewei Li, Haileleul Negussie, Yu Qiu, Vishwanatha R.A.P. Reddy, Bart Mateusen, Hans J. Nauwynck

Adapted from Research in Veterinary Science 105 (2016) 205–208

4.1 Abstract

Canine herpesvirus 1 (CaHV1) causes a systemic disease in newborn puppies, kennel cough at all ages and genital lesions in adult dogs. The aim of the present study was to elucidate the viral behavior during the early stage of infection in respiratory and genital mucosae, the portals of entry for CaHV1 by the use of ex vivo explants. CaHV1 infected and replicated in respiratory and vaginal mucosae in a plaque wise manner. CaHV1 started to penetrate the basement membrane (BM) only after 48 h post inoculation (hpi) in respiratory mucosal explants, but already after 24 hpi in vaginal explants. The plaque latitude and penetration depth increased over time and both were larger in the vaginal explants compared to the respiratory mucosal explants. The canine respiratory and genital mucosal explants were suitable to study the early pathogenesis of CaHV1. CaHV1 showed a better capacity to replicate and invade vaginal mucosa compared to respiratory mucosa, based on the latitude and penetration depth of the plaques of viral antigen positive cells.

4.2 Introduction

Canine herpesvirus-1 (CaHV1) is an alphaherpesvirus with a host range, and can mainly cause respiratory and genital diseases in dogs (Buonavoglia and Martella, 2007). CaHV1 is transmitted predominantly through licking, coughing, copulation and transplacental spread, and the mucosae of upper respiratory and genital tract are important gateways for virus entry (Evermann et al., 2011). Knowledge of the pathogenesis CaHV1 is limited. CaHV1 enters and replicates in epithelial cells, then it is transported via sensory neuronal axons to the neuronal cell bodies of trigeminal and dorsal root ganglia, where it replicates and spreads to neighbouring neurons. Thereafter, the virus either establishes a latent infection or is transported back to mucocutaneous sites where it is released and replicates, potentially leading to cell lysis and the characteristic lesions of a primary CaHV1 infection (Buonavoglia and

Martella, 2007). However, little is known about how CaHV1 behaves at respiratory and vaginal mucosae.

In order to better understand the primary infection kinetics of CaHV1, we set up an in vitro explant model of respiratory and genital tract mucosae derived from bitches to mimic the in vivo situation of CaHV1 invasion.

4.3 Materials and methods

4.3.1 Animals

Using tissues of euthanized animals is in agreement with the statement of the Local Ethical and Animal Welfare Committee of the Faculty of Veterinary Medicine, Ghent University. Three female dogs euthanized with phenobarbital (1 mL/1.5 kg; Kela Laboratories, Hoogstraten, Belgium) were used as tissue donors with informed owner consent. The reason for euthanasia was different from respiratory and genital problems. The animals did not show any symptom of respiratory or genital disease. Their history of prior exposure to respiratory viruses was not known. Blood was collected and examined for CaHV1-specific neutralizing antibodies with the complement-dependent seroneutralization test. The ages of the dogs were 5, 7 and 12 years. The trachea and vagina were isolated immediately after euthanasia. All isolation procedures were performed in a laminar flow.

4.3.2 Air-liquid tissue culture

Canine respiratory and genital mucosal explants were observed and cultivated based on a slightly modified protocol as previously described (Steukers et al., 2011). In brief, large pieces of trachea and vagina were transferred in a buffered saline solution (PBS), supplemented with 1µg/mL gentamycin (Invitrogen, Paisley, UK), 1 mg/mL streptomycin (Certa, Braine l'Alleud, Belgium), 1 mg/mL kanamycin (Sigma, St. Louis, MO, USA), 1000 U/mL penicillin (Continental Pharma, Puurs, Belgium) and

5μg/mL fungizone (Bristol- Myers Squibb, New York, USA) on ice. Next, the vaginal mucosa was stripped from the underlying layers. The tracheal mucosa was left on the cartilage. Then, tissues were cut into equal pieces with a size of approximately 25mm^2. All respiratory tissues were observed under a stereomicroscope for cilia beating, and only respiratory tissues in which cilia beating was present all over the explants were used. Finally, tissues were placed epithelium upwards on sterilized gauzes in 6-well plates for culture at an air-liquid interface. The explants were cultured in serum-free medium containing 50% DMEM (Invitrogen)/50% Ham's F-12 Gluta-MAX (Invitrogen) supplemented with 0.1 mg/mL streptomycin (Certa), 100 U/mL penicillin (Continental Pharma) and 1 μg/mL gentamycin (Invitrogen). Only a thin film of medium covered the explants, thereby mimicking the air-liquid interface found in the respiratory and genital tract of living animals. All explants were maintained at 37 °C and 5% CO_2.

4.3.3 Tissue viability

To determine the viability of the explants, the *In Situ* Cell Death Detection Kit (Roche Diagnostics, Switzerland) was used based on terminal deoxynucleotidyl transferase dUTP nick end-labeling (TUNEL), while a Hoechst staining was used to mark cell nuclei. The test was performed according to the manufacturer's guidelines. The amount of TUNEL-positive cells was counted from five randomly selected fields of 100 cells in both epithelium and lamina propria at 0, 24, 48, 72 and 96 h post cultivation. All samples were analyzed under a fluorescence microscope (Leica TCS SP2 confocal microscopy).

4.3.4 Virus inoculation

The CaHV1 F205 strain was purchased from ATCC (VR-1785TM). Stock virus was propagated in Madin-Darby canine kidney (MDCK) cells. The respiratory and vaginal mucosal explants were inoculated with the CaHV1 F205 strain as described for

BoHV1 before (Steukers et al., 2012b). Before inoculation, the explants were washed twice with PBS in a 24-well microplate (Nunc). Explants were then exposed to 1 ml virus suspension containing $10^{6.5}$ $TCID_{50}$/mL for 1h at 37°C. After inoculation with infectious virus, explants were washed three times and then placed back on the gauze. At each examined time point, a mock-inoculated tissue was enclosed. At 0, 24, 48 and 72 hpi respectively, respiratory and vaginal mucosal explants of each animal were collected and embedded in a cryoprotection medium (Methocel®, Fluka (Sigma)) and frozen at -70 °C.

4.3.5 Immunostaining

Consecutive cryosections (20 μm) were fixed in methanol (100%, -20°C) for 20 min. To evaluate the spread of CaHV1 in epithelial cells and its penetration depth underneath the basement membrane, a double staining was performed. Mouse anti-collagen VII antibodies (Sigma) (1:100 in PBS, 1h, 37°C) and goat anti-mouse IgG texas red (1:50, 1h, 37°C) were applied to visualize the BM. Afterwards, FITC-labeled anti-CaHV1 polyclonal antibodies (VMRD, Pullman, WA, USA) (undiluted, 1h, 37°C) were used to visualize virus positive cells in the explants. Samples were mounted and analyzed by confocal microscopy (Leica TCS SP2 confocal microscope).

4.3.6 Statistical analysis

Data were statistically evaluated by using SPSS software version 20. Normally distributed data were analyzed using ANOVA with Tukey *post hoc* test for comparison. The results were presented as means with standard deviation (SD). Data that were not normally distributed were analyzed with Mann-Whitney test. A p-value of < 0.05 was considered significant.

4.4 Results

4.4.1 Viability

The effect of cultivation on the viability of cells is shown in Table 1. The percentages of apoptotic cells in both epithelium and lamina propria were determined at each time point of cultivation using confocal microscopy. In the epithelium and lamina propria of both tissues, the number of apoptotic cells (TUNEL-positive cells) was slightly, but significantly ($p < 0.05$) increased over time. The percentages of apoptotic cells were less than 4% in the epithelium and less than 7% the lamina propria of the explants.

Table 1. *Occurrence of apoptosis in epithelium and lamina propria during in vitro culture of canine respiratory and genital mucosa explants.* *TUNEL-positive cells were counted from five randomly chosen fields of 100 cells. Values are given as means ± SD.*

Tissue	Layer	% of TUNEL-positive cells at…h post cultivation				
		0	24	48	72	96
Respiratory mucosa	Epithelium	0.4±0.5	0.7±0.6	0.6±0.5	1.6±0.9	1.8±1.3
	Lamina propria	0.6±0.6	1.9±2.6	4.3±3.0	5.9±2.6	5.5±3.0
Genital mucosa	Epithelium	0.3±0.4	0.7±0.6	0.7±0.5	2.4±1.4	3.7±2.8
	Lamina propria	0.4±0.7	2.7±3.3	4.7±2.8	4.1±2.6	6.2±4.5

SD, standard deviation

4.4.2 Evolution of CaHV1 mucosal spread (Figure 1)

The respiratory and vaginal mucosal explants of three dogs were inoculated with CaHV1 and evaluated at different time point post inoculation. Mock-inoculated explants (negative controls) did not show CaHV1 positive cells throughout the whole culture period in the respiratory and vaginal mucosae. CaHV1 was found to spread in a plaque-wise manner (Figure 1). CaHV1-induced individual plaques were observed

starting from 24 hpi in both explants. The evolution of plaque latitude and penetration depth underneath the BM could be followed up till the end of the experiment (72 hpi) in respiratory mucosal explants, but only up till 48 hpi as almost all epithelial cells in the canine vaginal tissues were infected.

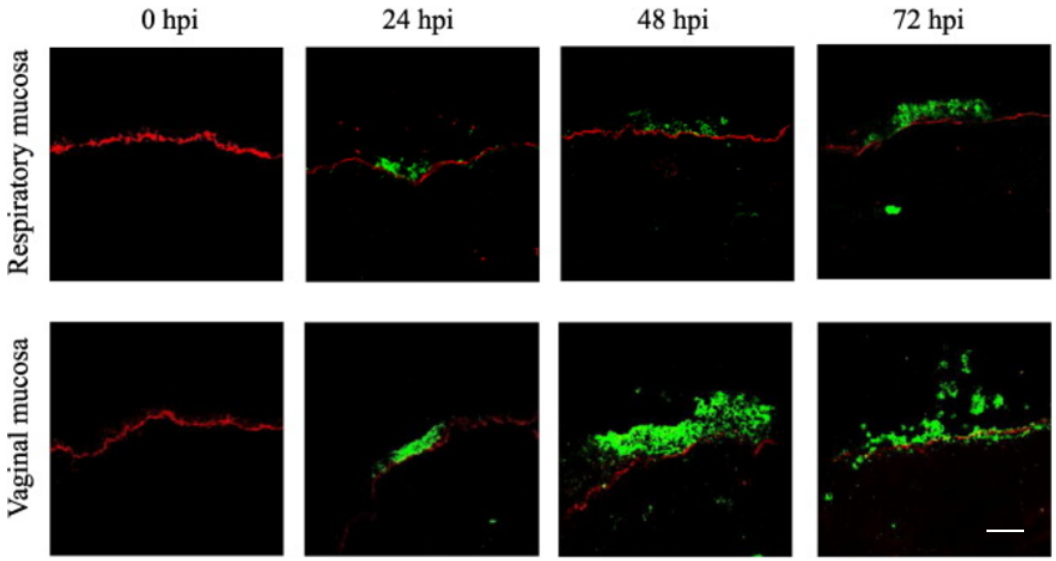

Figure 1. Confocal photomicrograph of CaHV1 infected canine respiratory and vaginal mucosa explants at 0, 24, 48 and 72 hpi. *Collagen VII of the basement membrane is stained red; viral antigen positive cells are stained green. Scale bar = 100 µm.*

4.4.3 CaHV1- induced plaque latitude (Figure 2)

The latitude of CaHV1-induced plaques in respiratory mucosal explants increased over time with an average of 106.0 ± 43.4 µm at 24 hpi, 138.9 ± 76.3 µm at 48 hpi and 170.3 ± 119.9 µm at 72 hpi in dog 1 (not significantly different; $p = 0.292$); an average of 70.3 ± 18.6 µm at 24 hpi, 133.6 ± 86.0 µm at 48 hpi and 162.6 ± 50.9 µm at 72 hpi in dog 2 (significantly different; $p = 0.021$); an average of 95.2 ± 67.3 µm at 24 hpi, 155.4 ± 54.7 µm at 48 hpi and 175 ± 45.8 µm at 72 hpi (significantly different; $p = 0.01$) in dog 3.

In the vaginal mucosal explants, the latitude of CaHV1-induced plaques increased significantly ($p < 0.001$) with an average of 106.7 ± 45.4 µm at 24 hpi and 401.4

±105.4 µm at 48 hpi in dog 1, 113.6 ± 42.3 µm at 24 hpi and 381.6 ± 108.6 µm at 48 hpi in dog 2, and 145.9 ± 46.0 µm at 24 hpi and 372.8 ± 102.2 µm at 48 hpi in dog 3. Taking together all results, the latitudes of CaHV1-induced plaques in respiratory mucosal explants were found to be significantly smaller ($p < 0.05$) than those in vaginal explants at 24 and 48 hpi.

4.4.4 Penetration depth

The plaque depth underneath the BM was evaluated at 0, 24, 48 and 72 hpi. There was a strong difference between respiratory tissues and genital tissues when comparing the penetration of the CaHV1-induced plaques through the BM, both in depth and rate.
In the respiratory mucosal explants, the plaque did not penetrate the BM in all dogs at 24 and 48 hpi. However, at 72 hpi, 1 out of 10 plaques and 4 out of 10 plaques crossed the BM in dog 2 and 3, respectively.

In the vaginal explants, only one plaque had penetrated the BM at 24 hpi whereas at 48 hpi, 44% of the CaHV1- infected cells plaques crossed the BM in all dogs. The average penetration depths in the vaginal explants increased significantly ($p < 0.001$) from 10.4 ± 19.5 µm at 48 hpi to 61.0 ± 13 µm at 72 hpi in dog 1; 38.7 ± 35.6 µm at 48 hpi to 51.9 ± 17.5 µm at 72 hpi in dog 2; from 3.0 ± 9.0 µm at 24 hpi, 23.2 ± 23.3 µm at 48 hpi and 63.9 ± 12.9 µm at 72 hpi.

The plaque penetration depth underneath the BM in the three independent experiments was significantly higher ($p < 0.05$) in the vaginal explants than in the respiratory mucosal explants at 48 and 72 hpi.

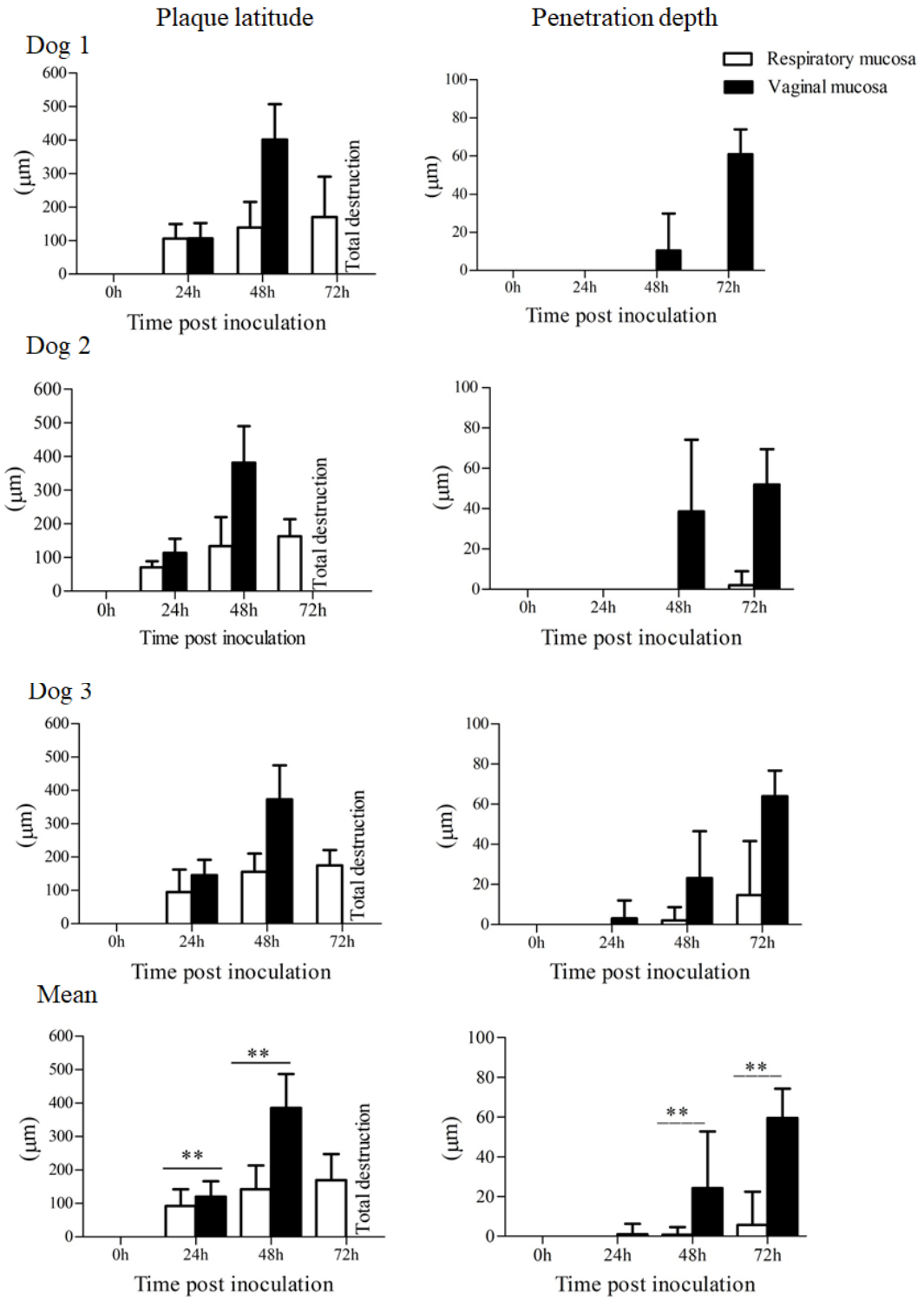

Figure 2. Evolution of CaHV1 plaque latitude and plaque penetration depth underneath the BM in the respiratory and vaginal mucosa explants at 24, 48 and 72 hpi (3 dogs, 10 plaques per dog). *Data represent the means and standard deviation of three independent experiments. Asterisks (**) indicate a significant difference between both types of explants.*

4.5 Discussion

Our study showed that plaque latitudes increased faster in the vaginal tissues than in the respiratory mucosal tissues between 24 and 48 hpi. This is similar to bovine herpesvirus 1 (Steukers et al., 2011), and can be explained by several reasons. Firstly, the vaginal tissues are less capable of generating local mucosal responses of the innate immunity compared to respiratory tissues (Russell and Mestecky, 2002). Secondly, the epithelial cell type and intercellular connections are different in these two different mucosae. The main cells of the respiratory epithelium are ciliated cells, which are of narrow columnar type (Pack et al., 1980). The main cells of the vaginal epithelium are squamous (Moll et al., 1983). Thus, more cells are present within the same area in the respiratory epithelium compared to the vaginal epithelium. When one considers one replication cycle and transmission to neighbouring cells every 12 h, a smaller area will be infected in respiratory mucosal explants than in vaginal explants. In addition, the stratified squamous epithelial cells of the vaginal mucosa are connected with more robust junctions than the ciliated epithelial of cells of the respiratory mucosa (Blaskewicz et al., 2011). These robust junctions may facilitate the cell-associated spread of the virus (Nauwynck et al., 2007).

In the vaginal mucosa, the replication characteristics of CaHV1 were similar to that of BoHV1, but both spread slower than HSV1/-2 in the stratified epithelium. In addition, HSV1/-2 induced prominent epithelial syncytia, which were not observed with CaHV1 or BoHV1 (Steukers et al., 2011; Steukers et al., 2014). The formation of syncytia in human tissues might be an example of co-evolution of human herpesvirus with their host. CaHV1 and BoHV1 have a better capacity to cross the BM of the vaginal explants compared to HSV1/2. In the near future, the underlying mechanism, which may give an explanation for this difference, will be elucidated.

CaHV1 is genetically closely related to feline herpes virus 1 (FeHV1), but unlike CaHV1, FeHV1 seldom induces reproductive problems (Thiry et al., 2009). Recent experiments with feline vaginal explants have demonstrated that upon FeHV1 inoculation plaques are formed which rarely penetrate the BM (unpublished data). The present study shows that CaHV1 had a main tropism for the genital epithelium, which agrees with in vivo findings with CaHV1-induced vesicles and ulcerations in the genital tract (Evermann et al., 2011).

In conclusion, ex vivo canine respiratory and genital mucosa explants were established, enabling research on CaHV1 replication and invasion. CaHV1 spreads in a plaque wise manner, and has a better tropism for genital than for respiratory tissues. Researchers may use these CaHV1 explant models to develop antiviral and safe attenuated vaccines in a research based way.

4.6 Conflict of interest statement

None of the authors of this paper has a financial or personal relationship with other people or organizations that could inappropriately influence or bias the content of the paper.

4.7 References

Blaskewicz, C.D., Pudney, J., Anderson, D.J., 2011. Structure and function of intercellular junctions in human cervical and vaginal mucosal epithelia. Biol Reprod 85(1), 97-104.

Buonavoglia, C., Martella, V., 2007. Canine respiratory viruses. Vet Res 38(2), 355-373.

Evermann, J.F., Ledbetter, E.C., Maes, R.K., 2011. Canine Reproductive, Respiratory, and Ocular Diseases due to Canine Herpesvirus. Vet Clin N Am-Small 41(6), 1097.

Moll, R., Levy, R., Czernobilsky, B., Hohlwegmajert, P., Dallenbachhellweg, G., Franke, W.W., 1983. Cytokeratins of Normal Epithelia and Some Neoplasms of the Female Genital-Tract. Lab Invest 49(5), 599-610.

Nauwynck, H., Glorieux, S., Favoreel, H., Pensaert, M., 2007. Cell biological and molecular characteristics of pseudorabies virus infections in cell cultures and in pigs with emphasis on the respiratory tract. Veterinary Research 38(2), 229-241.

Pack, R.J., Alugaily, L.H., Morris, G., Widdicombe, J.G., 1980. The Distribution and Structure of Cells in the Tracheal Epithelium of the Mouse. Cell Tissue Res 208(1), 65-84.

Russell, M.W., Mestecky, J., 2002. Humoral immune responses to microbial infections in the genital tract. Microbes Infect 4(6), 667-677.

Steukers, L., Vandekerckhove, A.P., Van den Broeck, W., Glorieux, S., Nauwynck, H.J., 2011. Comparative analysis of replication characteristics of BoHV1 subtypes in bovine respiratory and genital mucosa explants: a phylogenetic enlightenment. Veterinary Research 42.

Steukers, L., Weyers, S., Yang, X.Y., Vandekerckhove, A.P., Glorieux, S., Cornelissen, M., Van den Broeck, W., Temmerman, M., Nauwynck, H.J., 2014. Mimicking Herpes Simplex Virus 1 and Herpes Simplex Virus 2 Mucosal Behavior in a Well-Characterized Human Genital Organ Culture. J Infect Dis 210(2), 209-213.

Thiry, E., Addie, D., Belak, S., Boucraut-Baralon, C., Egberink, H., Frymus, T., Gruffydd-Jones, T., Hartmann, K., Hosie, M.J., Lloret, A., Lutz, H., Marsilio, F., Pennisi, M.G., Radford, A.D., Truyen, U., Horzinek, M.C., 2009. FELINE HERPESVIRUS INFECTION ABCD guidelines on prevention and management. Journal of Feline Medicine and Surgery 11(7), 547-555.

CHAPTER 5

Alphaherpesvirus infection activates the plasminogen activator-plasmin system in respiratory mucosa

Yewei Li, Jiexiong Xie, Jing Zhao, Haileleul Negussie, Vishwanatha R. A. P. Reddy,

Hans J. Nauwynck

Manuscript in preparation

5.1 Abstract

In the upper respiratory tract, the basement membrane (BM) is a barrier underlying the epithelial cell layer which is crossed during the invasion of alphaherpesviruses. Pseudorabies virus (PrV) directly breaches the BM barrier, which involves a serine protease. Here, we examined if the plasminogen activator-plasmin system, an enzymatic cascade for BM degradation, which is coordinated by serine proteases, is involved in the process of PrV BM penetration. In this study, porcine nasal mucosa explants were infected by pseudorabies virus. Immunofluorescence staining of porcine respiratory explants revealed that plasminogen and plasmin were present. Various forms of plasminogen and plasmin were found in porcine respiratory explants as demonstrated by Western blot. Plasmin was expressed in the epithelial virus plaque starting from 24 hours post inoculation (hpi) in porcine nasal mucosa explants. Further, the urokinase plasminogen activator (uPA) inhibitor WX-340 and the plasmin inhibitor tranexamic acid (TXA) were evaluated for their potential to inhibit the invasion of three pseudorabies virus (PrV) strains: NS374 (1971), 75V19 (1975) and 89V87 (1989). The penetration of the BM by NS374 and 75V19 was inhibited by both inhibitors, whereas 89V87 was significantly inhibited by TXA and only to a very limited extent by WX-340. These data revealed a clear role of the plasminogen activator-plasmin system in PrV invasion.

5.2 Introduction

Alphaherpesviruses use the upper respiratory mucosa for their primary replication and subsequent invasion. The passage of the virus through the basement membrane (BM) is a prerequisite for a successful host invasion (Steukers et al., 2012a). Alphaherpesviruses use different strategies to cross the BM in order to reach the underlying lamina propria. Some of alphaherpesviruses, including herpes simplex virus 1 (HSV1), pseudorabies virus (PrV), bovine herpesvirus 1 (BoHV1), feline herpesvirus 1 (FeHV1), and canine herpesvirus 1 (CaHV1) directly penetrate through the BM (Glorieux et al., 2011a; Glorieux et al., 2007; Li et al., 2016; Li et al., 2015;

Steukers et al., 2012b). Glorieux et al. (2011b) demonstrated that PrV crosses the BM by the use of a trypsin-like serine protease. In this study, the serine protease AEBSF inhibited the viral penetration through the BM. Further study using the Soybean Type I-S trypsin inhibitor of trypsin-like serine proteases, one of the serine protease subcategories, revealed the involvement of a trypsin-like serine protease in the PrV invasion process through the BM. Several cellular components associated with trypsin-like serine protease activity are differentially regulated upon infection with HSV1, including tissue-type plasminogen activator (tPA), urokinase plasminogen activator receptor (uPAR) and factor IX (Blanchard et al., 2006; Ray and Enquist, 2004). These cellular components are involved in the plasminogen activator-plasmin system (Stewart and Sayers, 2013).

The plasminogen activator-plasmin system contains the inactive proenzyme plasminogen, which is transformed into the proteolytically active plasmin mainly by two plasminogen activators, uPA and tPA (Syrovets and Simmet, 2004). uPA is an activator of extracellular proteolysis, and is involved in cell apoptosis, migration and proliferation (Collen and Lijnen, 1995; Plow et al., 1995). tPA facilitates fibrin break-down (Syrovets and Simmet, 2004). In general, plasminogen activation is more related to tissue damage and subsequent repair mechanisms than to specific pathological situations (Kramer et al., 1995). Epithelial cells release plasminogen activators which generate plasmin from plasminogen. Activation of the plasminogen activator-plasmin system leads to the degradation of both fibrin and fibronectin, as well as the laminin component of the BM (Berman et al., 1983). Due to these potential damaging activities, plasmin activity must be well regulated by the host.

The plasminogen activator-plasmin system may play a crucial role during pathogen infection. Plasminogen activation is tightly regulated by the balance between plasminogen activators tPA and uPA and their principal inhibitors-1 and 2 (Pepper,

2001). The balance may be broken by the entrance of pathogens into the epithelial cell. By doing this, plasmin may help the pathogen to cross the BM by degrading this barrier. Afterwards, the pathogen may disseminate to internal target organs. It has already been reported that HSV1 and 2, and cytomegalovirus (CMV) accelerate the proteolytic activation of plasminogen to plasmin by tPA (Gershom et al., 2012). Another human herpesvirus, Epstein-Barr virus (EBV), regulates uPA expression in tumors (Nakada et al., 1999). Induction or upregulation of the plasminogen activator-plasmin system in the upper respiratory mucosa during an alphaherpesvirus infection has not been reported yet. Whether this system can be activated during the viral-mucosa interaction and results in viral BM penetration is examined in the present study.

5.3 Materials and methods

5.3.1 Viruses

Three different Belgian PrV strains were used in this study. NS374, a mild PrV strain, and 75V19, a virulent PrV strain, were isolated from the brains of pigs with nervous symptoms in the 1970s. 89V87, a highly virulent PrV strain, was isolated in 1989 from an aborted foetus. All PrV strains were propagated in porcine testicle (ST) cells for 2 passages.

5.3.2 *Ex vivo* respiratory mucosa explant system

Porcine nasal mucosa explants were generated as previously described (Glorieux et al., 2009). At 24 h after cultivation, explants were placed in a 24-well plate and washed twice with warm medium. After 1h incubation with 1 ml inoculum containing 106.0 TCID50/ml of PrV, explants cultivated at 37 °C and 5% CO2. The explants were collected at 0, 24, 48 and 72 hpi and embedded in a cryoprotection medium (Methocel®, Fluka, Sigma) and frozen at -70 °C.

5.3.3 Western blot analysis of plasminogen and plasmin

SDS-PAGE and Western blot analyses were performed essentially as described previously (Setas Pontes et al., 2015). Briefly, porcine respiratory mucosa explant tissues were first homogenised. A loading buffer with the sample and the anionic detergent sodium dodecyl sulfate (SDS) was boiled at 100°C for 5 min to denature. Samples were run on a 12% polyacrylamide gel. After electrophoresis, the separated proteins were electroblotted onto nitrocellulose membranes. Blots were blocked for 60 min in a blocking solution (5% nonfat dry milk in PBS-Tween 20), and were subsequently incubated overnight with goat anti-plasminogen/plasmin antiserum (1:500; antibodies-online GmbH, Aachen, Germany). Following three washes with Tris-buffered saline, the membrane was incubated with rabbit anti-goat immunoglobulin HRP secondary antibody (1:3000, Dako, Denmark) for 1 h. Bovine plasminogen (biopur, Switzerland) was used as a positive control. The results were visualized with an ECL Western blot detection system (GE Healthcare).

5.3.4 Inhibitor assays in explants

We used tranexamic acid (TXA) as plasminogen inhibitor, which acts by competitively blocking the lysine binding sites of plasmin(ogen), thereby preventing binding to fibrin or cells (Dunn and Goa, 1999). WX-340, a highly specific and selective inhibitor of uPA, was also evaluated in this study (Endo-Munoz et al., 2015). At 24 h after cultivation, explants were placed in a 24-well plate and washed twice with warm medium. The explants were inoculated with 1 ml medium containing $10^{6.0}$ $TCID_{50}$/ml of PrV strains 89V87, 75V19 or NS374 for 1 h at 37 °C and 5% CO_2. At 1 hour post inoculation (hpi), explants were washed twice with warm medium and were immersed for 1 h in medium with or without inhibitor. In this assay, WX-340 was used at concentrations of 10, 30 and 100 µM, and TXA was used at concentrations of 1, 3 and 10 mM. Then, explants were transferred back from the 24-well plate to their

gauze with medium with or without the inhibitor. The ciliary beating of explants was checked on a daily basis using an Olympus CK40 light microscope.

5.3.5 Immunofluorescence stainings

To detect the distribution of plasmin(ogen) in porcine respiratory explants, cryosections were incubated with goat anti-plasminogen/plasmin antiserum (1:100 in PBS, 1 h, 37 °C), followed by FITC-labelled rabbit anti-goat IgG antibodies (1:100 in PBS, 1 h, 37 °C. Cell nuclei were counterstained with Hoechst 33342 (Molecular Probes) (1:100 in PBS) at 37 °C. The cryosections were mounted with glycerin-DABCO (Janssen Chimica, Belgium) after washed with PBS.

To detect the activated plasmin in PrV- infected explants, cryosections of PrV-infected explants were made and fixed in methanol (-20 °C, 100%) for 20 min. After washing, virus-infected cells were detected using FITC-labeled porcine polyclonal anti-PrV antibodies (Nauwynck and Pensaert, 1995) (1:100 in PBS, 1 h, 37 °C). Then, plasmin in explants was detected using the chromogenic substrate CS-41(03) (L-pyroglutamyl-L-phenylalanyl-Llysine-p- nitroaniline hydrochloride, HYPHEN BioMed, Neuville-sur-Oise, France) by monitoring the signal of p-nitroaniline release at 405 nm (1:1 in PBS, 5 min, 37 °C). Finally, cryosections were washed three times with PBS and mounted with glycerin-DABCO (Janssen Chimica, Belgium).

To evaluate the effect of inhibitors in explants, the following immunofluorescence staining was performed. Mouse anti-collagen VII (Sigma) (1:100 in PBS, 1 h, 37 °C) and goat anti-mouse IgG Texas Red (1:100 in PBS, 1 h, 37 °C) were used for the BM visualization. Next, PrV-infected cells were detected by FITC-labeled porcine polyclonal anti-PrV antibodies (1:100 in PBS, 1 h, 37 °C). Finally, after washing, the sections were incubated with Hoechst 33342 (1:100 in PBS) for 10 min. The cryosections were mounted with glycerin-DABCO (Janssen Chimica, Belgium).

5.3.6 Confocal microscopy imaging and plaque analysis

Series of immunofluorescent stained cryosections were analyzed using an SPE confocal microscope (Leica Microsystems GmbH, Heidelberg, Germany). For each condition, maximal plaque size and depth underneath the BM were measured for 10 plaques; triplicate independent experiments were performed. The plaques at the lateral and bottom edges of the explants were excluded from analysis.

5.3.7 Statistical analysis

Data are presented as means ± standard error of mean (SEM). Statistical analysis was performed with one-way ANOVA using GraphPad Prism 5.0 software. Since viral plaque penetration depth data were heteroscedastic after log-transformation, a Kruskal-Wallis' test followed by Mann-Whitney's post-hoc test was performed. A value of $P<0.05$ was considered to indicate a statistically significant difference.

5.4 Results

5.4.1 Detection of the plasminogen activator-plasmin system in porcine nasal mucosa explants

Plasminogen was found in respiratory epithelium, lamina propria and gland of porcine respiratory explants (Figure 1A). Different molecular forms of plasminogen and plasmin were detected by Western blot (Figure 1B). Under reducing conditions, Glu-plasminogen and Lys-plasminogen were detected in both virus infected and non-infected explants. Plasmin gave three bands corresponding to molecular masses of 68, 46 and 23 kDa, which correspond with the molecular weights of Glu-plasmin heavy chain, Lys-plasmin heavy chain, and plasmin light chain. In addition, two additional bands between 100 and 200 kDa appeared in most of the samples except in samples from 89V87 infected explants; a band with a molecular weight of approximately 30 kDa appeared in some samples.

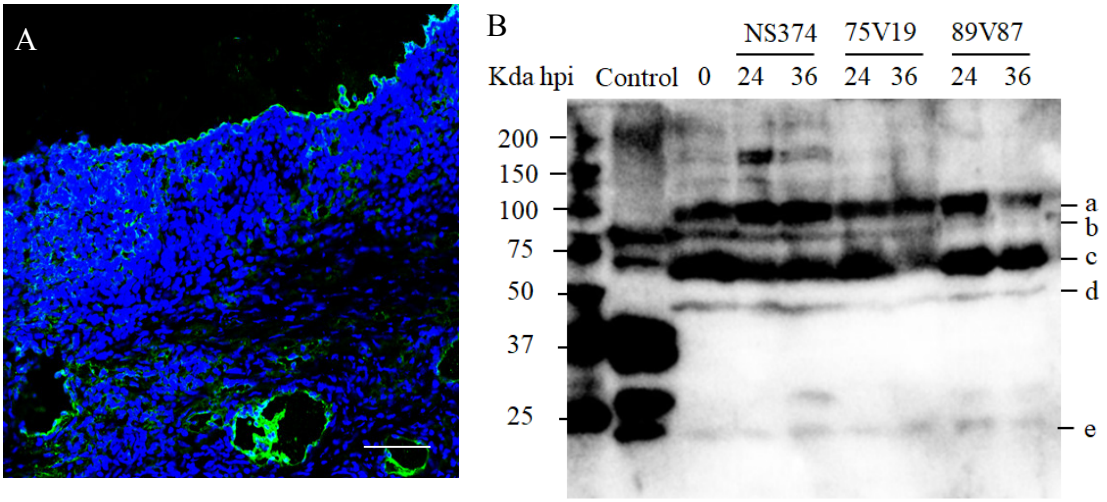

Figure 1. Detection of plasminogen/plasmin in porcine respiratory explants. *Immunofluorescence staining of porcine respiratory explants (A) showing the distribution of plasmin(ogen) (green) in the porcine respiratory mucosa explants. Nuclei were counterstained blue with Hoechst. Scale bar = 100 µm. Western blot analysis of plasminogen/plasmin at 0, 24 and 36 hours post inoculation (hpi) of porcine respiratory mucosa explant with PrV (B). Proteins from porcine respiratory mucosal explants were submitted to SDS-PAGE and Western blot. Plasminogen and plasmin were revealed with goat anti-plasminogen/plasmin serum and rabbit anti-goat immunoglobulin HRP secondary antibody. a=Glu-plasminogen; b=Lys-plasminogen; c=Glu-plamin heavy chain; d=Lys-plasmin heavy chain; e=plasmin light chain.*

5.4.2 Detection of plasmin in PrV plaques of porcine nasal mucosa explants

By the use of plasmin substrate and immunofluorescence staining, plasmin was detected starting from 24 hpi in PrV-infected explants.

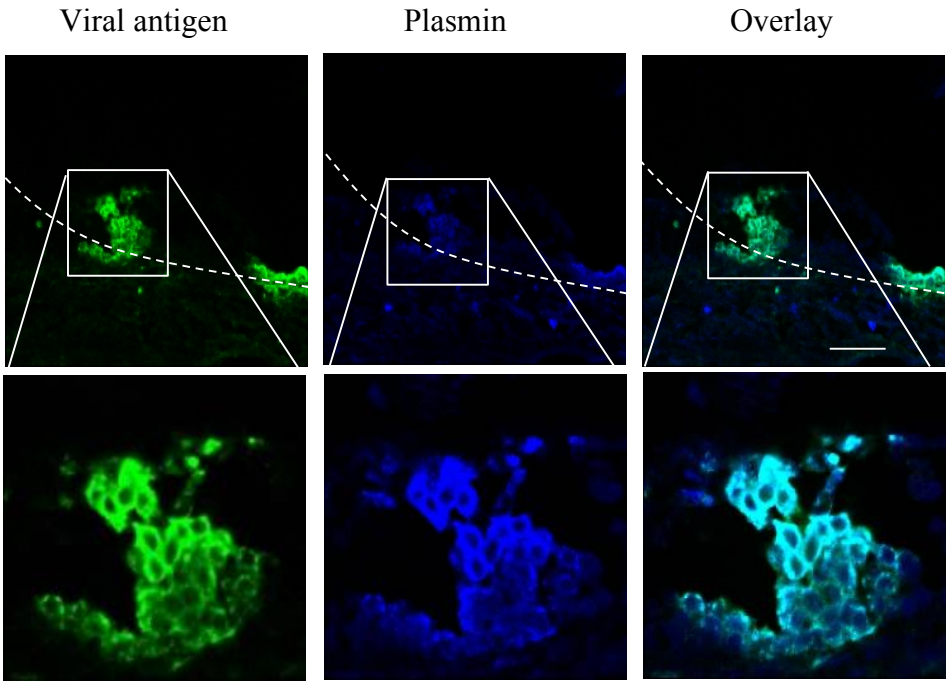

Figure 2. Representative confocal microscopic images of active plasmin in viral-induced plaques in porcine respiratory mucosa explants at 24 hpi. *Images for the individual channels are shown from left to right (green fluorescence, PrV viral antigens; blue fluorescence, active plasmin signal; overlay of viral antigens with active plasmin signal). White dotted line represents the BM. Scale bar = 100 µm.*

5.4.3 The effect of uPA/plasmin inhibitors on PrV invasion through the BM

Morphometric analysis of the kinetics of PrV spread in nasal mucosa explants was previously performed (Glorieux et al., 2009). In the present study, the effect of uPA and plasmin inhibitors on PrV invasion of the BM was evaluated in porcine nasal mucosa explants at 24 hpi. PrV replicated in a plaque-wise manner in inhibitor treated and mock-treated explants (Figure 3).

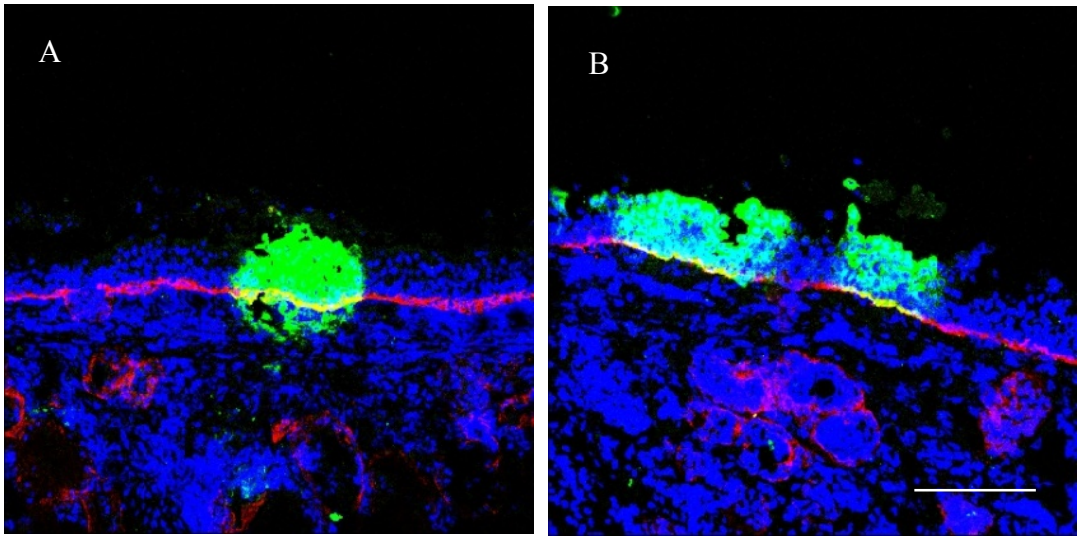

Figure 3. Confocal photomicrographs showing PrV (89V87 strain) plaques in (A) non-inhibitor treated and (B) plasmin inhibitor-treated (10 mM of TXA) porcine nasal mucosa explants at 24 hpi. *Green fluorescence visualizes PrV antigens; collagen VII (component of the basement membrane) is stained with Texas Red; blue fluorescence represents cell nuclei. Figure A shows a viral plaque crossing the BM. Figure B illustrates the blocked viral invasion underneath the BM in the presence of the plasmin inhibitor TXA. Scale bar = 100 µm.*

The plaque diameters of inhibitor-treated explants did not differ significantly with non-treated explants. In NS374 inoculated explants, a dose-dependent decrease in the plaque depth underneath the BM was observed with the uPA inhibitor WX-340 (10 µM- 60% reduction, 30 µM- 88% and 100 µM- 98%) and the plasmin inhibitor TXA (1 mM- 62%, 3 mM- 94% and 10 mM- 100%) (Figure 4). Incubation of PrV 75V19 inoculated explants with WX-340 at 10, 30 and 100 µM resulted in a 41%, 83% and 100% reduction in penetration depth underneath the BM, and with TXA at 1, 3 and 10 mM in a 45%, 88% and 96% reduction (Figure 4). WX-340 reduced the plaque depth of 89V87 strain with 31% at 10 µM, 23% at 30 µM, 31% at 30 µM. When using TXA at 1, 3, and 10 mM, the inhibitor reduced the plaque depth underneath the BM by 43%, 86% and 93%, respectively (Figure 4).

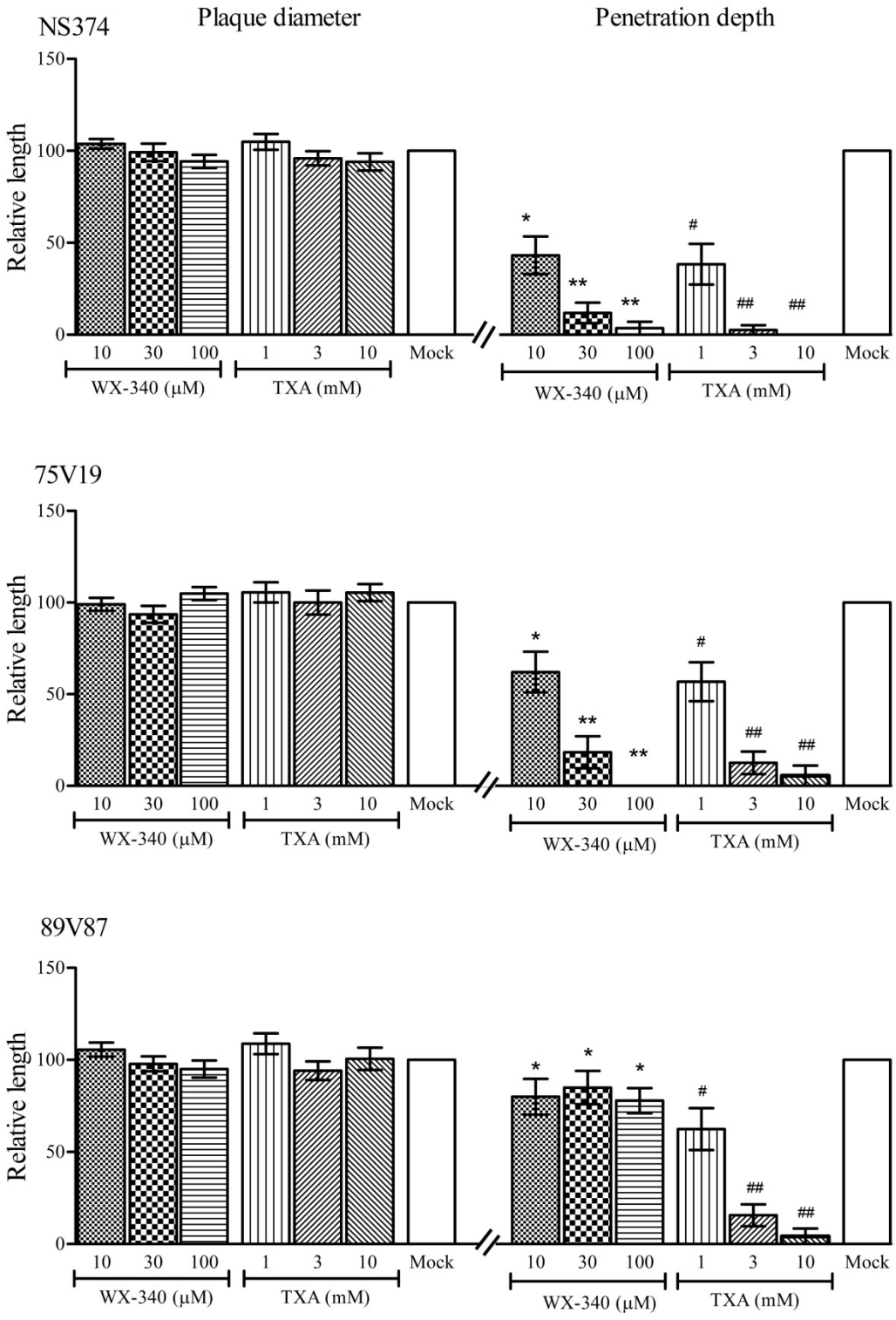

Figure 4. Plaque diameter and penetration depth underneath the basement membrane (BM) of plaques induced by different PrV strains at 24 hpi. *Data are represented as means of 10 plaques of triplicate independent experiments ± SEM (error bars). The percentages of reduction are relative to the mock treated group, which was set at 100%. Significant*

*differences are pointed out by the use of different numbers of * and #. Plaque diameter groups revealed no apparent differences with the mock groups. WX-340 had a strong inhibitory effect on the spread of PrV NS374 and PrV 75V19, and a minor effect on the spread of PrV 89v87. TXA strongly inhibited the penetration of the three PrV strains.*

5.5 Discussion

It is well known that plasmin plays a significant role in the degradation of BM components (Liotta et al., 1981). The plasminogen activator-plasmin system is well studied in blood vessels and skin, occasionally in some internal organs (Li et al., 2003). Previous studies have demonstrated the presence of uPA and their receptors and inhibitors in the upper respiratory tract, and tPA has only been demonstrated in nasal polyps so far (Stevens et al., 2015; Stewart and Sayers, 2013). Here, the presence of plasminogen/plasmin in the upper respiratory tract has been confirmed for pigs. Various forms of plasminogen/plasmin were found in the respiratory mucosa. We can conclude that the plasminogen activator-plasmin system exists and presumably can be activated in porcine respiratory explants, although it is hard to distinguish the different forms in situ.

In viral infected explants, unpredicted bands were detected by Western blot analysis. These unexpected bands could be proteins that are related to plasminogen, such as angiostatin and mini-plasmin. Both angiostatin and mini-plasmin are fragments of plasmin. Angiostatin contains 1-4 kringles of plasminogen, and plays a role in plasmin generation in tumors (Cao and Xue, 2004). Mini-plasmin is related to respiratory disorders (Murakami et al., 2001). So far, involvement of these proteins in the pathology of PrV has not been described yet.

Previously, a quantitative analysis of the kinetic evolution of PrV replication in porcine respiratory mucosa explants was evaluated (Glorieux et al., 2008). PrV

spreads in a plaque-wise manner and penetrates through the BM barrier between 12 and 24 hpi. PrV 89V87 strain was found to penetrate through the basement membrane around 16hpi (Glorieux et al. 2011b). Therefore, PrV BM crossing was analyzed starting from 24hpi.

Our study demonstrated that both the uPA inhibitor WX-340 and plasmin inhibitor TXA strongly reduced the plaque depth of the PrV NS374 and 75V19 strains underneath the BM in nasal mucosa, whereas only the plasmin inhibitor had a strong effect on the invasion of the 89V87 strain. Although speculative, a possible explanation may be that there are two pathways leading to plasmin activation that digests the BM afterwards: (i) indirectly via an upregulation of uPA expression and/or activation and (ii) directly upon contact with plasminogen. According to our findings, it seems that NS374 and 75V19 mainly activate the system by uPA, whereas 89V87 may directly convert plasminogen into plasmin. In addition, we further detected that a more recent PrV strain 00V72 can be inhibited by the plasmin inhibitor TXA, but not by the uPA inhibitor WX-340 (data not shown). Some older strains (NIA1, NIA3) can be inhibited by both the uPA inhibitor and the plasmin inhibitor (data not shown). Although additional experiments are needed to substantiate this, these results may possibly aid in explaining the increased virulence of PrV over the past decades.

The synthetic plasmin inhibitor TXA was used in this study. TXA blocks the lysine binding sites of plasminogen, which prevents the activation of plasminogen (Ollier et al., 2004). TXA is a cheap medicine that is available worldwide with proven efficacy in reducing blood loss. A high concentration (1 to 10 mM) of TXA was used in our study, which is equal with that used on cells by Ollier et al. (2004). In this study, influenza virus replication was reduced by TXA (Ollier et al., 2004). *In vivo*, a high concentration could only be reached during continuous intravenous infusion (Goobie

et al., 2013). Because pigs are difficult to restrain, oral drugs should be developed for *in vivo* use.

Based on the present work, it can be concluded that the plasminogen activator-plasmin system exists in the porcine respiratory mucosa. During PrV infection of the respiratory mucosa, the system is activated, resulting in the viral BM penetration, thereby enhancing the viral penetration of the BM. The uPA inhibitor WX-340 strongly inhibited the spread of PrV NS374 and PrV 75V19, but not 89V87, while the plasmin inhibitor TXA strongly inhibited the penetration of all the three PrV strains.

5.6 References

Berman, M., Manseau, E., Law, M., Aiken, D., 1983. Ulceration Is Correlated with Degradation of Fibrin and Fibronectin at the Corneal Surface. Invest Ophth Vis Sci 24(10), 1358-1366.

Blanchard, Y., Le Meur, N., Le Cunff, M., Blanchard, P., Leger, J., Jestin, A., 2006. Cellular gene expression survey of PseudoRabies Virus (PRV) infected human embryonic kidney cells (HEK 293). Vet Res 37(5), 705-723.

Cao, Y., Xue, L., 2004. Angiostatin. Semin Thromb Hemost 30(1), 83-93.

Collen, D., Lijnen, H.R., 1995. Molecular-Basis of Fibrinolysis, as Relevant for Thrombolytic Therapy. Thromb Haemostasis 74(1), 167-171.

Dunn, C.J., Goa, K.L., 1999. Tranexamic acid - A review of its use in surgery and other indications. Drugs 57(6), 1005-1032.

Endo-Munoz, L., Cai, N., Cumming, A., Macklin, R., de Long, L.M., Topkas, E., Mukhopadhyay, P., Hill, M., Saunders, N.A., 2015. Progression of Osteosarcoma from a Non-Metastatic to a Metastatic Phenotype Is Causally Associated with Activation of an Autocrine and Paracrine uPA Axis. Plos One 10(8).

Gershom, E.S., Vanden Hoek, A.L., Meixner, S.C., Sutherland, M.R., Pryzdial, E.L.,

2012. Herpesviruses enhance fibrin clot lysis. Thromb Haemost 107(4), 760-768.

Glorieux, S., Bachert, C., Favoreel, H.W., Vandekerckhove, A.P., Steukers, L., Rekecki, A., Van den Broeck, W., Goossens, J., Croubels, S., Clayton, R.F., Nauwynck, H.J., 2011a. Herpes simplex virus type 1 penetrates the basement membrane in human nasal respiratory mucosa. PLoS One 6(7), e22160.

Glorieux, S., Favoreel, H.W., Steukers, L., Vandekerckhove, A.P., Nauwynck, H.J., 2011b. A trypsin-like serine protease is involved in pseudorabies virus invasion through the basement membrane barrier of porcine nasal respiratory mucosa. Vet Res 42.

Glorieux, S., Van den Broeck, W., van der Meulen, K.M., Van Reeth, K., Favoreel, H.W., Nauwynck, H.J., 2007. In vitro culture of porcine respiratory nasal mucosa explants for studying the interaction of porcine viruses with the respiratory tract. J Virol Methods 142(1-2), 105-112.

Goobie, S.M., Meier, P.M., Sethna, N.F., Soriano, S.G., Zurakowski, D., Samant, S., Pereira, L.M., 2013. Population pharmacokinetics of tranexamic acid in paediatric patients undergoing craniosynostosis surgery. Clin Pharmacokinet 52(4), 267-276.

Kramer, M.D., Schaefer, B., Reinartz, J., 1995. Plasminogen activation by human keratinocytes: molecular pathways and cell-biological consequences. Biol Chem Hoppe Seyler 376(3), 131-141.

Li, W.Y., Chong, S.S., Huang, E.Y., Tuan, T.L., 2003. Plasminogen activator/plasmin system: a major player in wound healing? Wound Repair Regen 11(4), 239-247.

Li, Y., Negussie, H., Qiu, Y., Reddy, V.R., Mateusen, B., Nauwynck, H.J., 2016. Early events of canine herpesvirus 1 infections in canine respiratory and genital mucosae by the use of ex vivo models. Res Vet Sci 105, 205-208.

Li, Y., Van Cleemput, J., Qiu, Y., Reddy, V.R., Mateusen, B., Nauwynck, H.J., 2015.

Ex vivo modeling of feline herpesvirus replication in ocular and respiratory mucosae, the primary targets of infection. Virus Res 210, 227-231.

Liotta, L.A., Goldfarb, R.H., Brundage, R., Siegal, G.P., Terranova, V., Garbisa, S., 1981. Effect of plasminogen activator (urokinase), plasmin, and thrombin on glycoprotein and collagenous components of basement membrane. Cancer Res 41(11 Pt 1), 4629-4636.

Murakami, M., Towatari, T., Ohuchi, M., Shiota, M., Akao, M., Okumura, Y., Parry, M.A.A., Kido, H., 2001. Mini-plasmin found in the epithelial cells of bronchioles triggers infection by broad-spectrum influenza A viruses and Sendai virus. Eur J Biochem 268(10), 2847-2855.

Nakada, M., Yamashita, J., Okada, Y., Sato, H., 1999. Ets-1 positively regulates expression of urokinase-type plasminogen activator (uPA) and invasiveness of astrocytic tumors. J Neuropathol Exp Neurol 58(4), 329-334.

Nauwynck, H.J., Pensaert, M.B., 1995. Effect of specific antibodies on the cell-associated spread of pseudorabies virus in monolayers of different cell types. Arch Virol 140(6), 1137-1146.

Ollier, L., Caramella, A., Giordanengo, V., Lefebvre, J.C., 2004. High permissivity of human HepG2 hepatoma cells for influenza viruses. J Clin Microbiol 42(12), 5861-5865.

Pepper, M.S., 2001. Role of the matrix metalloproteinase and plasminogen activator-plasmin systems in angiogenesis. Arterioscler Thromb Vasc Biol 21(7), 1104-1117.

Plow, E.F., Herren, T., Redlitz, A., Miles, L.A., Hooverplow, J.L., 1995. The Cell Biology of the Plasminogen System. Faseb J 9(10), 939-945.

Ray, N., Enquist, L.W., 2004. Transcriptional response of a common permissive cell type to infection by two diverse alphaherpesviruses. J Virol 78(7), 3489-3501.

Setas Pontes, M., Devriendt, B., Favoreel, H.W., 2015. Pseudorabies virus triggers glycoprotein gE-mediated ERK1/2 activation and ERK1/2-dependent

migratory behavior in T cells. J Virol 89(4), 2149-2156.

Steukers, L., Glorieux, S., Vandekerckhove, A.P., Favoreel, H.W., Nauwynck, H.J., 2012a. Diverse microbial interactions with the basement membrane barrier. Trends Microbiol 20(3), 147-155.

Steukers, L., Vandekerckhove, A.P., Van den Broeck, W., Glorieux, S., Nauwynck, H.J., 2012b. Kinetics of BoHV1 dissemination in an in vitro culture of bovine upper respiratory tract mucosa explants. ILAR J 53(1), E43-54.

Stewart, C.E., Sayers, I., 2013. Urokinase receptor orchestrates the plasminogen system in airway epithelial cell function. Lung 191(2), 215-225.

Stevens, W.W., Ocampo, C.J., Berdnikovs, S., Sakashita, M., Mahdavinia, M., Suh, L., Takabayashi, T., Norton, J.E., Hulse, K.E., Conley, D.B., Chandra, R.K., Tan, B.K., Peters, A.T., Grammer, L.C., 3rd, Kato, A., Harris, K.E., Carter, R.G., Fujieda, S., Kern, R.C., Schleimer, R.P., 2015. Cytokines in Chronic Rhinosinusitis. Role in Eosinophilia and Aspirin-exacerbated Respiratory Disease. Am J Respir Crit Care Med 192(6), 682-694.

Syrovets, T., Simmet, T., 2004. Novel aspects and new roles for the serine protease plasmin. Cell Mol Life Sci 61(7-8), 873-885.

CHAPTER 6

General discussion

Alphaherpesviruses, a subfamily of the Herpesviridae, typically infect mucosal surfaces. Alphaherpesviruses replicate initially in the epithelial cells of the mucosae, after which they cross the basement membrane barrier and replicate and spread in the lamina propria underneath. Further, the virus may spread to some internal organs such as the central nervous system and pregnant uterus via lymph, blood and nerves. Viral replication at the mucosae and further spread may lead to respiratory, ocular and genital problems, nervous disorders and reproduction failures (Zaichick et al., 2011). The replication kinetics and invasion mechanism at the primary replication sites are not fully understood. In order to find novel treatment strategies, a better understanding of these parts of the pathogenesis is important. Although alphaherpesviruses are closely related, the replication and invasion strategies of these viruses at their primary entry sites differ to some extent. Previous research has shown that pseudorabies virus (PrV) directly penetrates the basement membrane in a plaque-wise manner, and that proteases mediate viral spread across the basement membrane (Glorieux et al., 2011b). BoHV1 also displays a plaque-wise spread during its dissemination in both respiratory and genital mucosae explants; it crosses the basement membrane more efficiently in the respiratory tract than in the genital tract (Steukers et al., 2011). Similar findings were also observed with HSV1 (Glorieux et al., 2011a; Steukers et al., 2014). HSV2 also exhibited a plaque-wise manner to across the basement membrane and induced prominent epithelial syncytia in genital tissues (Steukers et al., 2014). The invasion of EHV1 is quite different. EHV1 does not replicate in the lamina propria but infects resident immune cells in the epithelial cell layer and misuses their motile nature to invade the host (Vandekerckhove et al., 2010). EHV4 only replicates respiratory epithelium, and lacks the ability to cross the basement membrane (Vandekerckhove et al., 2011). These findings highlight the different strategies used by herpesviruses to cross the basement membrane barrier. Besides respiratory and genital mucosae, the ocular mucosa may be an important primary infection site for alphaherpesviruses, e.g. FeHV1. The current thesis first studied the mucosal invasion characteristics of FeHV1

and CaHV1 via newly established ocular, respiratory and genital explant models. These studies gave new insights in the interaction of FeHV1/CaHV1 with mucosae and were complementary with similar work that had been performed with other alphaherpesviruses (PrV, HSV1, BoHV1, EHV1) in the laboratory of the promoter. Additionally, the invasion mechanism of PrV was investigated in more detail.

In vitro tissue culture of ocular, respiratory and genital mucosae of feline and canine origin

In the present thesis, we have evaluated feline ocular and respiratory and canine respiratory and vaginal explant models to elucidate the interactions between FeHV1/CaHV1 and their host mucosae. *Ex vivo* tissue cultures are an elegant, reproducible and physiologically relevant compromise between *in vivo* and *in vitro* models. The use of an explant model can avoid sacrificing large numbers of experimental animals, which contributes to the important ethical dogma: Refinement, Reduction and Replacement (3R principle). In addition, the explant models allow a 3D viral infection, which is much more relevant than the 2D infection in monolayers of cell cultures because it mimics the *in vivo* situation. Characteristics of living tissues that are important for their function are cell-ECM interactions and cell-cell contacts (Page et al., 2013).

Feline and canine respiratory mucosae explants were already described before. They were used to study FeHV1 and bacterial infections (Anderton et al., 2004; Leeming et al., 2006). However, in these studies, the viability of the cell was not evaluated, and the integrity of the lamina propria and submucosa was not assessed during inoculation. To compare the infection kinetics of herpesviruses in respiratory and genital explants from different species, *ex vivo* explant models were developed consisting of respiratory and genital mucosae of horses, pigs, cattle, chicken and humans following a standardized way in the promoter's research team (Glorieux et al., 2007; Glorieux et

al., 2011a; Reddy et al., 2014; Steukers et al., 2012; Steukers et al., 2014; Vandekerckhove et al., 2009). In general, these explants are cultivated at 37 °C, 5% CO_2, in serum-free conditions and can be maintained for 3 to 4 days. The viability of different cells did not significantly decrease over time. The use of similar culture conditions allows to compare the replication characteristics of different alphaherpesviruses.

Alphaherpesvirus FeHV1 and CaHV1 invasion characteristics in different mucosae

The alphaherpesvirus FeHV1 is the causal agent of conjunctivitis, keratitis and rhinotracheitis. FeHV1 is highly host specific. Although FeHV1 is well-known to cause ocular and respiratory problems, the underling pathogenesis during primary infection remains poorly understood. In Chapter 3, we determined the replication kinetics of FeHV1 and the viral primary invasion in the mucosae of their natural host, the cat. FeHV1 virus infection occurred at the edges, but not in the intact center of corneal tissues. Absence of herpesvirus infection in the intact corneal tissue in the present study may be due to 1) the mucins at the cornea surface that may hamper the attachment of herpesviruses to corneal epithelial cells; 2) absence of receptors at the surface of the epithelial cells, leading to a state of resistance; 3) attenuation/modification of the FeHV1 C27 strain during passaging. This finding suggests that FeHV1 seems to exhibit a higher affinity for the conjunctiva than for the cornea, and that FeHV1 may spread in a cell associated manner from the open edges into corneal tissues during the initial infection. FeHV1 infection of ocular explants may be a valuable model for ocular HSV1 infection studies, since the ocular disease induced by FeHV1 is quite similar to that of HSV1 (Maes, 2012). Clinically, the primary infection of HSV1 is usually a nonspecific self-limiting conjunctivitis, often in early childhood and usually without corneal involvement (Azari and Barney, 2013).

In Chapter 3, we showed that feline conjunctival mucosa and tracheal mucosa explants are susceptible to FeHV1 infection. In both conjunctival and tracheal tissue, the virus was able to quickly disseminate in a plaque-wise manner and invade by breaching the basement membrane barrier. This clearly shows that the virus is well adapted to disseminate within conjunctival and tracheal mucosae. This potent invasive capacity in these tissues may explain why ulceration and osteolytic changes in the turbinate bones are part of the clinical entity caused by FeHV1.

The alphaherpesvirus CaHV1 infects the respiratory tract and reproductive organs of dogs. In Chapter 4, we established canine respiratory and genital mucosae explant models to study CaHV1 infection. CaHV1 spreads in a plaque-wise manner in both respiratory and genital explant models, and has a better tropism for genital than for respiratory tissues. When comparing the replication kinetics of CaHV1 in different tissues, CaHV1 plaques were found to have a bigger plaque diameter in vaginal epithelium compared to plaques in tracheal epithelium. This trend has also been observed for BoHV1 and HSV1 in respiratory and genital tissues (Glorieux et al., 2011a; Steukers et al., 2011; Steukers et al., 2014). This might be due to differences in local mucosal immune responses between vaginal and tracheal tissue or the different cell types and intercellular connections between vaginal and tracheal epithelial cells (Blaskewicz et al., 2011; Nauwynck et al., 2007).

In Chapter 4, it was found that CaHV1 can spread efficiently in the depth in vaginal tissues. CaHV1 replication in the vaginal mucosa is associated with clinical symptoms, as it causes vaginal lesions under natural conditions. When we combine the clinical reports with our findings, we could propose that in pregnant dogs, localized genital lesions occur at the site of viral inoculation after initial exposure. As a result, puppies may become infected during delivery when passing the vagina. This represents an important transmission route from pregnant bitches to puppies at birth.

Different replication kinetics and dissemination of alphaherpesviruses in mucosae can be linked with differences in clinical symptoms. The highly invasive PrV, BoHV1 and FeHV1 have the power to cause severe acute respiratory distress. In contrast, CaHV1, EHV1 and EHV4, which lack the ability to penetrate plaque-wise through the basement membrane in the respiratory tissue, only cause mild respiratory problems.

FeHV1 and CaHV1 are genetically closely related (Gaskell et al., 2007), however their clinical behaviors differ significantly in genital tissues. FeHV1 seldomly induces reproductive lesions while CaHV1 may cause reproductive problems (Thiry et al., 2009). Recent experiments with feline vaginal explants have demonstrated that upon FeHV1 inoculation, plaques are formed which rarely penetrate the basement membrane although the virus can easily spread laterally (unpublished data). Our data indicate that CaHV1 shows a main tropism for the genital epithelium and is able to cross the basement membrane, which appears to be in line with the findings *in vivo* (Evermann et al., 2011). Compared with FeHV1, CaHV1 showed a more restricted replication in respiratory explants. This is also in accordance with the *in vivo* findings, since respiratory signs of CaHV1 infection are less severe or absent compared to those following infections with FeHV1. The capacity of alphaherpesviruses to penetrate through the basement membrane may vary depending on the mucosa (conjunctival, respiratory and genital), host and viral species. The underlying mechanism is still not clear. Because CaHV1 causes a serious systemic fatal heamorrhagic disease in puppies, we predict that the virus may penetrate the basement membrane in the upper respiratory tract early in life. It is not clear if this occurs via a local destruction of the basement membrane or if leukocytes are used as invasion vehicles.

In conclusion, mucosa explant models were developed to study virus-mucosa interactions. These *ex vivo* models enable the evaluation of the kinetic evolution of the

horizontal and vertical spread of feline/canine alphaherpesviruses in the mucosa, which is close to the *in vivo* situation. With the rapid development of genome sequencing technology, more information will be available for animal alphaherpesviruses research. Comparing tissue tropism of different alphaherpesvirus strains and their genomic backgrounds can provide more insights in the invasion mechanism of alphaherpesviruses.

The plasminogen activator-plasmin system is involved in the plaque-wise crossing of the basement membrane by PrV

In Chapter 3 and 4, we described that FeHV1 plaques cross the basement membrane in conjunctiva and trachea explants at 48 hpi, and CaHV1 penetrates the basement membrane in vaginal explants at 48 hpi. Similar observations were described for PrV in respiratory mucosa explants at 16 hpi (Glorieux et al., 2011b). We were interested in which cellular effectors are involved in the viral invasion mechanism. During previous work in the laboratory of the promoter, it was found that a trypsin-like serine protease is involved in PrV penetration of the basement membrane, and it was indicated that the plasminogen activator-plasmin system might be involved in this process (Glorieux, 2009; Glorieux et al., 2011b).

In Chapter 5, plasminogen and plasmin were detected in the porcine respiratory mucosa using Western blot and immunostainings. Since other components of the plasminogen activator-plasmin system such as uPA their receptors and inhibitors are also described in these tissues, and tPA has been demonstrated in nasal polyps (; Stevens et al.2015; Stewart and Sayers, 2013), we believed that the plasminogen activator-plasmin system exists in the mucosa and is kept at a dynamic equilibrium.

Swine respiratory explants were first treated with uPA or plasmin inhibitors, followed by inoculation with different virulent strains of PrV. The penetration of the basement

membrane by two older PrV strains was inhibited by both inhibitors, whereas a more recent strain 89V87 was only inhibited by the plasmin inhibitor. Therefore, depending on the virus strain, plasmin that digests the basement membrane may be activated indirectly via an upregulation or activation of uPA or directly upon contact with plasminogen. Plasmin inhibitors may be the most suitable candidates to inhibit PrV invasion through the basement membrane.

In Chapter 5, the synthetic plasmin inhibitor TXA was used to inhibit PrV invasion. PrV is a cofactor of the porcine respiratory disease complex (PRDC). The most common agents involved in PRDC include viral and bacterial pathogens (Thacker, 2001). An important viral agent, influenza virus, enhances plasmin generation during respiratory infection (Kido et al., 1999; Windeyer et al., 2012). A preliminary experiment in our lab demonstrated that plasmin inhibitor TXA can limit influenza virus replication in the porcine respiratory mucosa explant model (unpublished data). In addition, many bacteria can stimulate plasminogen activation (Bhattacharya et al., 2012). Plasmin inhibitors may inhibit such plasmin generation. Thus, these plasmin inhibitors may have a potential as drugs to interfere with PRDC.

Hypothesis

We have found that the cellular components uPA and plasmin are associated with alphaherpesvirus penetration through the basement membrane. However, the viral proteins that are involved in this process are still not identified. Recent studies in our department demonstrated that a US3 deleted PrV mutant has a limitation to penetrate the basement membrane (Lamote et al., 2016). Because US3 encodes a serine/threonine protein kinase (PK) (Jung et al., 2011), and uPA expression is normally regulated by cellular serine/threonine protein kinases (Leslie et al., 1990; Witowsky et al., 2003), it could be that in the viral infected cells, the viral US3 PK stimulates cells to express and secrete uPA, resulting in activation of plasminogen.

uPA plays an important role in this pathway, thus old strains (75V19 and NS374) might mainly use this pathway to activate plasminogen. We deduced the following, although highly speculative hypothesis illustrated in Figure 1.

Our results indicated that strain 89V87 might activate plasminogen by direct contact. Thus, a possible hypothesis is that the PrV virion interacts with plasminogen, and directly converts plasminogen into plasmin. This would result in proteolytic plasmin activity in close proximity of the virus particle enabling virus passage through the basement membrane barrier. Further work will be necessary to unravel the exact mechanism of plasminogen activation by PrV.

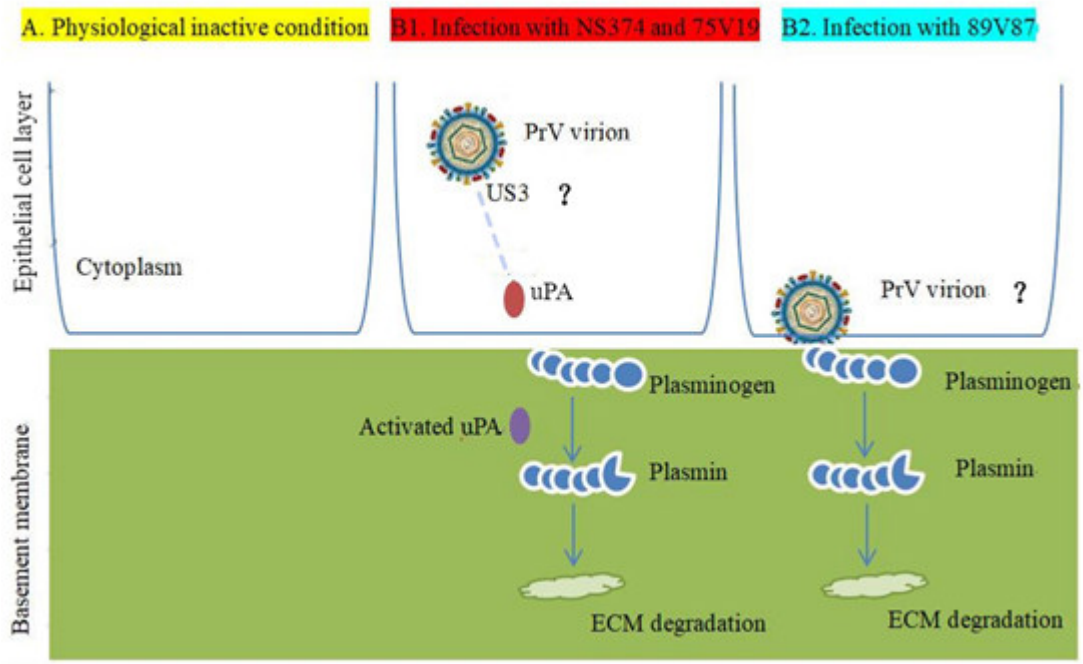

Figure 1. Hypothetical model for BM penetration of PrV via the plasminogen activator-plasmin system. *A. Physiological situation- In the absence of specific stimuli, the extracellular matrix (ECM) remains intact. No uPA present in the cells. B. Situation of PrV infection- (1) For strains NS374 and 75V19, uPA generation may be stimulated, possibly via the viral serine/threonine protein kinase (PK) encoded by US3. Afterwards, activated uPA converts plasminogen into plasmin. As a result, plasmin takes part in extracellular matrix (ECM) degradation. (2) For strain 89V87, viral proteins may directly convert plasminogen into plasmin, thereby leading to ECM degradation.*

Future perspectives

FeHV1 and CaHV1 cross the basement membrane in a plaque-wise manner similar to the mechanism previously described for PrV, BoHV1 and HSV.Our research revealed that the plasminogen activator-plasmin system plays an important role in the viral passage across the basement membrane. Based on this new information, a topical use of antiviral compounds such as plasmin inhibitor could be an interesting antiviral strategy. The current antiviral drugs that target viral DNA synthesis have been proven to be effective against herpesvirus infections. These drugs can inhibit virus replication and even suppress clinical manifestations but are not a cure for the disease. Different from these drugs, products like plasmin inhibitors may be effective during clinical episodes or used as preventive measures during exposure periods.

Induction of virus-specific cellular and humoral immunity via vaccination is another antimicrobial (preventive) measure. If the hypothesis (Figure 1) mentioned above holds true for viral penetration of the BM, use of genetically modified viruses may elicit a robust adaptive immune response while preventing viruses from breaching the BM. Our research suggests that the established explant models can be effective tools to screen for genetically modified, live attenuated vaccines.

Herpesviruses can cause co-infections with other viruses. In humans, epidemiological evidence between HSV and HIV infections has been documented (Wald and Corey, 2007). In HIV-infected patients, the uPA and uPAR expression are upregulated, and uPA/uPAR appear to be nonredundant signals counteracting virus invasion (Alfano et al., 2003). Similar to PrV, HSV infection may also activate the plasminogen activator-plasmin system, resulting in viral basement membrane penetration. It was reported that HSV1 enhances the generation of plasmin and plasmin enhances cell infection by HSV (Pryzdial et al., 2014). Based on these results reported, we speculate

that HIV might facilitate HSV replication and basement membrane penetration through plasminogen activator-plasmin system. This may explain why HSV infection is frequently associated with HIV acquisition. This valuable knowledge would contribute to the development of antiviral measures for HSV and HIV in humans in the future.

The plasminogen activator-plasmin system plays a crucial role in hemostasis. HSV1 envelope receptors exploit these proteases to enhance cellular infection by triggering host signaling mechanisms (Pryzdial et al., 2014). Some other enveloped viruses like influenza virus, SARS-CoV, may also use the system to affect hemostasis. As mentioned in 1.5.4, uPA activity increased in a dose-dependent manner following SARS-CoV infection (Gralinski et al., 2013). During influenza virus infection, plasminogen could contribute to the pathogenesis of the virus infection by promoting virus replication or by inducing a fibrinolysis-dependent harmful inflammatory response in the respiratory tract (Berri et al., 2013). It could be that these viruses have a similar mechanism to regulate some components expression/activation in the plasminogen activator/plasmin enzymatic cascade. The system may further demonstrate the delicate balance between virus invasion and ECM remodeling. Further work may concentrate on revealing the consistency mechanism of the above mentioned enveloped viruses.

References

Alfano, M., Sidenius, N., Blasi, F., Poli, G., 2003. The role of urokinase-type plasminogen activator (uPA)/uPA receptor in HIV-1 infection. J Leukoc Biol 74(5), 750-756.

Anderton, T.L., Maskell, D.J., Preston, A., 2004. Ciliostasis is a key early event during colonization of canine tracheal tissue by Bordetella bronchiseptica. Microbiol-Sgm 150, 2843-2855.

Azari, A.A., Barney, N.P., 2013. Conjunctivitis: a systematic review of diagnosis and

treatment. JAMA 310(16), 1721-1729.

Berri, F., Rimmelzwaan, G.F., Hanss, M., Albina, E., Foucault-Grunenwald, M.L., Le, V.B., Vogelzang-van Trierum, S.E., Gil, P., Camerer, E., Martinez, D., Lina, B., Lijnen, R., Carmeliet, P., Riteau, B., 2013. Plasminogen controls inflammation and pathogenesis of influenza virus infections via fibrinolysis. PLoS Pathog 9(3), e1003229.

Bhattacharya, S., Ploplis, V.A., Castellino, F.J., 2012. Bacterial plasminogen receptors utilize host plasminogen system for effective invasion and dissemination. J Biomed Biotechnol 2012, 482096.

Blaskewicz, C.D., Pudney, J., Anderson, D.J., 2011. Structure and Function of Intercellular Junctions in Human Cervical and Vaginal Mucosal Epithelia. Biol Reprod 85(1), 97-104.

Evermann, J.F., Ledbetter, E.C., Maes, R.K., 2011. Canine reproductive, respiratory, and ocular diseases due to canine herpesvirus. Vet Clin North Am Small Anim Pract 41(6), 1097-1120.

Gaskell, R., Dawson, S., Radford, A., Thiry, E., 2007. Feline herpesvirus. Vet Res 38(2), 337-354.

Glorieux, S., 2009. Invasion of pseudorabies virus in porcine nasal respiratory mucosa explants Ghent University.

Glorieux, S., Van den Broeck, W., van der Meulen, K.M., Van Reeth, K., Favoreel, H.W., Nauwynck, H.J., 2007. In vitro culture of porcine respiratory nasal mucosa explants for studying the interaction of porcine viruses with the respiratory tract. J Virol Methods 142(1-2), 105-112.

Glorieux, S., Bachert, C., Favoreel, H.W., Vandekerckhove, A.P., Steukers, L., Rekecki, A., van den Broeck, W., Goossens, J., Croubels, S., Clayton, R.F., Nauwynck, H.J., 2011a. Herpes Simplex Virus Type 1 Penetrates the Basement Membrane in Human Nasal Respiratory Mucosa. Plos One 6(7).

Glorieux, S., Favoreel, H.W., Steukers, L., Vandekerckhove, A.P., Nauwynck, H.J.,

2011b. A trypsin-like serine protease is involved in pseudorabies virus invasion through the basement membrane barrier of porcine nasal respiratory mucosa. Vet Res 42.

Gralinski, L.E., Bankhead, A., 3rd, Jeng, S., Menachery, V.D., Proll, S., Belisle, S.E., Matzke, M., Webb-Robertson, B.J., Luna, M.L., Shukla, A.K., Ferris, M.T., Bolles, M., Chang, J., Aicher, L., Waters, K.M., Smith, R.D., Metz, T.O., Law, G.L., Katze, M.G., McWeeney, S., Baric, R.S., 2013. Mechanisms of severe acute respiratory syndrome coronavirus-induced acute lung injury. MBio 4(4).

Griffiths, J.B., Electricwala, A., 1987. Amplification of tissue plasminogen activator expression from epithelial cell lines. Dev Biol Stand 66, 417-422.

Hajjar, K.A., Krishnan, S., 1999. Annexin II: a mediator of the plasmin/plasminogen activator system. Trends Cardiovasc Med 9(5), 128-138.

Jung, M., Finnen, R.L., Neron, C.E., Banfield, B.W., 2011. The alphaherpesvirus serine/threonine kinase us3 disrupts promyelocytic leukemia protein nuclear bodies. J Virol 85(11), 5301-5311.

Kido, H., Murakami, M., Oba, K., Chen, Y., Towatari, T., 1999. Cellular proteinases trigger the infectivity of the influenza A and Sendai viruses. Mol Cells 9(3), 235-244.

Lamote, J.A., Glorieux, S., Nauwynck, H.J., Favoreel, H.W., 2016. The US3 Protein of Pseudorabies Virus Drives Viral Passage across the Basement Membrane in Porcine Respiratory Mucosa Explants. J Virol 90(23), 10945-10950.

Leeming, G., Meli, M.L., Cripps, P., Vaughan-Thomas, A., Lutz, H., Gaskell, R., Kipar, A., 2006. Tracheal organ cultures as a useful tool to study Felid herpesvirus 1 infection in respiratory epithelium. J Virol Methods 138(1-2), 191-195.

Leslie, N.D., Kessler, C.A., Bell, S.M., Degen, J.L., 1990. The chicken urokinase-type plasminogen activator gene. J Biol Chem 265(3), 1339-1344.

Maes, R., 2012. Felid herpesvirus type 1 infection in cats: a natural host model for

alphaherpesvirus pathogenesis. ISRN Vet Sci 2012, 495830.

Michael, K., Klupp, B.G., Mettenleiter, T.C., Karger, A., 2006. Composition of pseudorabies virus particles lacking tegument protein US3, UL47, or UL49 or envelope glycoprotein E. J Virol 80(3), 1332-1339.

Nauwynck, H., Glorieux, S., Favoreel, H., Pensaert, M., 2007. Cell biological and molecular characteristics of pseudorabies virus infections in cell cultures and in pigs with emphasis on the respiratory tract. Veterinary Research 38(2), 229-241.

Page, H., Flood, P., Reynaud, E.G., 2013. Three-dimensional tissue cultures: current trends and beyond. Cell Tissue Res 352(1), 123-131.

Pryzdial, E.L., Sutherland, M.R., Ruf, W., 2014. The procoagulant envelope virus surface: contribution to enhanced infection. Thromb Res 133 Suppl 1, S15-17.

Reddy, V.R.A.P., Steukers, L., Li, Y.W., Fuchs, W., Vanderplasschen, A., Nauwynck, H.J., 2014. Replication characteristics of infectious laryngotracheitis virus in the respiratory and conjunctival mucosa. Avian Pathol 43(5), 450-457.

Steukers, L., Vandekerckhove, A.P., Van den Broeck, W., Glorieux, S., Nauwynck, H.J., 2011. Comparative analysis of replication characteristics of BoHV-1 subtypes in bovine respiratory and genital mucosa explants: a phylogenetic enlightenment. Vet Res 42, 33.

Steukers, L., Vandekerckhove, A.P., Van den Broeck, W., Glorieux, S., Nauwynck, H.J., 2012. Kinetics of BoHV-1 Dissemination in an in Vitro Culture of Bovine Upper Respiratory Tract Mucosa Explants. Ilar J 53(1), E43-E54.

Steukers, L., Weyers, S., Yang, X., Vandekerckhove, A.P., Glorieux, S., Cornelissen, M., Van den Broeck, W., Temmerman, M., Nauwynck, H.J., 2014. Mimicking herpes simplex virus 1 and herpes simplex virus 2 mucosal behavior in a well-characterized human genital organ culture. J Infect Dis 210(2), 209-213.

Stewart, C.E., Sayers, I., 2013. Urokinase receptor orchestrates the plasminogen system in airway epithelial cell function. Lung 191(2), 215-225.

Stevens, W.W., Ocampo, C.J., Berdnikovs, S., Sakashita, M., Mahdavinia, M., Suh, L., Takabayashi, T., Norton, J.E., Hulse, K.E., Conley, D.B., Chandra, R.K., Tan, B.K., Peters, A.T., Grammer, L.C., 3rd, Kato, A., Harris, K.E., Carter, R.G., Fujieda, S., Kern, R.C., Schleimer, R.P., 2015. Cytokines in Chronic Rhinosinusitis. Role in Eosinophilia and Aspirin-exacerbated Respiratory Disease. Am J Respir Crit Care Med 192(6), 682-694.

Thacker, E.L., 2001. Immunology of the porcine respiratory disease complex. Vet Clin North Am Food Anim Pract 17(3), 551-565.

Thiry, E., Addie, D., Belak, S., Boucraut-Baralon, C., Egberink, H., Frymus, T., Gruffydd-Jones, T., Hartmann, K., Hosie, M.J., Lloret, A., Lutz, H., Marsilio, F., Pennisi, M.G., Radford, A.D., Truyen, U., Horzinek, M.C., 2009. Feline herpesvirus infection. ABCD guidelines on prevention and management. J Feline Med Surg 11(7), 547-555.

Vandekerckhove, A.P., Glorieux, S., Gryspeerdt, A.C., Steukers, L., Duchateau, L., Osterrieder, N., Van de Walle, G.R., Nauwynck, H.J., 2010. Replication kinetics of neurovirulent versus non-neurovirulent equine herpesvirus type 1 strains in equine nasal mucosal explants. J Gen Virol 91, 2019-2028.

Vandekerckhove, A.P., Glorieux, S., Gryspeerdt, A.C., Steukers, L., Van Doorsselaere, J., Osterrieder, N., de Walle, G.R.V., Nauwynck, H.J., 2011. Equine alphaherpesviruses (EHV-1 and EHV-4) differ in their efficiency to infect mononuclear cells during early steps of infection in nasal mucosal explants. Vet Microbiol 152(1-2), 21-28.

Wald, A., Corey, L., 2007. Persistence in the population: epidemiology, transmission. In: Arvin, A., Campadelli-Fiume, G., Mocarski, E., Moore, P.S., Roizman, B., Whitley, R., Yamanishi, K. (Eds.), Human Herpesviruses: Biology, Therapy, and Immunoprophylaxis, Cambridge.

Windeyer, M.C., Leslie, K.E., Godden, S.M., Hodgins, D.C., Lissemore, K.D., LeBlanc, S.J., 2012. The effects of viral vaccination of dairy heifer calves on

the incidence of respiratory disease, mortality, and growth. J Dairy Sci 95(11), 6731-6739.

Witowsky, J., Abell, A., Johnson, N.L., Johnson, G.L., Cuevas, B.D., 2003. MEKK1 is required for inducible urokinase-type plasminogen activator expression. Journal of Biological Chemistry 278(8), 5941-5946.

Zaichick, S.V., Bohannon, K.P., Smith, G.A., 2011. Alphaherpesviruses and the cytoskeleton in neuronal infections. Viruses 3(7), 941-981.

CHAPTER 7

Summary-Samenvatting

Summary

Different animal species host various alphaherpesviruses and may suffer from a diverse array of pathologies induced by these pathogens. During the primary infection of alphaherpesviruses, the host possesses several barriers that hamper invasion of pathogens. One essential barrier is the basement membrane (BM) underneath the epithelia. Previous studies in our laboratory have shown that alphaherpesviruses behave differently at the BM. The replication of equine herpesvirus 4 (EHV4) is restricted to the respiratory epithelium of the upper respiratory tract. Herpes simplex virus 1 (HSV1), suid herpesvirus 1 (PrV) and bovine herpesvirus 1 (BoHV1) penetrate through the BM, to reach and infect susceptible cells located in the underlying connective tissues. Equine herpesvirus 1 (EHV1) infects epithelial cells, but not underlying fibroblasts. Instead, it hijacks monocytes in the epithelium to cross the BM and invade its host. Feline herpesvirus 1 (FeHV1) and Canine herpesvirus 1 (CaHV1), two important pathogens of cats and dogs, are not well studied. In the current thesis, we sought to establish models that allow the study of the mucosal invasion mechanism used by FeHV1 and CaHV1. In addition, since many alphaherpesviruses cause respiratory infections in their host, a better characterization of the pathogenesis of one of the infections may contribute to better insights in the pathogenesis of others.

In Chapter 1, a general introduction of herpesviruses and an overview of the characteristics of ocular, respiratory and genital mucosae is provided.

Subchapters 1.1-1.3 consist of a brief introduction of herpesvirus biology in general. Because the major focus in this thesis is on FeHV1, CaHV1 and PrV, more information is provided about the respective pathogenesis and symptomatology of these viruses.

Subchapter 1.4 mainly describes the structure and functions of the ocular surface, upper respiratory and lower genital tract tissues with emphasis on the basement membrane.

Subchapter 1.5 focuses on the current knowledge of the plasminogen activator-plasminogen system.

Chapter 2 formulates the aims of the thesis.

In chapter 3, *ex vivo* models are described that allow to study feline herpesvirus replication in ocular and respiratory mucosae, which are represent the primary targets of infection.

Feline herpesvirus 1 (FeHV1) is one of the major viral pathogens involved in rhinotracheitis and ocular disease in cats. Little is known about how the virus replicates in and invades the mucosae of the respiratory tract and eyes, resulting in lesions. In the present study, viral behavior during the early stage of infection was examined in the respiratory and ocular mucosae, the portals of entry of FeHV1 by using *ex vivo* explants. Three FeHV1 seronegative cats without ocular or respiratory problems were used in this study. Equal pieces ($25mm^2$) of corneal, conjunctival and tracheal mucosa explants were maintained in an air-liquid culture at 37 °C and 5% CO_2, and their viability was examined during 96 h of cultivation. All tracheal tissues were observed under a stereomicroscope for cilia beating, and only tracheal tissues in which cilia beating was present all over the explants were used. Corneal, conjunctival and tracheal explants were inoculated with the FeHV1 C-27 strain at 24 hours after cultivation and sampled at 0, 24, 48 and 72 hours post inoculation (hpi). Viral antigen positive cells were visualised via a direct immunofluorescence staining and series of stained cryosections were analysed with a Leica TCS SP2 confocal microscope. A quantitative morphological analysis of viral replication and invasion in the mucosae was performed by measuring plaque latitudes and penetration depths underneath the

basement membrane. The explants of three cats were maintained in an air-liquid culture up to 96 hours with a little decrease in tissue viability. After inoculation, FeHV1 was found to replicate in conjunctival and tracheal mucosae in a plaque wise manner but no infection was observed in corneal epithelium except for damaged sites. The plaques were observed from 24 hpi and plaque latitude increased over time. The viral plaque latitudes increased over time at a similar speed in trachea and conjunctiva. FeHV1 penetrated the BM in conjunctival and tracheal explants between 24 and 48 hpi, and most plaques crossed the BM at 72 hpi. FeHV1 invaded the lamina propria more efficiently in tracheal tissues than in conjunctival tissues. In conclusion, the feline ocular and respiratory explants were suitable to study the early events of the pathogenesis of FeHV1 infections. Our study indicates that FeHV1 has a better capacity to invade the respiratory mucosa than the conjunctival mucosa, and prefers the conjunctiva but not the cornea as a portal of entry during ocular infection.

Chapter 4 demonstrates CaHV1 respiratory and genital mucosal dissemination and invasion.

The pathogenesis of canine herpesvirus 1 is not well characterized. We aimed to investigate the early steps in the pathogenesis of this pathogen known for its contribution to cases of respiratory and genital diseases. The replication kinetics and invasion characteristics of CaHV1 in tracheal and vaginal mucosae were compared using explants. The canine tracheal and vaginal mucosae explants were inoculated with CaHV1 F205 strain. The explants were collected at 0, 24, 48, and 72h pi, cryosections were made, fixed and stained for viral antigens by a double immunofluorescence labeling. A fluorescent terminal deoxynucleotidyl transferase mediated dUTP nick end labeling (TUNEL) staining was used to analyze the viability of the canine tracheal and vaginal mucosal explants. The explant models were maintained up to 96h without significant changes in cell viability. Both explants were successfully infected with CaHV1. The virus spread in a plaque wise manner, as

shown by immunofluorescence analysis. Upon inoculation, the plaques were already observed at 24 hpi, their size increased over time. CaHV1 started to penetrate the BM only after 48 hpi in tracheal explants but already after 24 hpi in vaginal explants. The plaque penetration depth increased over time and was larger in vaginal mucosa explants compared to tracheal mucosa explants. The canine respiratory and genital explants were established in this study, enabling research on CaHV1 replication and invasion in the mucosae. CaHV1 showed a better capacity to replicate and invade vaginal mucosa compared to tracheal mucosa, based on both the latitude and penetration depth of the plaques of viral antigen positive cells.

According to our findings in the former two chapters, both FeHV1 and CaHV1 are able to penetrate the basement membrane in a plaquewise manner, which is similar to what was previously observed for pseudorabies virus (PrV). Therefore, we were interested in which viral effectors are required for the viral invasion mechanism of this group of alphaherpesvirus and used the established model of PrV on respiratory mucosa for investigation.

Chapter 5 shows pseudorabies virus invasion through the basement membrane barrier occurs via activation of the uPA-plasmin system.

Previous studies showed that a trypsin-like serine protease is involved in pseudorabies virus (PrV) invasion through the basement membrane barrier of porcine nasal respiratory mucosa and it was hypothesized that this serine protease might be uPA, which can convert plasminogen into active plasmin. Different strains of PrV, namely 89V87, 75V19 and NS374, were tested in this experiment. In a first step, porcine respiratory explants were infected with PrV. As demonstrated by Western blot, various forms of plasminogen and plasmin were found in non-infected and virus-infected porcine respiratory explants. As demonstrated by IF staining, plasmin was expressed in the virus plaque starting from 24 hours post inoculation (hpi) in porcine respiratory explants. In a second step, a detailed quantitative analysis system

was used to determine the kinetics of horizontal and vertical virus spread in nasal explants, in the presence or absence of WX-340 (an uPA inhibitor) and tranexamic acid (an plasmin inhibitor). Plaque latitudes and penetration depths underneath the basement membrane were determined at 24h post inoculation (pi). Basement membrane penetration of two older PrV strains, NS37 and 75V19, were blocked by both the uPA inhibitor and the plasmin inhibitor, while basement membrane passage of the more recent strain 89V87 was only blocked by the plasmin inhibitor.

In chapter 6, all experimental studies are discussed.

Samenvatting

Alfaherpesvirussen worden teruggevonden bij verscheidene diersoorten en kunnen een divers spectrum aan ziektebeelden induceren. Gedurende de primaire infectie worden deze pathogenen geconfronteerd met verschillende barrières binnen de gastheer, die de invasie trachten te verhinderen. De basale membraan (BM) onder het epitheel vormt een dergelijk belangrijke barrière. Voorgaande studies binnen ons laboratorium hebben aangetoond dat elk alfavirus zich anders gedraagt ter hoogte van de BM. Bijvoorbeeld, de replicatie van het equiene herpesvirus 4 (EHV-4) beperkt zich tot het respiratoire, mucosale epitheel van de bovenste luchtwegen. Herpes simplex virus 1 (HSV-1), suid herpesvirus 1 (of pseudorabiës virus, PrV) en boviene herpesvirus 1 (BoHV-1) zullen na primaire infectie ter hoogte van de mucosa de BM doorboren om zo de gevoelige target cellen in het onderliggende bindweefsel te bereiken. Het equiene herpesvirus 1 (EHV-1) daarentegen infecteert de mucosale epitheelcellen maar niet de onderliggende fibroblasten. Als gevolg, maakt EHV-1 gebruik van een alternatief mechanisme om de BM te doorkruisen. EHV-1 zal typisch de aanwezige monocyten in het epitheel 'hijacken' om de BM te doorboren en zo zijn gastheer te invaderen. Het feliene herpesvirus 1 (FeHV-1) en caniene herpesvirus 1 (CaHV-1) zijn twee belangrijke pathogenen van de kat en hond maar werden tot op heden onvoldoende bestudeerd. In de huidige thesis werd er dan ook getracht modellen op te stellen die de studie van de mucosale invasiemechanismen van zowel FeHV-1 als CaHV-1, zal toelaten. Aangezien vele alfaherpesvirussen respiratoire infecties veroorzaken in hun gastheer, zal de karakterisatie van de invasiemechanismen van deze twee alfaherpesvirussen bijdragen tot betere inzichten in de pathogenese van andere alfaherpesvirussen.

In hoofdstuk 1, werd een algemene introductie gegeven over herpesvirussen evenals een beschrijving van de eigenschappen van de oculaire, respiratoire en

genitale mucosa. In tussenhoofdstuk 1.1 tot 1.3 kwam de algemene biologie van herpesvirussen aan bod. Aangezien er binnen deze thesis wordt toegespitst op FeHV-1, CaHV-1 en PrV, werd de pathogenese en symptomatologie van deze virussen in meer detail weer gegeven. In tussenhoofdstuk 1.4 werd een overzicht gegeven van de structuur en functie van de oogweefsels, de bovenste luchtwegen en de lagere genitale weefsels waarbij extra aandacht besteed werd aan de BM. In tussenhoofdstuk 1.5 wordt de huidige kennis van het 'plasminogeen activator-systeem' beschreven.

In hoofdstuk 2, werden de doelstellingen van deze thesis uiteengezet.

In hoofdstuk 3, werden *ex vivo* modellen beschreven die ons toelaten de replicatie van feliene herpesvirussen in de oculaire en respiratoire mucosa, de primaire plaats van infectie, te bestuderen. FeHV-1 is één van de voornaamste virale oorzaken van rhinotracheitis en oculaire infecties bij de kat. Er is weinig geweten over de replicatie van dit virus en hoe deze de oculaire en respiratoire mucosa binnendringt om zo aanleiding te geven tot lesies. In de huidige studie werd gebruik gemaakt van *ex vivo* explantmodellen om de vroege stadia van infectie ter hoogte van de toegangspoorten voor FeHV-1, met name de respiratoire en oculaire mucosa, te bestuderen. Drie FeHV-1-seronegatieve katten zonder oculaire of respiratoire symptomen werden geïncludeerd in deze studie. Uniforme explanten ($25mm^2$) van de cornea, conjunctiva en trachea werden gecultiveerd als een "air-liquid interface culture" bij 37 °C en 5% CO_2 en de vitaliteit werd gecontroleerd na 96 uur in cultuur. Verder werd ook de activiteit van de cilia nagegaan voor alle trachea explanten via stereomicroscopie en enkel de explanten waarbij ciliabeweging werd waargenomen over de gehele explant werden gebruikt in verdere experimenten. De explanten van de cornea, conjunctiva en trachea werden geïnoculeerd met FeHV-1 stam C-27. Op specifieke tijdstippen (0, 24, 48 en 72 uur) post inoculatie (p.i.) werden cryosecties gemaakt en deze ondergingen vervolgens directe immunofluorescentiekleuring. Deze

kleuring werd dan gevisualiseerd met de Leica TCS SP2 confocale microscoop en het aantal positieve cellen werd bepaald. Een kwantitatieve, morfologische analyse van de virusreplicatie en mucosale invasie gebeurde via het opmeten van de plaquelatitude en penetratiediepte onder de BM. Explanten van drie katten konden gecultiveerd worden als een 'air-liquid interface culture" gedurende 96 uur met een beperkt verlies aan explant vitaliteit. Na inoculatie met FeHV-1, kon plaquegewijze virusreplicatie geobserveerd worden in de mucosa van de conjunctiva en trachea. In het corneale epitheel kon echter geen infectie waargenomen worden met als uitzondering ter hoogte van beschadigde sites. Plaques werden typisch geïnduceerd vanaf 24 uur p.i. en de plaquelatitude nam progressief toe met de tijd. Deze toename gebeurde met eenzelfde snelheid in zowel de trachea als de conjunctiva explanten. FeHV-1 doorboorde de BM van de conjunctiva en trachea explanten tussen 24 uur en 48 uur p.i. waarbij de meeste plaques de BM doordrongen bij 72 uur p.i. De invasie van de lamina propria gebeurde op een veel efficiëntere manier in de trachea explanten in vergelijking met de conjunctiva explanten. Deze bevindingen leiden tot de conclusie dat de feliene oculaire en respiratoire explanten uiterst geschikt zijn om de initiële infectiestadia gedurende FeHV-1 infectie te bestuderen. Met deze studie konden we eveneens aantonen dat FeHV-1 met grotere efficiëntie de respiratoire mucosa invadeert (in vergelijking met de mucosa van de conjunctiva) en dat deze een voorkeur heeft voor de conjunctiva maar niet de cornea als predominante toegangspoort gedurende oculaire infecties bij de kat.

In hoofdstuk 4, werd de invasie en disseminatie van CaHV-1 in de respiratoire en genitale mucosa aangetoond. De pathogenese van het CaHV-1 is slechts in beperkte mate gekarakteriseerd. Het doel van deze studie was dan ook om de vroege replicatiestadia van CaHV-1, het causatief agens van respiratoire en genitale aandoeningen bij de hond, verder uit te klaren. Hiervoor werd allereerst de replicatiekinetiek en het invasiemechanisme van CaHV-1 in de mucosa van de trachea

en vagina met elkaar vergeleken door opnieuw gebruik te maken van explantmodellen. Tracheale en vaginale mucosa explanten van de hond werden geïnoculeerd met CaHV-1 stam F205. Op specifieke tijdstippen p.i. (0, 24, 48 en 72 uur) werden de explanten ingevrozen om cryosecties te maken. Deze cryosecties werden nadien gefixeerd en gekleurd voor virale antigenen via dubbele immunofluorescentielabeling. De "Terminal deoxynucleotidyl transferase dUTP Nickend Labeling" of TUNEL-kleuring werd gebruikt om de vitaliteit van de caniene trachea en vagina explanten na te gaan. Beide explantmodellen konden in cultuur gehouden worden tot 96 uur zonder de vitaliteit significant te beïnvloeden. De trachea en vagina explanten werden vervolgens geïnfecteerd met CaHV-1 en via immunofluorescentie analyse werd er aangetoond dat dit virus zich verspreid in een plaquegewijze manier. Na inoculatie konden plaques waargenomen worden op 24 uur p.i. en de grootte van deze plaques nam toe met de tijd. In het trachea explantmodel, penetreerde CaHV-1 de BM pas op 48 uur p.i. In tegenstelling tot de penetratie in de trachea explanten, werd in de vagina explanten reeds op 24 h p.i. penetratie van de BM waargenomen. De plaquediepte nam in beide modellen toe met de tijd en was typisch hoger in vaginale mucosa explanten in vergelijking met tracheale mucosa explanten. Samengevat werden in deze studie twee explantmodellen, een respiratoir en genitaal explant model, tot stand gebracht die ons toelaten de replicatie en invasiemechanismen van CaHV-1 in de mucosa te bestuderen. Op basis van de waargenomen latitude en penetratiediepte van de plaques in cellen positief voor virale antigenen konden we besluiten dat CaHV-1 een hogere capaciteit heeft om te repliceren en door te dringen in de vaginale mucosa in vergelijking met de tracheale mucosa. In overeenkomst met onze bevindingen in de twee voorgaande hoofdstukken, kunnen we concluderen dat FeHV-1 en CaHV-1 beiden de basale membraan kunnen penetreren door middel van plaques, op een gelijkaardige wijze als geobserveerd voor het pseudorabies virus (PrV). Om in een volgende stap de virale effectors die essentieel zijn tijdens het

invasieproces van deze alfaherpesvirussen te achterhalen, werd dan ook gebruik gemaakt van het PrV infectiemodel in de respiratoire mucosa.

In **hoofdstuk 5**, **werd gedemonstreerd dat PrV invasie van de BM gebeurt via activatie van het uPA-plasmine systeem**. Vorige studies hebben aangetoond dat een trypsine-like serine protease een rol speelt in de invasie van PrV doorheen de BM van de porciene nasale respiratoire mucosa. Volgens onze hypothese is dit serine protease een urokinase-type plasminogeen activator enzym, dat plasminogeen omzet naar het actieve plasmine protease. Verschillende stammen van PrV (89V87, 75V19 en N374) werden getest in dit experiment. Allereerst, werden porciene respiratoire mucosa explanten geïnfecteerd met PrV. Verschillende vormen van plasminogeen en plasmine werden terug gevonden in zowel niet-geïnfecteerde als virus-geïnfecteerde explanten na western blot analyse. In de respiratoire explantmodellen werd plasmine expressie in de virus plaques waargenomen op 24 uur p.i. Verder werd een detailleerde, kwantitatieve analyse uitgevoerd om de kinetiek van zowel horizontale als verticale virusspreiding in nasale explanten in de aan- of afwezigheid WX-340 (een uPA inhibitor) en tranexamic zuur (een plasmine inhibitor) te bepalen. Plaquelatitude en penetratiediepte onder de BM werden bepaald op 24 uur p.i. De BM penetratie van twee oudere PrV stammen, NS37 en 75V19, werd geïnhibeerd door zowel de uPA inhibitor als de plasmine inhibitor. De BM penetratie van de meer recentere PrV stam, 89V87 daarentegen werd enkel geïnhibeerd door de plasmine inhibitor.

In **hoofdstuk 6,** werd alle bekomen data geëvalueerd en kritisch besproken.

Acknowledgement

At the end of this thesis, I would like to take some time to thank all the people without whom this project would never have been possible.

First of all, I wish to thank my advisor, Prof. Dr. Hans Nauwynck, Director of the Laboratory of Virology. He helped me come up with the thesis topic and guided me over four years of development. I greatly appreciate the time and efforts he has exerted to guide me throughout the research and thesis writing.

I also want to take a moment to thank my thesis committee members, Prof. Dr. Sylvie Daminet, Prof. Dr. Koen Chiers, Prof. Dr. Herman Favoreel, Prof. Dr. Wim Van den Broeck, Prof. Dr. Peter Delputte and Dr. Sarah Glorieux. Thank you for investing time and providing interesting and valuable feedback. I feel proud and honored that you have accepted to be on my committee.

Next, some people of outstanding importance for my research. Dr. Sarah Glorieux and Dr. Lennert Steukers, your work has formed the basis for my research. Amy Yang in the herpersvirus group has also been amazing help during my first two years of the PhD research. I also appreciate the support and help from Dr. Sjouke Van Pouke for her help to contact veterinary clinics to donate cats and dogs for my experiments. A special acknowledgement goes to my office mate: Dr. Haileleul Negussie. He was a true friend ever since we began to share an office in 2013. And I also thank Jason Xie, Bo Yang, my colleagues and also roommates who have been supportive in every way. I am also thankful to Wendy Baetens for translating the summary. Also thank you to the past and current colleagues at the laboratory who have helped with the project and supported me in many ways: Jing Zhao, Ivan Trus, Ruifang Wei, Tingting Cui, Katrien Poelaert, Jolien Van Cleemput, Vishwanatha Reddy, Sebastiaan Theuns,

Caroline Bonckaert, Ilias Frydas, Lowiese Desmarets, Inge Roukaerts, Delphine Acar, Vo Van Tuan, Thuong Van Khuong, Garba Abubakar and Gaëtan De Gryse.

I would like to thank the China Scholarship Council, for providing the scholarship allowing me to pursue PhD study, and thank the Faculty of Veterinary Medicine of Ghent University for providing funding to support my research and also the opportunity to attend conferences and meet so many interesting people.

I also want to thank my parents and parents in-laws for believing in me and being there for practical support in all those things of life beyond doing a PhD, and finally my wife Yu Qiu, for her continued support and encouragement in all aspects of my life and throughout the ups and downs of my research. Please hold my hand forever.